

(200)
WR.

W. 94-4103

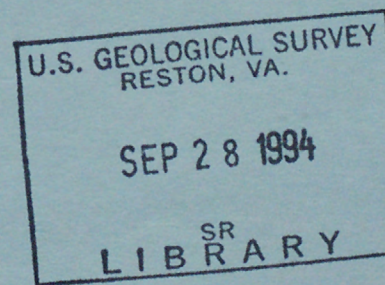
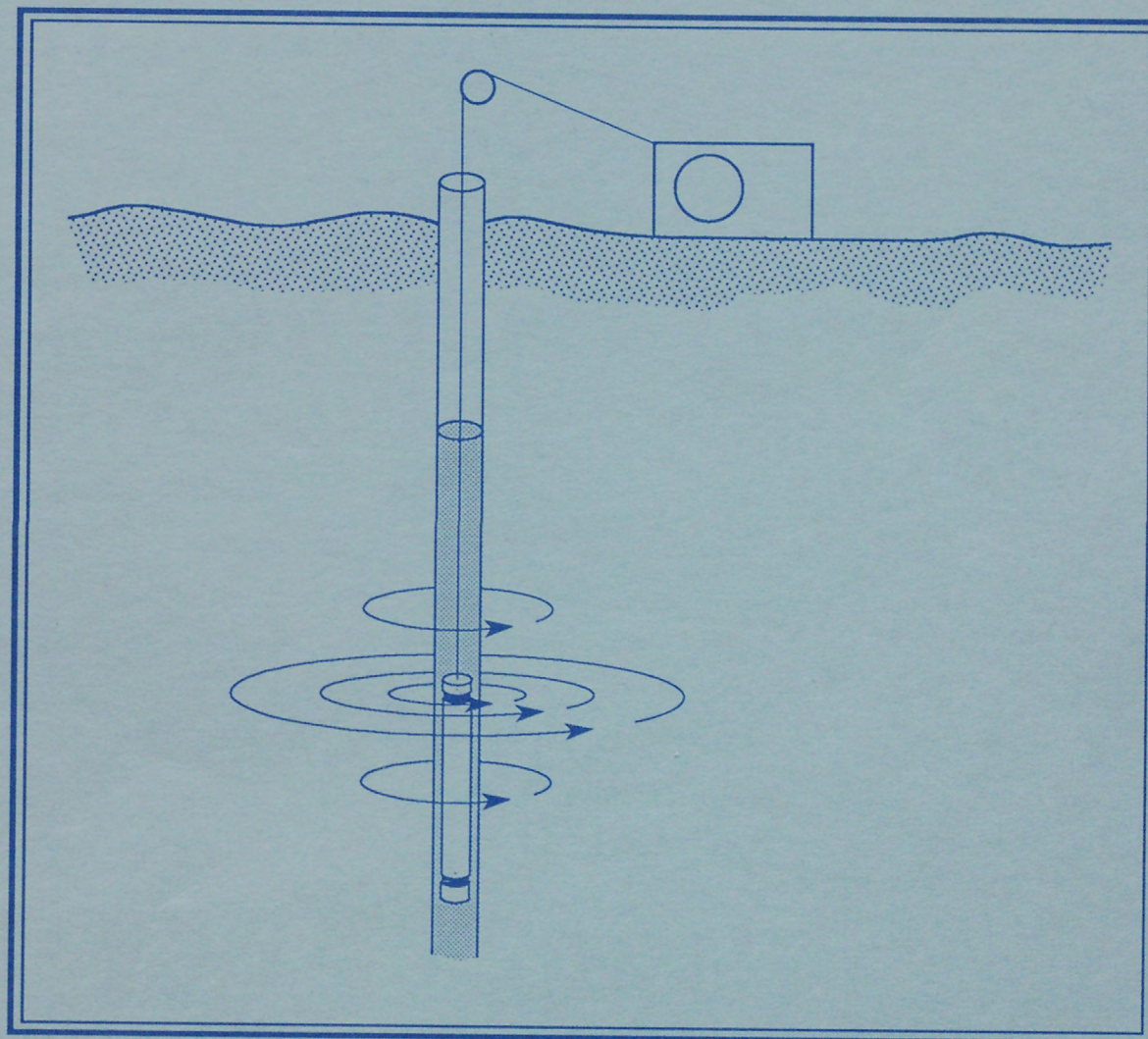
PROCEEDINGS OF THE U.S. GEOLOGICAL SURVEY WORKSHOP ON THE APPLICATION OF
BOREHOLE GEOPHYSICS TO GROUND-WATER INVESTIGATIONS

ALBANY, NEW YORK

JUNE 2-4, 1992

U.S. GEOLOGICAL SURVEY

Water-Resources Investigations Report 94-4103



Cover: Electromagnetic-induction logger used in ground-water investigation.



92023495

C.1

PROCEEDINGS OF THE U.S. GEOLOGICAL SURVEY WORKSHOP ON THE APPLICATION OF
BOREHOLE GEOPHYSICS TO GROUND-WATER INVESTIGATIONS, ALBANY, NEW YORK,
JUNE 2-4, 1992

Edited by Frederick L. Paillet and John H. Williams

U.S. GEOLOGICAL SURVEY
Water-Resources Investigations Report 94-4103



Denver, Colorado
1994

U.S. DEPARTMENT OF THE INTERIOR
BRUCE BABBITT, Secretary
U.S. GEOLOGICAL SURVEY
Gordon P. Eaton, Director

Use of trade names in this report is for identification purposes only and does not constitute endorsement by the U.S. Geological Survey.

For additional information
write to:

Chief, Branch of Regional Research
U.S. Geological Survey
Box 25046, MS 418
Denver Federal Center
Denver, CO 80225

Copies of this report can be
purchased from:

U.S. Geological Survey
Earth Science Information Center
Open-File Reports Section
Box 25286, MS 517
Denver Federal Center
Denver, CO 80225

CONTENTS

Preface.....	VII
PART I -- RECENT DEVELOPMENTS.....	1
A generalized approach to quantitative interpretation of borehole geophysical logs in hydrogeologic studies, by F.L. Paillet.....	2
Application of electromagnetic-induction logging to ground-water- quality studies, by John H. Williams.....	9
Flowmeter logging--a review, by F.L. Paillet and A.E. Hess.....	13
Acoustic logging--a review, by F.L. Paillet.....	22
PART II -- CASE STUDIES.....	28
Use of borehole-geophysical logs to define the areal extent, source, and thicknesses of confining units in the Owens Valley, California, by Kenneth J. Hollett and Wesley R. Danskin.....	29
Use of borehole-geophysical logs to delineate the position of the freshwater/saline-water interface in the Michigan basin, by D.B. Westjohn.....	33
Use of borehole geophysics for delineation of the contributing area to a supply well in a dipping, sedimentary-bedrock aquifer, by Gary J. Barton and Randall W. Conger.....	40
Use of geophysical logs in hydrogeologic investigations at selected Superfund sites in north-central Illinois, by P.C. Mills, James Ursic, R.T. Kay, and D.J. Yeskis.....	49
Use of borehole geophysical methods to investigate aquifer cross contamination by volatile organic compounds in the Stockton Formation, Hatboro, Pennsylvania, by Ronald A. Sloto, Paola Macchiaroli, and Michael T. Towle.....	54
Delineation of the saltwater-freshwater interface in Great Neck, Long Island, New York, by Frederick Stumm.....	60
Delineation and estimated time of travel of a road-salt plume by use of borehole induction logs, by Peter E. Church and Paul J. Friesz.....	66
Detection of contaminant plumes by borehole geophysical logging, by Thomas J. Mack.....	71
Use of borehole electromagnetic logging to delineate a septage- effluent plume in glacial outwash, Orleans, Massachusetts, by Leslie A. DeSimone and Paul M. Barlow.....	75

ILLUSTRATIONS

1. Gamma, neutron, and density logs for a sandstone aquifer in central Texas; A, B, and C denote sandstone or carbonate beds discussed in text.....	7
2. Profiles of effective porosity computed by use of a gamma log to correct neutron and density for clay-mineral effects.....	8
3. Measured response of two slimhole electromagnetic-induction probes: A. Radial distance, B. Vertical distance.....	11

4. Electromagnetic-induction and lithologic logs, specific conductance of ground-water samples, and geoelectric section for a monitoring-well pair near the Albany landfill in east-central New York.....	12
5. U.S. Geological Survey thermal-pulse flowmeter.....	18
6. Calibration curves for U.S. Geological Survey thermal-pulse flowmeter.	19
7. Example of thermal-pulse flowmeter data collected from a borehole in fractured dolomite that illustrates the distribution of vertical flow under ambient conditions during pumping at a rate of about 2.0 gallons per minute.....	20
8. Example of the distribution of vertical flow induced in an observation borehole when an adjacent borehole is about 50 feet away and is being pumped at a rate of about 3 gallons per minute.....	21
9. A. Single-source acoustic logging probe. B. Dual-source compensated acoustic logging probe.....	25
10. Empirical calibration of interval transit-time in porosity units using the Wyllie time-average equation.....	26
11. Acoustic-waveform logs compared to televiewer logs indicating the effects of fractures on acoustic propagation along boreholes: A. Horizontal-fracture zone intersecting a vertical borehole. B. Near-vertical fracture intersecting a vertical borehole.....	27
12. Location and structural division of Owens Valley into Bishop and Owens Lakes basins, hydrologically connected through the geomorphic "narrows" east of and adjacent to Poverty Hills.....	31
13. Borehole geophysical logs of three wells, location of the three wells in the Bishop basin, and geophysical correlation of major clay layers in the southern part of the Bishop basin.....	32
14. Electrical-resistivity/spontaneous potential log indicating the presence of freshwater to a depth of 180 meters.....	37
15. Dual-induction resistivity logs before and after pumping 17,000 gallons of brine from an interval packed-off at a depth of 570 feet...	38
16. Suite of neutron-porosity/dual-induction logs run in borehole shown in figure 15.....	39
17. Map showing geology and zone of contribution for supply-well NP61 at the North Penn Water Authority Hospital well field, Lansdale, Pennsylvania.....	44
18. Graphs and schematic diagrams showing geophysical logs of supply well NP61.....	45
19. Photograph showing hydrogeologic characteristics of sedimentary bedrock of Triassic age near the Hospital well field, Lansdale, Pennsylvania.....	46
20. Schematic diagram showing conceptual hydrogeologic model of the North Penn Water Authority Hospital well field, Lansdale, Pennsylvania.....	47
21. Graphs and schematic diagram showing geophysical logs of observation-well NP62 at the North Penn Water Authority Hospital well field, Lansdale, Pennsylvania.....	48
22. Maps showing location of U.S. Environmental Protection Agency Superfund sites in north-central Illinois.....	51
23. Diagram showing correlation of geologic units at three U.S. Environmental Protection Agency Superfund sites in north-central Illinois.....	52
24. Graphs showing gamma logs for the bedrock units of Ordovician age at	

the Byron Salvage Yard and Parson's Casket Hardware sites in north-central Illinois.....	53
25. Location of study area, boreholes, and monitoring-well clusters.....	58
26. Diagram showing lithostratigraphic correlation approximately along strike.....	59
27. Location of the Great Neck study area and observation wells GN-1 to GN-10.....	64
28. Generalized geologic section of the Great Neck peninsula.....	65
29. Geophysical logs (gamma and electromagnetic induction) of observation wells.....	66
30. Location of study area in southeastern Massachusetts and location of wells relative to Route 25, altitude of water table on August 1, 1989, and the direction of ground-water flow at site B in Wareham, Massachusetts.....	69
31. Induction logs and water-quality data collected on July 25, 1991 from well clusters B1 (upgradient from the highway) and B2 (downgradient from the highway) along the same path of ground-water flow.....	70
32. Maximum induction conductivities of the road-salt plumes from March 1988 through March 1991 at monitoring wells B2303 and B2403.....	71
33. Map showing location of study area, landfills, and monitoring wells and water-table altitude in September 1991.....	73
34. Diagram showing borehole geophysical logs, geologic section, screened interval and associated specific conductance of ground water for selected wells at Landfill B.....	74
35. Diagram showing geologic section, screened intervals, and associated specific conductance of ground water at Landfill A.....	75
36. Map showing water-table altitude and configuration, and areal distribution of specific conductance of ground water, March 1991.....	78
37. Graphs showing lithologic, natural-gamma, and induction logs for: (A) Well 93 and (B) Well 96.....	79

TABLES

1. Generalized approach to geophysical-log analysis in ground-water studies and application to sandstone/shale example.....	4
2. Summary of numerical inversion formulation in geophysical log analysis.....	5
3. Summary of high-resolution borehole-flow and related measurement techniques.....	17
4. Cementation exponents and porosities measured of sandstone core samples from selected depths.....	36
5. Estimated quantity of volatile organic compounds moving downward in borehole fluid in nine sampled boreholes.....	56

CONVERSION FACTORS, ABBREVIATIONS, AND SEA LEVEL DATUM

<u>Multiply</u>	<u>By</u>	<u>To obtain</u>
micrometer (μm)	0.00003937	inch
centimeter (cm)	0.3937	inch
millimeter (mm)	0.03937	inch
meter (m)	3.281	foot
kilometer (km)	0.6214	mile
hectometer (hm)	100	meter
centimeter per second (cm/s)	0.0328	foot per second
square centimeter (cm^2)	0.1550	square inch
square meter (m^2)	10.765	square foot
milligram (mg)	0.00003527	ounce
gram (g)	0.035	ounce
kilogram (kg)	2.205	pound
microgram per milliliter ($\mu\text{g/ml}$)	133.5×10^{-6}	ounce per gallon
microgram per liter ($\mu\text{g/L}$)	1×10^{-6}	ounce per ounce
milligram per liter (mg/L)	1	part per million
gram per liter (g/L)	0.06243	pound per cubic foot
grams per cubic centimeter (g/cm^3)		
milliliter (mL)	0.0338	ounce, fluid
liter (L)	1.0567	quart
	0.2642	gallon
cubic decimeter per second	15.85	gallons per minute

CONVERSION FACTORS--ENGLISH TO METRIC

<u>Multiply</u>	<u>By</u>	<u>To obtain</u>
quart (qt)	0.9464	liter
gallon (gal)	3.785	liter
gallon per minute (gal/min)	0.06309	liter per second
foot (ft)	0.3048	meter
inch (in)	25.4	millimeter
mile (mi)	1.609	kilometer
pound (lb)	0.4536	kilogram
pound per square inch (lb/in^2)	6.895	kilopascal

To convert degrees Fahrenheit ($^{\circ}\text{F}$) to degrees Celsius ($^{\circ}\text{C}$), use the following formula: $^{\circ}\text{C} = (^{\circ}\text{F}-32)1.8$.

To convert degrees Celsius ($^{\circ}\text{C}$) to degrees Fahrenheit ($^{\circ}\text{F}$), use the following formula: $^{\circ}\text{F} = (^{\circ}\text{C}+32)1.8$.

The following terms and abbreviations also are used in this report:

kilohertz (kHz)
 microsiemens per centimeter at 25 degrees Celsius ($\mu\text{S/cm}$)
 ohm-meter (ohm-m)
 count per second (cps)
 foot per day (ft/d)
 meter per day (m/d)
 American Petroleum Institute (API)

PREFACE

Ground-water hydrologists are faced with increasingly complex problems, such as delineation of the sources of recharge to well fields, determination of the direction and rate of contaminant transport, and assessment of aquifer-remediation efforts. In order to address these and other ground-water problems adequately, detailed information on subsurface conditions is needed. Borehole geophysical methods can be used to measure hydraulic and water-quality properties *in situ* and can be used to generate data critical to understanding aquifer systems. For this reason, conventional geophysical logging and recently developed log interpretation are expected to have an expanding role in ground-water studies conducted by the U.S. Geological Survey.

This report presents a compilation of papers presented at the Borehole Geophysics Workshop held on June 2-4, 1992, in Albany, New York. The workshop was sponsored by the Borehole Geophysics Advisory Group of the U.S. Geological Survey, Water Resources Division (WRD), as a means of acquainting various WRD scientists with the latest developments in the application of borehole geophysics to ground-water studies. The report is divided into two parts: The first part is a review of recent developments in borehole geophysical techniques where such developments are expected to have a significant effect on ground-water studies. This review includes the generalized mathematical techniques used in quantitative interpretation of geophysical logs, and the most recent equipment and analytical techniques used for electromagnetic-induction, flow and acoustic logging. The second part describes a number of field studies to illustrate how borehole geophysical-logging techniques are being applied in these studies. Each of these study descriptions illustrates the specific way in which logs can be calibrated and interpretations can be made on the basis of prevailing hydrogeologic conditions at the study site. We hope that this overview of borehole geophysical activities within WRD will lead to improved understanding of the equipment and analytical techniques available to the ground-water hydrologist, and identification of individuals having specific types of experience in geophysical logging and log analysis who may be available for consultation. We also expect that the 1992 Borehole Geophysics Workshop represents the first step in a continuing effort to coordinate geophysical-logging activities across district boundaries and, thereby, to improve effectiveness of available geophysical-logging techniques and equipment.

PART 1

RECENT DEVELOPMENTS

A GENERALIZED APPROACH TO QUANTITATIVE INTERPRETATION OF BOREHOLE
GEOPHYSICAL LOGS IN HYDROGEOLOGIC STUDIES
By F.L. Paillet¹

A number of software packages are available for the quantitative interpretation of digital borehole geophysical logs. These packages use a variety of mathematical techniques to provide estimates of hydrogeologic properties; one use of this information is to generate parameters for models of ground-water flow. However, borehole geophysical-well-log interpretation is highly dependent on site-specific assumptions included in inversion-problem formulation. Here the term "inversion-problem formulation" is given in the formal mathematical sense as described by Parker (1977). In that limited definition, inversion-problem formulation refers to the establishment of a linear or weakly nonlinear set of equations relating a given set of geophysical measurements to another set of geophysical or hydraulic variables. These equations can then be "inverted" by the formal application of well-known mathematical techniques to establish an unambiguous relation between the measured quantities and the variables of interest. It is also common for the set of site-based assumptions used in the interpretation to change over time, as the hydrogeologist improves his/her understanding of ground-water flow in the study area. The mathematical and geophysical sophistication of log-inversion software and the requirements of this software to incorporate as much site-specific information as possible may be such that all of the quantitative information contained in the log may not be used and (or) the results may be unreliable. This paper describes a generalized interpretation technique designed to guide the hydrogeologist in the analysis of borehole geophysical logs in ground-water applications and to provide specific criteria for recognizing when quantitative inversion is not possible and should not be attempted with a given data set.

The general approach begins by identifying the three specific contributions that borehole geophysical logs can make to an aquifer study: (1) Logs provide a detailed, continuous depth profile of selected lithologic properties; (2) logs measure lithologic properties *in situ* and in a volume of rock or sediment larger than that in conventional cores; and (3) logs provide multiple, statistically independent measurements that can be related to more than one lithologic property. These three attributes can be related to five interpretation steps in log analysis (table 1). The critical step in quantitative interpretation is the third step--inversion-problem formulation. The numerical inversion is performed by software that uses coupled equations in which n logs represent n independent measurements, each of which is modeled by a specific equation (table 2). The numerical test for whether quantitative interpretation is warranted for a given data set is determined by the ability of the analyst to form an overdetermined inversion problem (Doveton, 1986; Merkel and others, 1976). If such an inversion is possible, then a systematic iteration to a local minimum in the difference between a given model and the data set can be performed, and a quantitative interpretation can be made on the basis of these calculations.

Inversion-problem formulation is illustrated using a set of three typical logs (gamma, neutron, and density logs) for a sandstone aquifer (fig. 1). The objective is to estimate aquifer transmissivity from these logs. The

¹U.S. Geological Survey, MS 403, Box 25046, Denver, CO 80225

formulation of an overdetermined inversion is found to be possible (table 2) and yields consistent results (fig. 2). This analysis gives a quantitative description of the vertical distribution of porosity within the aquifer (Paillet, 1991), and indicates that the site-specific assumptions used to formulate the inversion are either consistent over the aquifer, because porosities derived by two different sets of equations give the same answer, or discrepancies can be disregarded, as in the depth interval from 1,045 to 1,055 ft, where negative porosity values are associated with a dense, low-permeability dolomite.

The generalized interpretation method can be illustrated by application to the sandstone-aquifer analysis; the results are summarized in table 1. The first interpretation step involves correlating beds in the logs and adjusting depth scales so that similar beds are given at the same depths on each log. In figure 1, three prominent beds (A, B, and C) can be identified on the logs, and are correlated across the figure. In the second step, neutron and density log calibrations are corrected for measured hole diameter, and the caliper log (not shown) is scanned for washouts. In the third step, various inversions are formulated and tested (table 2). One final model is selected as the best fit between model and data; the distribution of porosity given by this model is computed in the fourth interpretation step. The fifth and final step involves relating this porosity profile to transmissivity. This analysis requires integration of the well-log data with other, larger-scale hydraulic data, such as aquifer tests and tracer experiments. In this example, the interval-averaged porosity and clay-mineral fraction are correlated with aquifer-test data to develop a large-scale calibration relating quantitative log interpretations to aquifer properties.

REFERENCES

Doveton, John H., 1986, Log analysis of subsurface geology--concepts and computer methods: New York, Wiley-Interscience, 273 p.

Merkel, R.H., MacCary, L.M., and Chicko, R.S., 1976, Computer techniques applied to formation evaluation: *The Log Analyst*, v. 17, no. 3, p. 3-10.

Paillet, F.L., 1991, Graphical overlap applications in geotechnical log analysis, in *Proceedings of the 4th International MGLS/KEGS Symposium on Borehole Geophysics for Minerals, Geotechnical and Groundwater Applications*, August, 1991, Toronto, Canada, p. 294-264.

Parker, R.L., 1977, Understanding inverse theory: *Annual Reviews in Earth and Planetary Sciences*, v. 5, p. 35-64.

Table 1. Generalized approach to geophysical log analysis in ground-water studies and application to sandstone/shale example

Interpretation step	Contribution from logs	Sandstone/shale example
1. Depth alignment and correlation with samples.	Detailed depth profile.	Compare logs for beds (A, B, C, and so forth in fig. 1).
2. Remove effect of borehole on measurement.	In-situ measurements.	Check for diameter calibration and possible washouts.
3. Inversion formulation and testing.	Multiple independent measurements.	Trial solution of $n=3$ logs for $m=2$ unknowns (porosity and clay-mineral fraction).
4. Select solution with best inversion, if possible.		Conclude an under-determined solution is possible; recompute porosity as the average of values from neutron and density using optimized inversion.
5. Second or large-scale interpretation--integrate into complete data set.	Integrate log data into interpretation.	Calibrate porosity distribution using T and S from aquifer tests.

Table 2. Summary of numerical inversion formulation in geophysical log analysis

1. GEOPHYSICAL MEASUREMENTS AS COUPLED EQUATIONS

$$Y_1 = a_{10} + a_{11}X_1 + a_{12}X_2 + \dots + a_{1m}X_m \quad Y_i(z_j) = \text{Geophysical measurements}$$

i indexes tool

$$Y_2 = a_{20} + a_{21}X_1 + a_{22}X_2 + \dots + a_{2m}X_m \quad j \text{ indexes depth point}$$

$$Y_n = a_{n0} + a_{n1}X_1 + a_{n2}X_2 + \dots + a_{nm}X_m \quad X_k(z_j) = \text{Geological variable in}$$

interpretation model, such as

or, written in complete matrix form: $\quad \text{porosity or clay-mineral fraction}$

$m \quad k \text{ indexes variable}$

$$Y_i(z_j) = a_{i0} + \sum_{k=1}^m a_{ik}X_k(z_j)$$

2. CLASSES OF INVERSIONS:

If $n < m$, equations are underdetermined: There are too many possible unknowns; these may be combined in many different ways to give a solution to the equations.

If $n = m$, equations are fully determined: There is one solution, and it is solved by direct solution of the matrix equations above; however, there is no way to know if the "best" values of the calibration constants a_{ik} have been used.

If $n > m$, equations are overdetermined: There are not enough unknowns X_k to match the data set for any given set of a_{ik} ; we can vary the values of a_{ik} to minimize the mismatch between model and solution.

Table 2. Summary of numerical inversion formulation in geophysical log analysis
continued

3. SANDSTONE/SHALE INVERSION EXAMPLE:

Formulate overdetermined solution with $n = 3$ and $m = 2$;

X_1 = Effective porosity (volume fraction-dimensionless)

X_2 = Clay-mineral fraction (volume fraction-dimensionless)

LOG	INTERPRETATION EQUATION	KNOWN a_{ik}	UNKNOWN a_{ik}
Gamma	$Y_1 = G_{ss}(1-X_1-X_2) + G_{cl}X_2$	$a_{11}=0$	$a_{10}=G_{ss}$ $a_{12}=(G_{cl}-G_{ss})$

Neutron	$Y_2 = X_1 + P_{cl}X_2$	$a_{21}=1$	$a_{22}=P_{cl}$
		$a_{20}=0$	

Density	$Y_3 = X_1 + D_{cl}X_2 + 2.65(1-X_1-X_2)$,	$a_{30}=2.65$	$a_{32}=(2.65-D_{cl})$
		$a_{31}=1.65$	

where the undetermined calibration parameters are given by--

G_{ss} = gamma activity of clay-free sandstone; estimate from "clean" interval;

G_{cl} = gamma activity of clays in shale; estimate from shale interval;

P_{cl} = noneffective porosity of shale (use initial guess of 0.30, final value of 0.20 optimizes model); and

D_{cl} = density of shale (initial guess of 2.50 g/cm³; final value of 2.60 optimizes model).

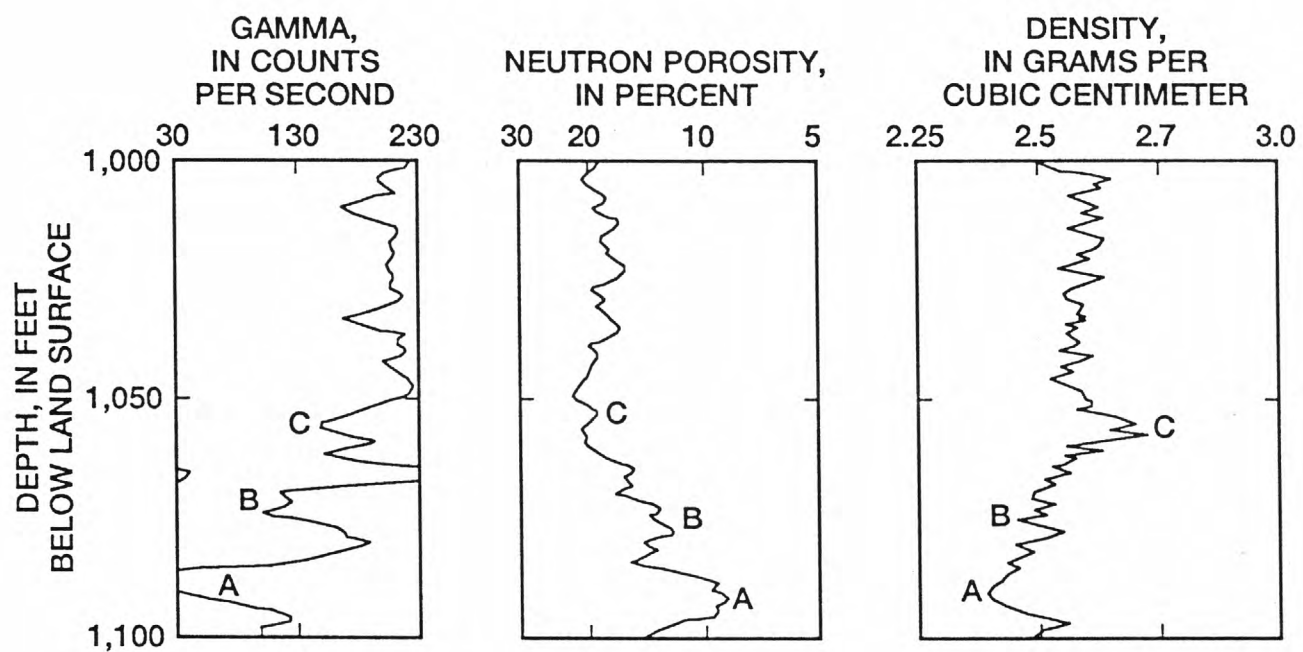


Figure 1. Gamma, neutron, and density logs for a sandstone aquifer in central Texas; A, B, and C denote sandstone or carbonate beds discussed in text.

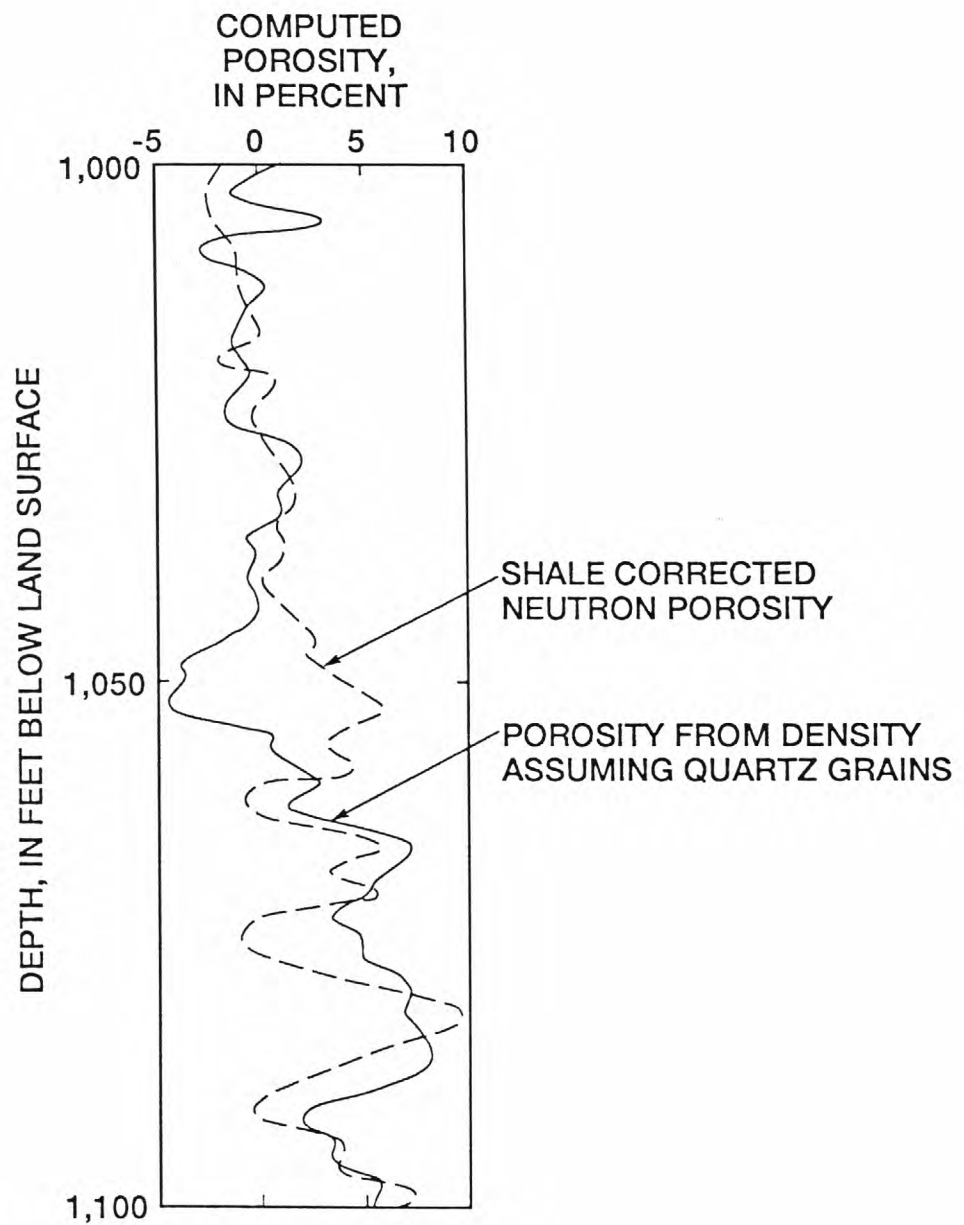


Figure 2. Profiles of effective porosity computed by use of a gamma log to correct neutron and density logs for clay-mineral effects.

APPLICATION OF ELECTROMAGNETIC-INDUCTION LOGGING TO
GROUND-WATER-QUALITY STUDIES
By John H. Williams¹

Electromagnetic-induction logging has been used in the petroleum industry since the 1950's (Doll, 1949). Induction probes specifically designed for ground-water applications in small-diameter borehole (slim-hole) monitoring wells were not commercially available until the mid-1980's. Since the late 1980's, induction logging has become an integral part of a wide range of ground-water-quality studies conducted by the U.S. Geological Survey in New England and New York.

Induction logs measure the conductivity of the medium surrounding a borehole; conductivity can be recorded through PVC casing and in water-, air-, and mud-filled holes. Slim-hole induction probes consist of transmitter and receiver coils that operate at a frequency of about 40 kHz and are spaced about 0.5 m apart, and one or more focusing coils that minimize the effects of the borehole fluid and maximize the vertical resolution.

The measured response in relation to radial distance from the borehole axis of two slim-hole induction probes, the Geonics EM39 and Century 9510, indicates that the instruments are insensitive to the medium within 7.5 and 5 cm, respectively, of the borehole axis (fig. 3A). Therefore, the effect of the conductivity of the borehole fluid is essentially negligible in wells with a diameter less than about 15 cm for the Geonics EM39 probe and less than about 10 cm for the Century 9510 probe. Physical experiments and numerical models show that approximately one-half of the measured response of two induction probes is determined by formation properties at a radial distance greater than 0.5 m.

The measured response in relation to vertical distance from the center of the induction probes is somewhat asymmetrical and is averaged over a vertical interval above and below the probe center (fig. 3B). The maximum value for the Geonics EM39 probe is offset 23 cm, and that for the Century 9510 probe is offset 10 cm. The vertical separation between one-half of the maximum response for the Geonics EM39 probe is 65 cm, and that for the Century 9510 probe is 48 cm. The measured response of the probes to an abrupt contact between conductive and resistive zones is smoothed over an interval of about 1 m; the measured response of conductive zones less than about 0.5 m thick is less than one-half of their true conductivity (Taylor and others, 1989).

The major geohydrologic factors that affect induction logs in sand-and-gravel aquifers are the dissolved-solids concentration in the ground water and the silt and clay content of the aquifer. Lithologic information from drilling samples and (or) other geophysical logs is needed to determine whether the increased conductivity of a given zone is related to the dissolved-solids concentration or to the silt and clay content. Induction and lithologic logs, specific conductance of ground-water samples, and geoelectric section at a pair of monitoring wells near the Albany landfill in east-central New York are presented in figure 4. The leachate plume from the landfill contains increased dissolved-solids concentrations and is clearly delineated by the induction logs. The geoelectric section determined from the EM logs by use of a computer program developed by McNeill

¹U.S. Geological Survey, P.O. Box 1669, Albany, NY 12201

and others (1990) suggests the presence of an abrupt contact between contaminated and uncontaminated water at 11.5 m below land surface.

Induction logging is an efficient method for high-resolution, vertical mapping of the dissolved-solids concentration in ground water that would not be practical by use of monitoring wells alone. As suggested by the previous example (fig. 4), dissolved-solids concentrations in sand-and-gravel aquifers can vary by more than an order of magnitude within a vertical distance of less than 1 m. At a single location, the water quality sampled from monitoring wells can vary widely, depending on the placement of screened intervals and, thus, is not necessarily representative of the actual conditions (Benson and others, 1988). Induction logs provide a nearly continuous vertical profile of water quality from which the optimum depth for monitoring-well screens can be determined and repeated induction logging can be used to monitor ground-water quality over time.

Applications of induction logging to ground-water-quality studies conducted by the USGS presented in this proceedings include the following:

1. delineation of the saltwater-freshwater interface in northwestern Long Island,
2. monitoring of road-salt contamination in southeastern Massachusetts,
3. mapping of leachate plumes from two municipal landfills in west-central Vermont, and
4. definition of the development of the contaminant plume from a sewage-disposal facility on Cape Cod.

REFERENCES

Benson, R.C., Turner, M., Turner, P., and Vogelsong, W., 1988, In situ, time-series measurements for long-term ground-water monitoring, in Collins, A.G., and Johnson, A.I., eds., *Ground-Water Contamination Field Methods*: Philadelphia, Pennsylvania, ASTM STP 963, p. 58-72.

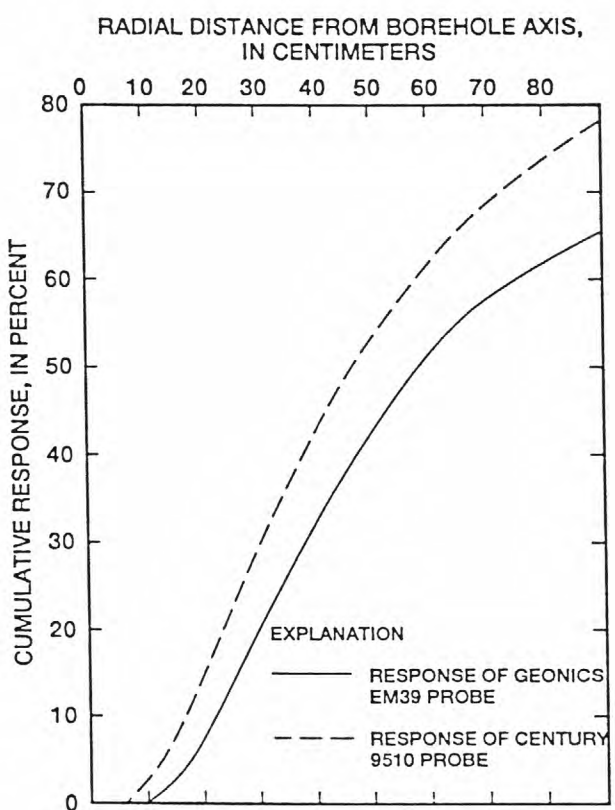
Doll, H.G., 1949, Introduction to induction logging and application of logging to wells drilled with oil-base mud: *Journal of Petroleum Technology*, TP2641, Petroleum Transactions Association, Institute of Mining, Metallurgical and Petroleum Engineering, p. 148-162.

McNeill, J.D., 1986, Geonics EM39 borehole conductivity meter-theory of operation: Mississauga, Ontario, Geonics Limited Technical Note 20, 11 p.

McNeill, J.D., Bosnar, M., and Snelgrove, F.B., 1990, Resolution of an electromagnetic borehole conductivity logger for geotechnical and ground water applications: Mississauga, Ontario, Geonics Limited Technical Note 25, 28 p.

Taylor, K.C., Hess, J.W., and Mazzella, A., 1989, Field evaluation of a slim-hole induction tool: *Ground Water Monitoring Review*, v. 9, no. 1, p. 100-104.

A



B

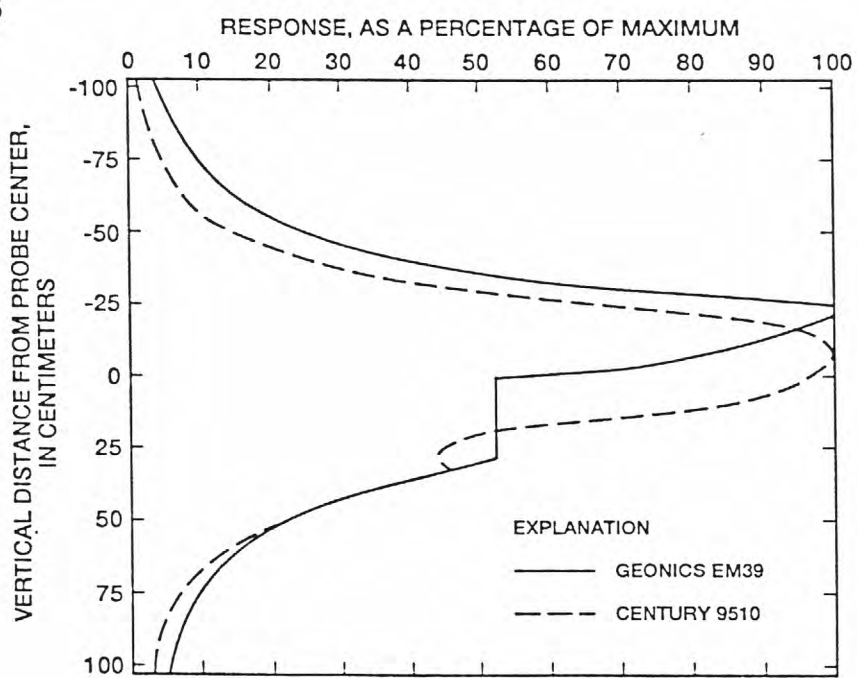


Figure 3. Measured response of two slimhole electromagnetic-induction probes:
A. radial distance, B. vertical distance. [Graphs based on data from McNeill (1986) and Century Geophysical Corporation (written commun., 1992).]

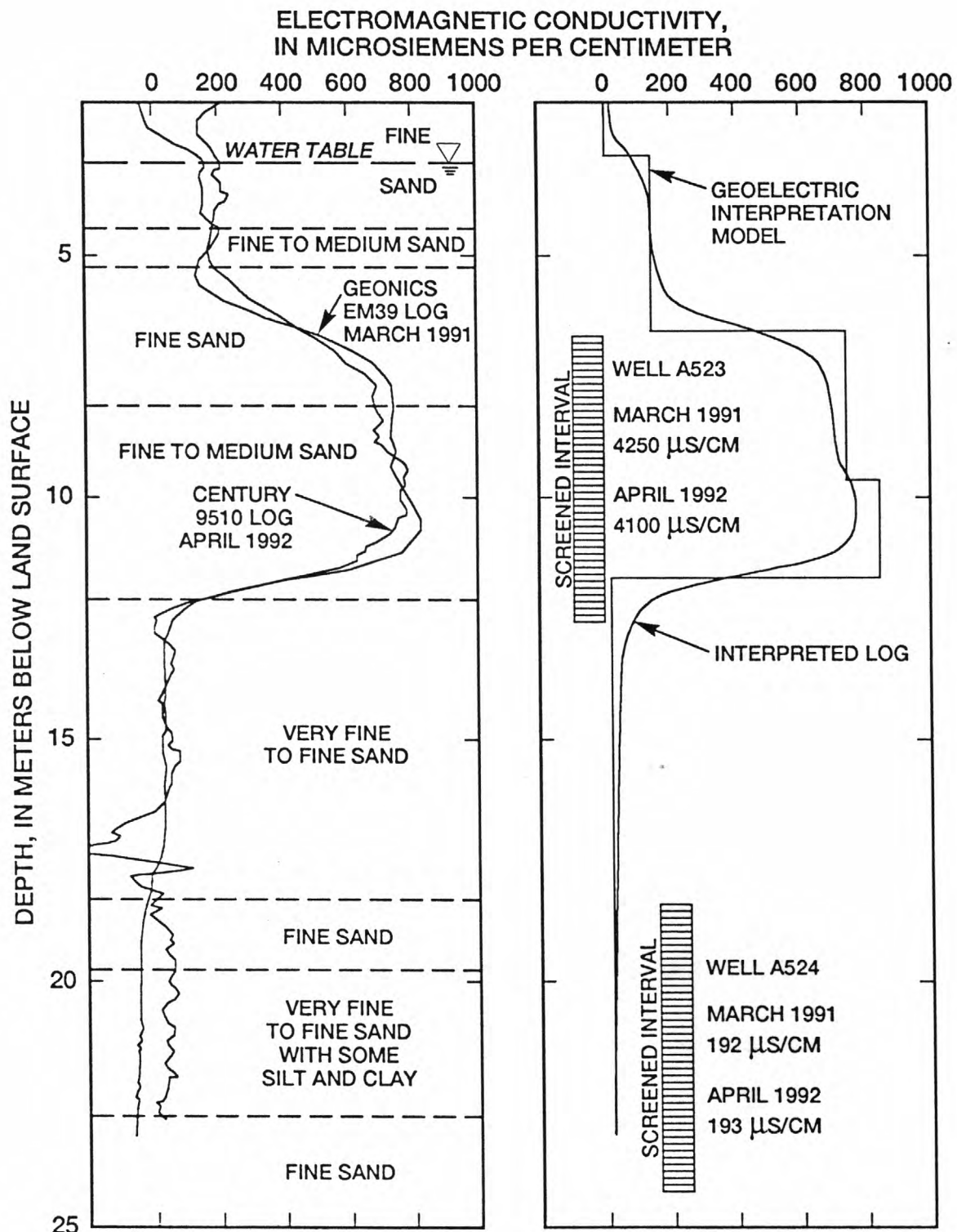


Figure 4. Electromagnetic-induction and lithologic logs, specific conductance of ground-water samples, and geoelectric section for a monitoring-well pair near the Albany landfill in east-central New York.

FLOWMETER LOGGING -- A REVIEW
F.L. Paillet¹ and A.E. Hess¹

Almost all geophysical measurements made in boreholes measure quantities that are at best indirectly related to the hydraulic properties of aquifers. One notable exception is the measurement of borehole flow either along the borehole axis or across the borehole at a given depth. These measurements are directly related to the flow of water in the adjacent aquifer or to naturally occurring hydraulic-head differences that can drive flow along an open borehole intersecting two or more hydraulically conductive intervals, and can be used to interpret the hydraulic properties of aquifers *in situ*. However, no one method for flow logging is effective under all conditions and flow regimes. A variety of flow-measurement techniques are available for use in many different applications and under various borehole conditions.

Several conventional well logs, such as borehole-fluid-resistivity, temperature, and formation-resistivity logs, can be used as indicators of flow under some conditions. These geophysical measurements are generally referred to as "passive" in that flow measurements are made by inferring the presence of flow rather than actively measuring flow. These passive measurements involve situations where the logs can be used to interpret the flow of waters containing different solutes and solute concentrations, or having different temperatures along the well bore. In other situations, appropriate solutes or radioactive or nonradioactive tracers can be injected in the borehole at specified locations ("active" methods), and successive logs made to characterize the dispersal of these tracers in the borehole (Patten and Bennett, 1962). Injection of hot or cold water can be especially effective in defining flow regimes, because the injected water heats or cools the formation at depths where water is leaving the borehole, so that flow regimes can be identified even after the injection has ceased (Keys and Brown, 1978).

The most frequently cited "active" borehole flow-measurement technique is based on use of a sensitive impeller that is installed in a borehole probe in such a way that the rotation rate of the impeller system can be calibrated in terms of axial borehole flow. Such devices are of limited use, because a minimum flow of about 2 ft/min is required to turn the most sensitive impeller (Keys, 1990). Somewhat smaller changes in flow can be detected by comparing the impeller rotation rates measured while moving the flowmeter up or downhole at a constant speed. The calibrations of more sensitive impellers tend to vary during the course of measurement as bearings wear and debris accumulates in the wire mesh or other structure protecting the impeller. In spite of these limitations, impeller flowmeters have been used effectively to document inflow and outflow in large-capacity boreholes (Keys and Sullivan, 1979; Schimschal, 1981).

Because of the limitations on flow measurement by conventional impeller flowmeters, a number of experimental, high-resolution flowmeters have been developed or proposed that are based on thermal-pulse, electromagnetic, borehole-fluid-conductivity, laser-doppler, and acoustic-doppler methods and measure either flow along the borehole axis or flow across the borehole (table 3). The U.S. Geological Survey thermal-pulse flowmeter (TPFM) is presented as an example of these experimental high-resolution flowmeters

¹U.S. Geological Survey, MS 403, Box 25046, Denver, CO 80225

(Hess, 1986). The TPFM measures the time required for a parcel of water, heated by a pulse of electric current in a grid placed across the borehole flow, to travel about 0.8 in. up or down the borehole (fig. 5). A downhole-inflated packer can be used to block the annulus around the flow-measurement section to increase flow sensitivity and allow the TPFM response to be calibrated independent of borehole diameter (Hess and Paillet, 1991). The TPFM is designed to indicate whether flow is up or down and can detect flows as small as 0.01 gal/min. This flow rate corresponds to an average velocity of about 0.02 ft/min in a 6-in.-diameter borehole. TPFM calibration relates the inverse of pulse transit time to average flow or discharge and has a slight upflow bias, because of the buoyancy of the pulse of heated water (fig. 6).

The TPFM can be used to identify flow in boreholes induced by naturally occurring differences in hydraulic head between fractures or aquifers (fig. 7), to define the vertical distribution of flow induced in a borehole below a pump (fig. 7), or to indicate the pattern of flow induced in an observation borehole adjacent to a pumped borehole (fig. 8). One of the most difficult problems associated with the interpretation of TPFM measurements is distinguishing differences in measured flows at different measurement depths associated with inflow or outflow at depths between those measurement depths from the effects of transient variations in the flow field (Paillet and others, 1992). In some studies, the transient effects are removed by normalizing the measurements, using water-level measurements to correct for the effects of an enlarging cone of depression during an aquifer test (Paillet, 1991). In other situations, TPFM measurements are labeled to distinguish those made shortly after the start of the experiment ("early" measurements) from those made much later in the experiment ("late" measurements) (fig. 8). However, the transient evolution of such flow fields can, in principle, be defined by means of TPFM measurements, and such analyses have the potential to characterize the transmissivity and storage coefficient of individual zones within unconsolidated-rock aquifers and individual fractures within bedrock aquifers (Paillet and others, 1992).

Although much of the literature on use of flowmeters in hydrogeologic studies has focused on the measurement of vertical flow along the well bore, there has been some effort to measure horizontal flow across the well bore and vertical flow behind casing. Two factors affect measurement of horizontal flow in addition to the factors associated with measuring the flow itself: (1) the effects of the borehole on the local seepage flow field, and (2) the effects of aquifer heterogeneity on the statistical significance of individual measurements. The borehole acts to distort the ground-water-flow field, and it is not certain that the local horizontal-flow vector is representative of the larger scale average of horizontal flow.

Vertical flow behind casing has been measured by experimental logging equipment by means of acoustic-doppler and acoustic scattering techniques. The acoustic doppler is analogous to optical laser-doppler measurements, except that the acoustic measurements can be made through casing (Rambow, 1991). One unusual technique is labeled as "active listening." In this measurement, the acoustic energy scattered from behind casing is compared over short time delays (Rambow, 1991). Changes in the pattern of scattered acoustic energy can be used to identify movement of the particles causing the scattering. This technique does not require the sophisticated electronic equipment used in other techniques to define flow behind casing, and it

appears to have some potential for application in ground-water studies.

REFERENCES

Hess, A.E., 1986, Identifying hydraulically conductive fractures with a slow-velocity borehole flowmeter: *Canadian Geotechnical Journal*, v. 23, no. 1, p. 69-78.

Hess, A.E., and Paillet, F.L., 1991, Measurement of vertical flow in borehole UE-3e 4 using geophysical logs, Nevada Test Site, Nye County, Nevada: *U.S. Geological Survey Water-Resources Investigations Report 90-4185*, 17 p.

Kerfoot, W.B., 1988, Monitoring well construction, and recommended procedures for direct ground-water flow measurements using heat-pulsing flowmeter, *in* *Ground Water Contamination--field methods*, A.G. Collins and A.I. Johnson, eds.: *American Society for Testing Materials 963*, p. 146-161.

Keys, W.S., 1990, Borehole geophysics applied to ground-water investigations: *U.S. Geological Survey Techniques of Water-Resources Investigations*, book 2, chap. E2, 150 p.

Keys, W.S. and Brown, R.F., 1978, The temperature logs to trace the movement of injected water: *Ground Water*, v. 16, no. 1, p. 32-48.

Keys, W.S. and Sullivan, J.K., 1979, Role of borehole geophysics in defining the physical characteristics of the Raft River geothermal reservoir, Idaho: *Geophysics*, v. 44, no. 6, p. 1116-1141.

Molz, F.J. and Young, S.C., 1993, Development and application of borehole flowmeters for environmental assessment: *The Log Analyst*, v. 34, no. 1, p. 13-23.

Momii, K., Jinno, K., and Hirano, F., 1993, Laboratory studies on a new LDV system for horizontal groundwater velocity measurements in a borehole: *Water Resources Research*, v. 29, no. 2, p. 283-291.

Paillet, F.L., 1991, The 1st core hole at Mirror Lake, New Hampshire--comparing geophysical logs to core and cross-hole flow logging: *U.S. Geological Survey Toxic Substance Hydrology Conference, Monterey, California, Proceedings*, 1991, *Water-Resources Investigations Report 91-4034*, p. 162-171.

Paillet, F.L., Novakowski, Kent, and Lapcevic, Pat, 1992, Analysis of transient flows in boreholes during pumping in fractured formations, *in* *Society of Professional Well Log Analysts Annual Logging Symposium, 33rd, 1992, Transactions, Oklahoma City, Oklahoma: Society of Professional Well Log Analysts, Houston, Texas*, p. S1-S22.

Patten, E.P., Jr. and Bennett, G.D., 1962, Methods of flow measurement in well bores: *U.S. Geological Survey Water-Supply Paper 1544-C*, 28 p.

Rambow, F.H.K., 1991, Active listening--an alternative method for detecting flow and measuring flow velocity behind casing: *The Log Analyst*, v. 32, no. 6, p. 645-653.

Schimschal, Ulrich, 1981, Flowmeter analysis at Raft River, Idaho: *Ground Water*, v. 19, no. 1, p. 93-97.

Tsang, C-F., Hufschmied, Peter, and Hale, F.V., 1990, Determination of fracture inflow parameters and with a borehole fluid conductivity logging method: *Water Resources Research*, v. 26, no. 4, p. 561-578.

Young, S.C. and Waldrop, W.R., 1989, An electromagnetic borehole flowmeter for measuring hydraulic conductivity, *in* Molz, F.J., Guven, O., and Melville, J.G. eds., *Proceedings of the Conference on New Field*

Techniques for Quantifying the Physical and Chemical Properties of
Heterogeneous Aquifers: Auburn, Alabama, Water Resources Research
Institute.

Table 3. Summary of high-resolution borehole-flow and related measurement techniques

Technique	Physical principle	Application	Reference
Conventional well logs			
Temperature	Passive tracer	Vertical flow	Keys (1990) Keys and Brown (1978)
Fluid resistivity or conductivity probe	Passive tracer	Vertical flow	Paillet (1991) Keys (1990)
Impeller flowmeter	Flow turns impeller	Vertical flow	Keys (1990) Keys and Sullivan (1979) Schimschal (1981)
Brine injection	Tag/trace with ions	Vertical flow	Patten and Bennett (1962)
Thermal-pulse flowmeter flow	Tag/trace with heat pulse	Vertical or horizontal	Hess (1986) Hess and Paillet (1990) Kerfoot (1988)
Hydrophysical logging	Replace fluid and monitor conductivity	Vertical flow	Tsang and others (1990)
Electromagnetic flowmeter	Currents induced by flow through generator	Vertical flow	Young and Waldrop (1989) Molz and Young (1993)
Laser doppler flowmeter	Doppler shift of reflected laser	Vertical or horizontal	Momii and others (1993)
Acoustic doppler flowmeter	Doppler shift of acoustic beam	Vertical flow behind casing	Rambow (1991)
Active listening	Movement of scattering pattern	Vertical flow behind casing	Rambow (1991)

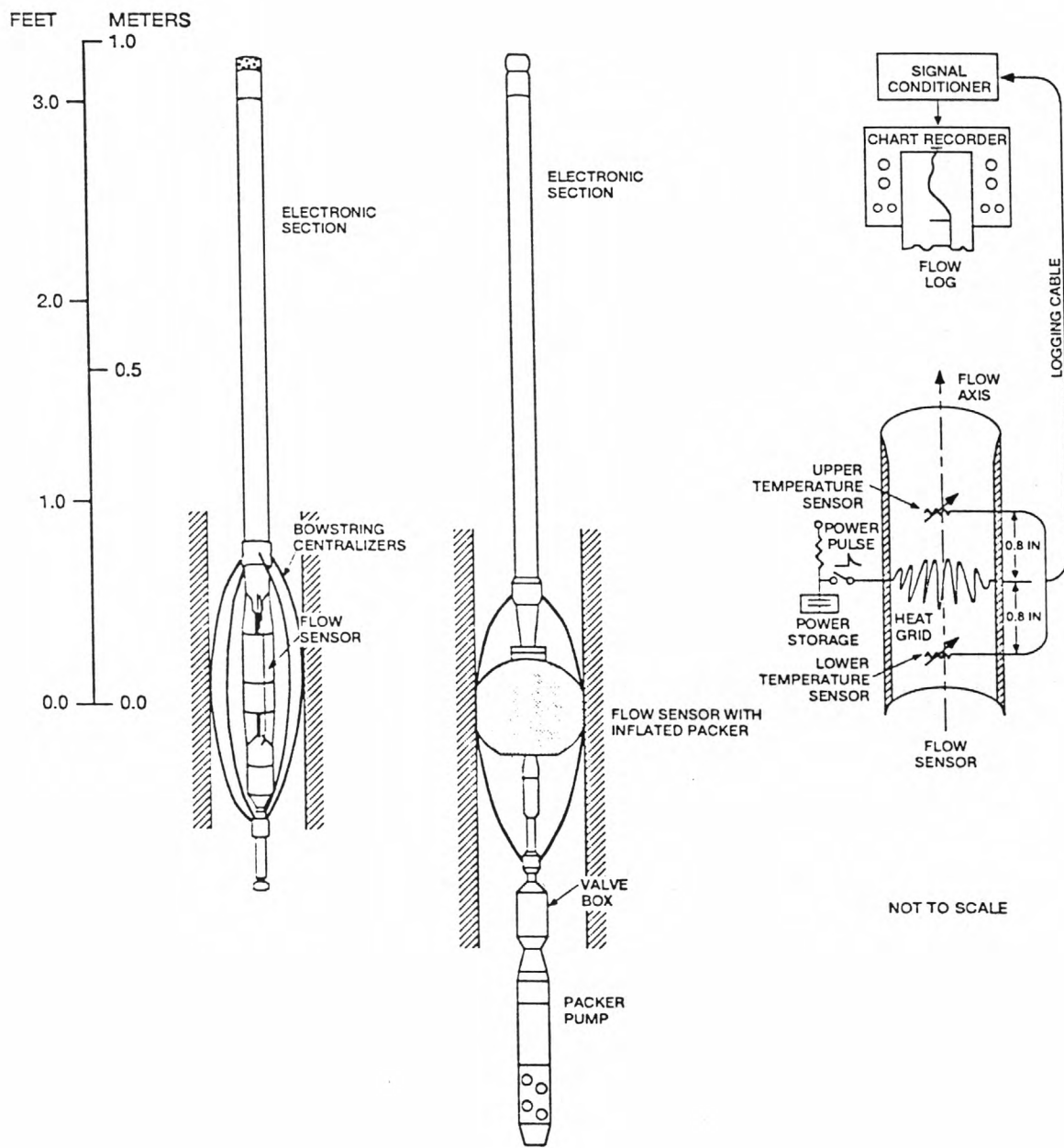


Figure 5. U.S. Geological Survey thermal-pulse flowmeter.

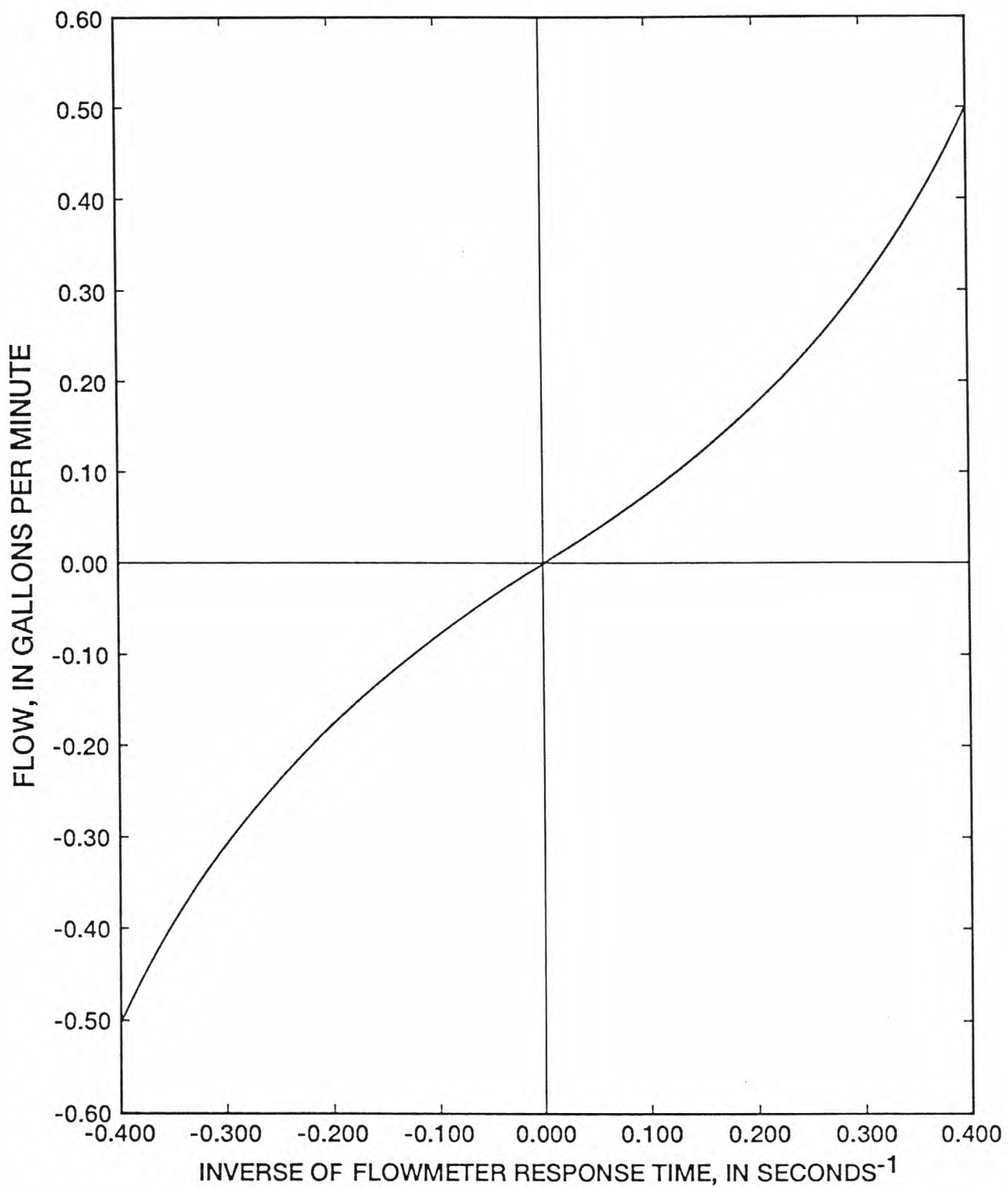


Figure 6. Calibration curves for U.S. Geological Survey thermal-pulse flowmeter.

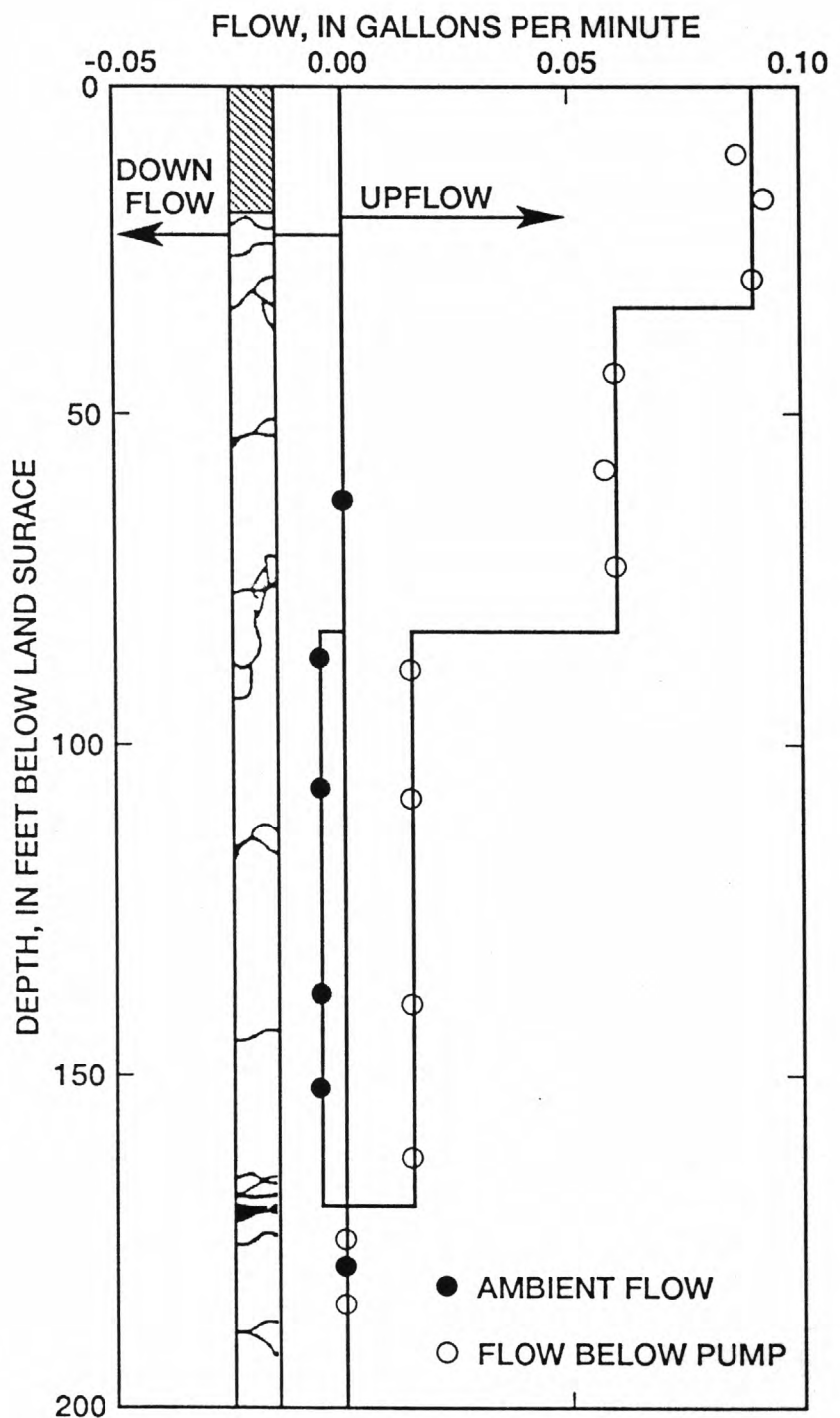


Figure 7. Example of thermal-pulse flowmeter data collected from a borehole in fractured dolomite that illustrates the distribution of vertical flow under ambient conditions during pumping at a rate of about 2.0 gallons per minute.

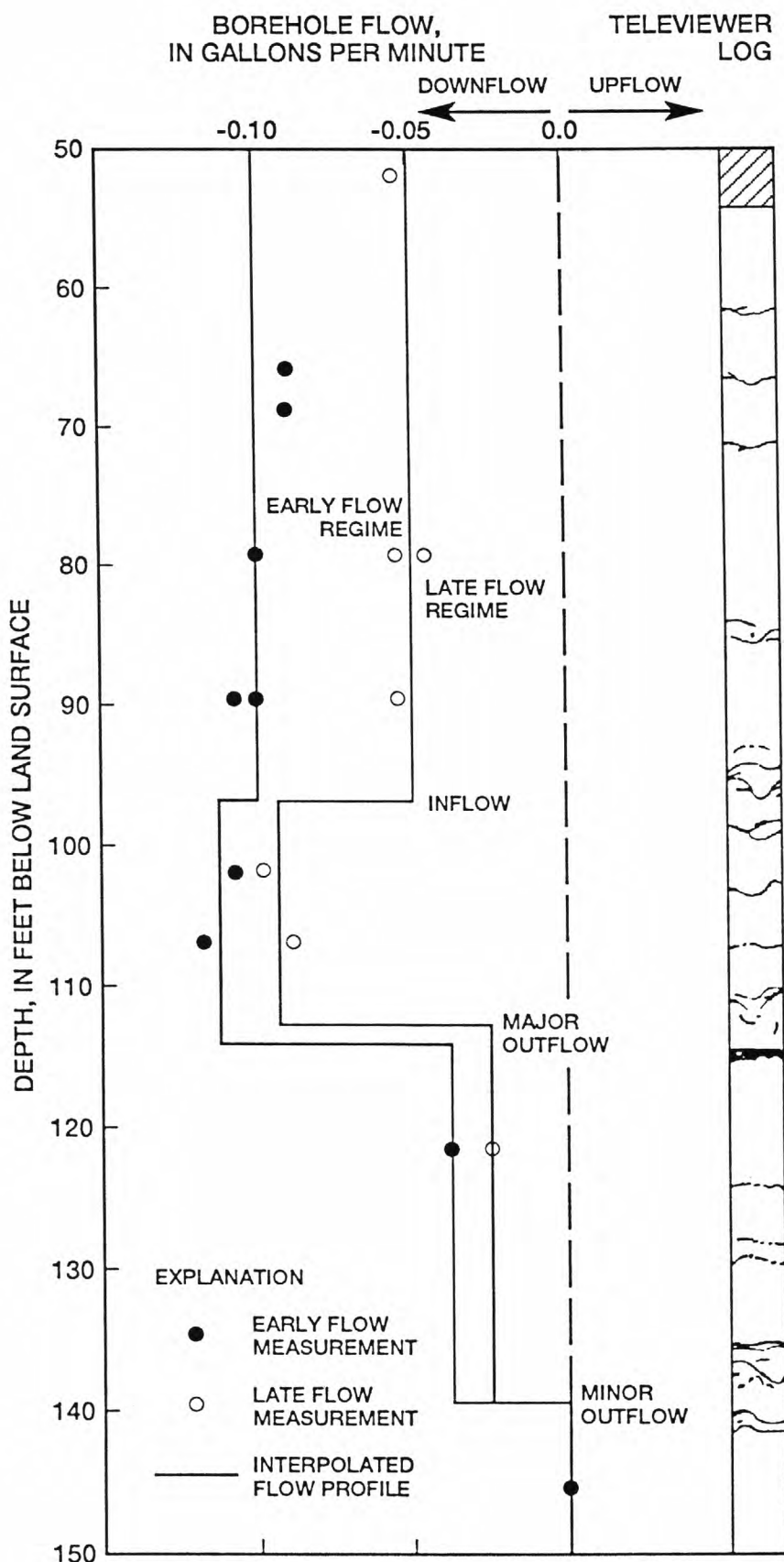


Figure 8. Example of the distribution of vertical flow induced in an observation borehole when an adjacent borehole is about 50 feet away and is being pumped at a rate of about 3 gallons per minute.

ACOUSTIC LOGGING -- A REVIEW
F.L. Paillet¹

Conventional acoustic-logging systems are designed to measure the "acoustic" or compressional velocity of rocks adjacent to the borehole (Guyod and Shane, 1969; Paillet and Cheng, 1991). In principle, this velocity is a scalar property averaged over a sample volume related to the acoustic wavelength (10-50 cm at typical logging frequencies of 10-30 kHz).

Acoustic-logging tools operate by measuring the transit time for propagation of critically refracted acoustic waves between a source and two receivers. The velocity computation is based on the difference between arrivals at the two receivers to remove the effects of "fluid delay" associated with the part of the wave-propagation path in the borehole (fig. 9A). "Compensated" acoustic logging tools use pairs of sources and receivers to average the propagation times up and down the well bore; this averaging suppresses the effects of abrupt borehole-diameter changes in the transit-time measurements (fig. 9B). In either situation, the logging tool is run in the center of the borehole and the signals are averaged around the circumference of the cylindrical receiver. Up-hole processing computes and plots the inverse of acoustic velocity--interval transit time--in units of microseconds per meter or foot.

Acoustic logs are sometimes used to sample such properties as Young's modulus and shear strength of rocks for geotechnical studies or for the calibration and interpretation of surface-seismic studies. More often, acoustic logs are used to measure porosity, under the assumption that measured transit time is volume-weighted average of wave propagation in fluid-filled pores and mineral grains (fig. 10). Two significant problems are associated with this kind of porosity logging. First, the acoustic velocity of the mineral framework of sedimentary rocks depends on the depth of burial, so that the acoustic velocity for a given rock sample varies directly with confining pressure. This effect becomes unimportant at pressures equivalent to a depth of a few thousand feet, beyond which velocities become only weakly dependent on pressure, and variations in interval transit time can be unambiguously related to porosity. Unfortunately, most aquifers are shallow, and effects of confining pressure greatly complicate the quantitative interpretation of acoustic logs in many ground-water applications. In addition, acoustic velocities in clays and shale are relatively low so that increases in transit time caused by the presence of clays can be much greater than those caused by local increases in porosity.

Acoustic logging recently has been expanded to include full-waveform logging by digitizing the pressure signals received at the two acoustic receivers (fig. 11). This method was first developed as a means of performing small-scale seismic-refraction studies in the borehole (Christensen, 1964). In spite of the obvious analogy between surface and borehole seismic-refraction surveys, mathematical analysis shows that the borehole-waveform experiment is fundamentally different from a surface-refraction survey (Paillet and Cheng, 1986). Waveforms recorded several wavelengths away from the acoustic source along the borehole axis (from 0.5 to 2.0 m for typical logging frequencies from 5-30 kHz) are

¹U.S. Geological Survey, MS Box 403, Box 25046, Denver, CO 80225

dominated by resonances that travel along the borehole. These guided waves can be very effective in characterizing the properties of fractures that intersect the borehole wall. When fractures are transverse to the borehole axis and are located between acoustic source and receiver (fig. 11A), all pulses of wave energy traveling along the borehole are scattered and attenuated. The mean energy (mean-square wave amplitude) in any time interval correlates with the hydraulic aperture of the fracture or fracture zone. When fractures intersect the borehole at an oblique angle, there is always one side of the borehole where waves can propagate through unfractured rocks (fig. 11B). In this situation, the effects of the fracture on wave propagation along the borehole are much more complicated. However, one particular pulse in the waveform appears to respond only to borehole-wall permeability--the tube-wave mode or Stoneley wave (Paillet, 1983, 1991). A number of recent studies indicate that various techniques can be used to interpret tube-wave properties and to relate measured tube-wave attenuation to fracture permeability (Schmitt and others, 1988a; Tang and others, 1991; Hornby and others, 1989, 1992).

Until 1985, almost all acoustic-logging systems used axisymmetric sources centralized in the borehole. White (1967) and Kitsunezaki (1980) proposed that shear-wave properties (velocity and attenuation) could be characterized with greatly improved accuracy using nonaxisymmetric sources. These sources are usually called dipole or quadrupole sources as opposed to axisymmetric or monopole sources. Although some authors refer to the data given by these logging tools as shear-wave logs, the waveforms generated by dipole sources are also dominated by resonances in the fluid column. Wave-propagation studies show that dipole and quadrupole logging generates waveforms that can be used effectively to interpret shear velocities in situ and especially in soft or poorly consolidated sediments. Another important result is that nonaxisymmetric tube waves generated by dipole sources give permeability responses that are only weakly affected by mudcake and drilling damage to the borehole wall. This is explained by noting that axisymmetric tube waves produce an oscillatory transfer of fluid across the borehole wall, so that these waves are sensitive to alteration of rocks immediately adjacent to the borehole wall (the so-called "skin" effect). Nonaxisymmetric waves produce oscillatory motion in pore spaces in the formation but do not produce a net displacement across the borehole wall and are, therefore, not very sensitive to drilling-induced skin effects.

REFERENCES

Christensen, M.D., 1964, A theoretical analysis of wave propagation in fluid filled drill holes for the interpretation of 3-dimensional velocity logs, in Society of Professional Well Log Analysts Annual Logging Symposium, Midland, Texas, 5th, 1964, Transactions: Society of Professional Well Log Analysts, Houston, Texas, p. K1-K30.

Guyod, Hubert, and Shane, L.E., 1969, Geophysical well logging--introduction to geophysical well logging; acoustic logging: Houston, Texas, Hubert Guyod (pub.), v. 1, 256 p.

Hornby, B.E., Johnson, D.L., Winkler, K.W., and Plumb, R.A., 1989, Fracture evaluation using reflected Stoneley-wave arrivals: Geophysics, v. 54, p. 1274-1288.

Hornby, B.E., Luthi, S.M., and R.A. Plumb, 1992, Comparison of fracture

apertures computed from electrical borehole scans and reflected Stoneley waves--An integrated interpretation: *The Log Analyst*, v. 33, no. 1, p. 50-66.

Kitsunezaki, Choro, 1980, A new method for shear-wave logging: *Geophysics*, v. 45, no. 10, p. 1489-1506.

Paillet, F.L., 1983, Acoustic characterization of fracture permeability at Chalk River, Ontario: *Canadian Geotechnical Journal*, v. 20, no. 3, p. 468-476.

_____, 1991, Qualitative and quantitative interpretation of fracture permeability using acoustic full-waveform logs: *The Log Analyst*, v. 32, no. 3, p. 256-270.

Paillet, F.L., and Cheng, C.H., 1986, A numerical investigation of head waves and leaky modes in fluid-filled boreholes: *Geophysics*, v. 51, no. 7, p. 1438-1449.

_____, 1991, Acoustic waves in boreholes--the theory and application of acoustic full-waveform logs: Boca Raton, Florida, CRC Press, 264 p.

Schmitt, D.P., Bouchon, Michel, and Bonnet, Guy, 1988a, Full-wave synthetic acoustic logs in radially semi-infinite saturated porous media: *Geophysics*, v. 53, no. 6, p. 807-823.

Schmitt, D.P., Zhu, Y., and Cheng, C.H., 1988b, Shear wave logging in semi-infinite saturated porous formations: *Journal of Acoustical Society of America*, v. 84, p. 2230-2244.

Tang, X.M., Cheng, C.H., and Paillet, F.L., 1991, Modeling borehole Stoneley wave propagation across permeable in-situ fractures, in *Society of Professional Well Analysts Annual Logging Symposium*, 32nd, 1991, Transactions, Midland, Texas: Society of Professional Well Log Analysts, Houston, Texas, p. GG1-GG25.

White, J.E., 1967, The hula log--a proposed acoustic tool, in *Society of Professional Well Log Analysts Annual Logging Symposium*, 8th, 1967, Denver, Colorado: Society of Professional Well Log Analysts, Houston, Texas, p. I1-I6.

A

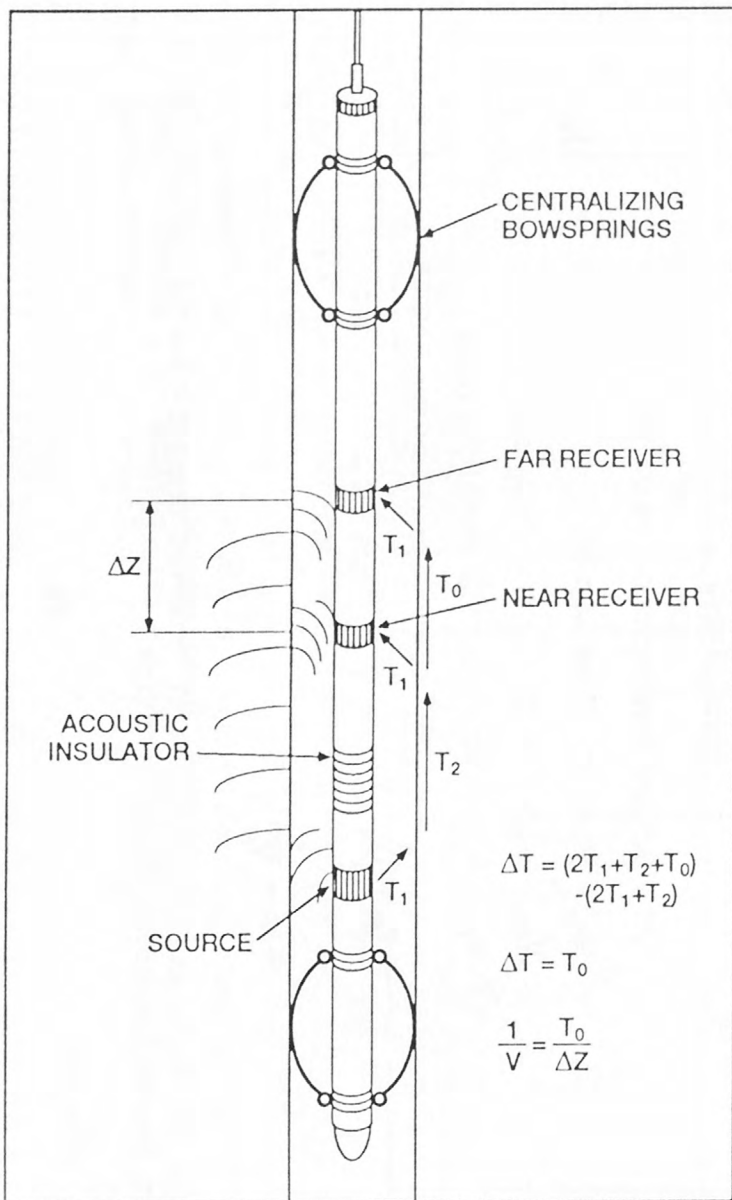
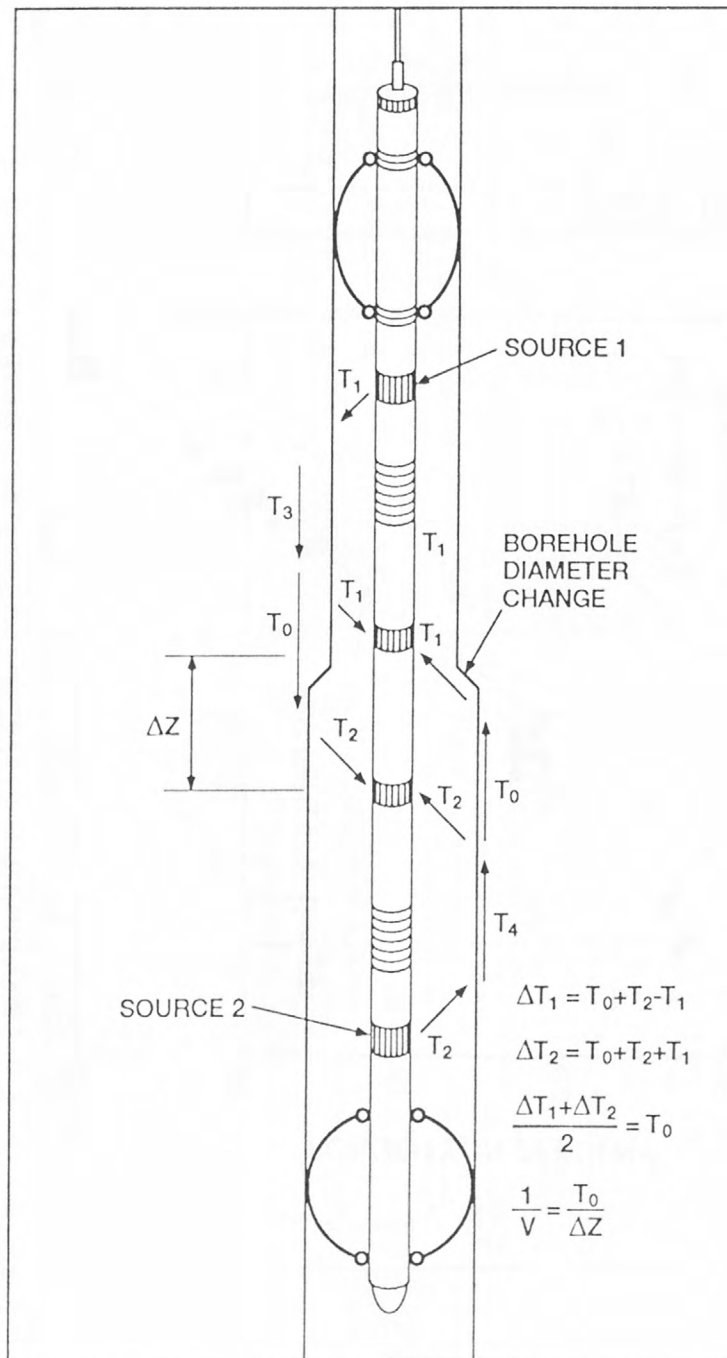


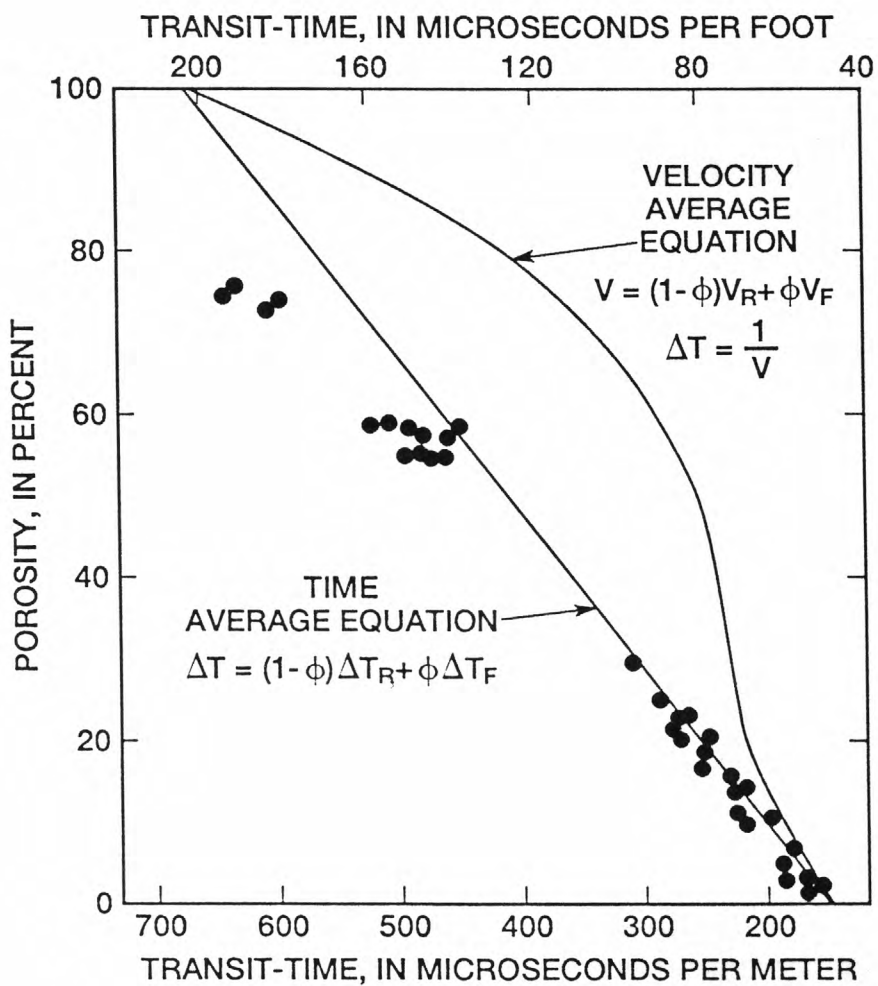
Figure 9. A. Single-source acoustic logging probe. B. Dual-source compensated acoustic logging probe.

B



EXPLANATION

- T_0 TRAVEL TIME ON PATH T_0
- T_1 TRAVEL TIME ON PATH T_1
- T_2 TRAVEL TIME ON PATH T_2
- ΔZ DISTANCE BETWEEN NEAR AND FAR RECEIVERS
- V ACOUSTIC VELOCITY OF FORMATION



EXPLANATION

V = ACOUSTIC VELOCITY OF FORMATION

ϕ = POROSITY OF FORMATION

V_R = ACOUSTIC VELOCITY OF MINERAL GRAINS

V_F = ACOUSTIC VELOCITY OF BOREHOLE FLUID

$$\Delta T_R = \frac{1}{V_R}$$

$$\Delta T_F = \frac{1}{V_F}$$

Figure 10. Empirical calibration of interval transit-time in porosity units using the Wyllie time-average equation.

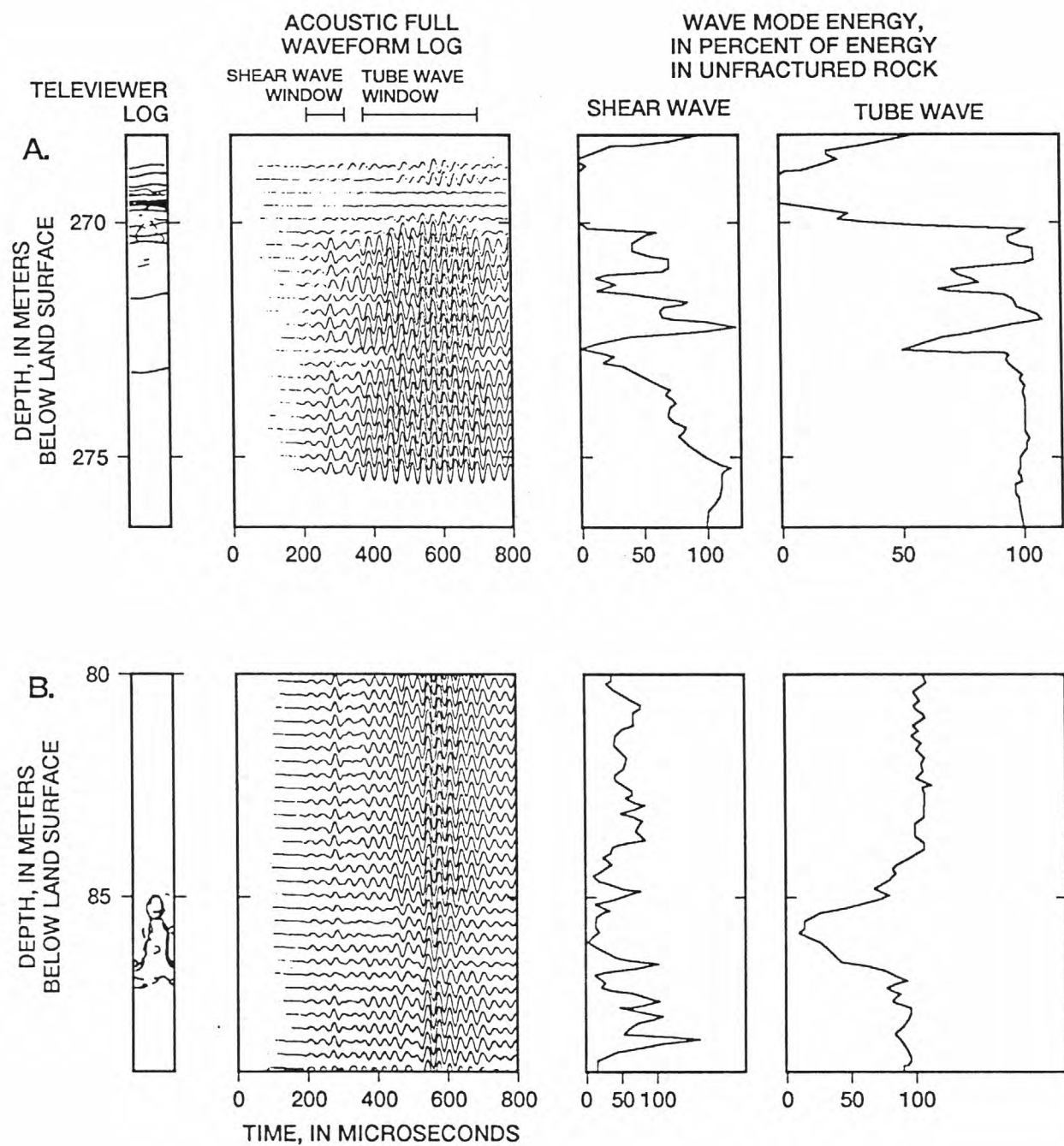


Figure 11. Acoustic-waveform logs compared to televiewer logs indicating the effects of fractures on acoustic propagation along boreholes:

- A. Horizontal-fracture zone intersecting a vertical borehole.
- B. Near-vertical fracture intersecting a vertical borehole.

Part 2

CASE STUDIES

USE OF BOREHOLE-GEOPHYSICAL LOGS TO DEFINE THE AREAL EXTENT, SOURCE, AND THICKNESSES OF CONFINING UNITS IN THE OWENS VALLEY, CALIFORNIA
By Kenneth J. Hollett¹ and Wesley R. Danskin²

Delineation of the areal extents and thicknesses of the confining units that separate the unconfined and confined aquifers in the Bishop Basin (fig. 12) of Owens Valley, California, plays a significant role in managing the water resources of the valley. Most of the water exported to Los Angeles, more than 200 miles to the south, is diverted runoff from precipitation that falls on the Sierra Nevada. Since 1970, a significant quantity of precipitation also has been withdrawn from the confined aquifer system. During times of below-normal runoff, ground-water withdrawals are increased, within legal limits, to meet water demand. These increased withdrawals pose an important hydrologic question: Do the confining units, which are discontinuous in the valley fill, isolate hydraulic-head declines within the confined aquifer or will these declines lower water levels in the unconfined aquifer to the possible detriment of the desert-scrub communities that depends on shallow ground water?

Numerous holes have been drilled in the valley to address this question. Three of the boreholes drilled in the southern part of the Bishop Basin were geophysically logged (fig. 13). Analysis of these logs indicates the presence of a number of significant clay layers, such as the three laterally extensive blue and green clay layers in the southern part of the basin (fig. 13) that represent episodes of lacustrine sedimentation in the Bishop Basin valley fill. These clay layers are confining units in the aquifer system in the valley. The lower most of the blue clay layers is directly underlain by the green clay and, together, these form a single confining unit in the basin-fill aquifer. On the basis of geologic information from the three logs depicted in figure 13 and logs from other boreholes in the Bishop basin (Hollett and others, 1991), the lower most, green clay layer progressively thins towards the west, whereas the immediately overlying blue clay layer thins to the east. The closely spaced pair of blue and green clay layers extends and thins from the narrows near Poverty Hills to the north near Big Pine (fig. 13). Deposition of the clay occurred in a shallow Holocene lake formed by the damming of the ancestral Owens River by basalt flows extruded during part of the Holocene Epoch. Alternating beds of lacustrine clay and fluvial sands and gravels in the stratigraphic sequence at the narrows suggest that a sequence of blockage and breaching may have occurred several times, both before and after deposition of the blue and blue-green clay layers. The surface and near-surface fluvial sediments at the narrows reflect a breached condition that allowed the Owens River to flow from the Bishop Basin to the Owens Lake Basin (Hollett and others, 1991). Furthermore, the borehole geophysical logs depict a characteristically different geophysical signature for the blue and green clays. In particular, the natural-gamma logs in boreholes USGS 16 and 17 (fig. 13) indicate that the natural-gamma signature for the green clay is significantly lower than the average natural-gamma response of about 100 counts per second associated with the valley-fill deposits. In contrast, the natural-gamma response for the blue clay is significantly higher than the average. Both clays, however,

¹U.S. Geological Survey, MS 411, Reston, VA 22092

²U.S. Geological Survey, 5735 Kearney Villa Rd., San Diego, CA 92123

produce a similar, characteristically small response on the electrical-resistivity log. Geophysical traces for the uncalibrated gamma-gamma and neutron logs also show distinctive signatures for the blue and green clays.

On the basis of a comparison of samples of the green clay collected from boreholes in the southern part of the Bishop Basin and samples of Paleozoic green marine shales that crop-out to the east in the White Mountains, the green clays are similar in both color and composition to the shales, which suggests that the green clays may be eroded material from the marine shales. This interpretation is further supported by the westward thinning of the green clay layer and, to some extent, by the relatively low natural-gamma response which is typical of the older marine shale at the eastern margin of the valley. In contrast, the relatively higher natural-gamma response for the blue clays may reflect, in part, the presence of variable amounts of glacial and alluvial material eroded from the younger and more tectonically active Sierra Nevada to the west. Characteristically, deposits eroded from the granitic Sierra Nevada produce natural-gamma responses of 90 to 200 counts per second in boreholes logged with equipment similar to that used for this study. The responses for fine-grained material eroded from the Sierra Nevada are typically at the higher end of this range.

The many erosional episodes are represented in the sediments and recorded by the geophysical logs. These borehole-geophysical records were crucial in developing an understanding of the depositional framework of the aquifer system, in determining the relation of the unconfined and confined aquifers in the southern part of the Bishop Basin, and in defining the hydrogeologic boundary conditions for a subsequent numerical simulation of ground-water flow and evaluation of management alternatives.

REFERENCES

Hollett, K.J., Danskin, W.R., McCaffrey, W.F., and Walti, C.L., 1991, Geology and water resources of Owens Valley, California: U.S. Geological Survey Water-Supply Paper 2370-B, 77 p.

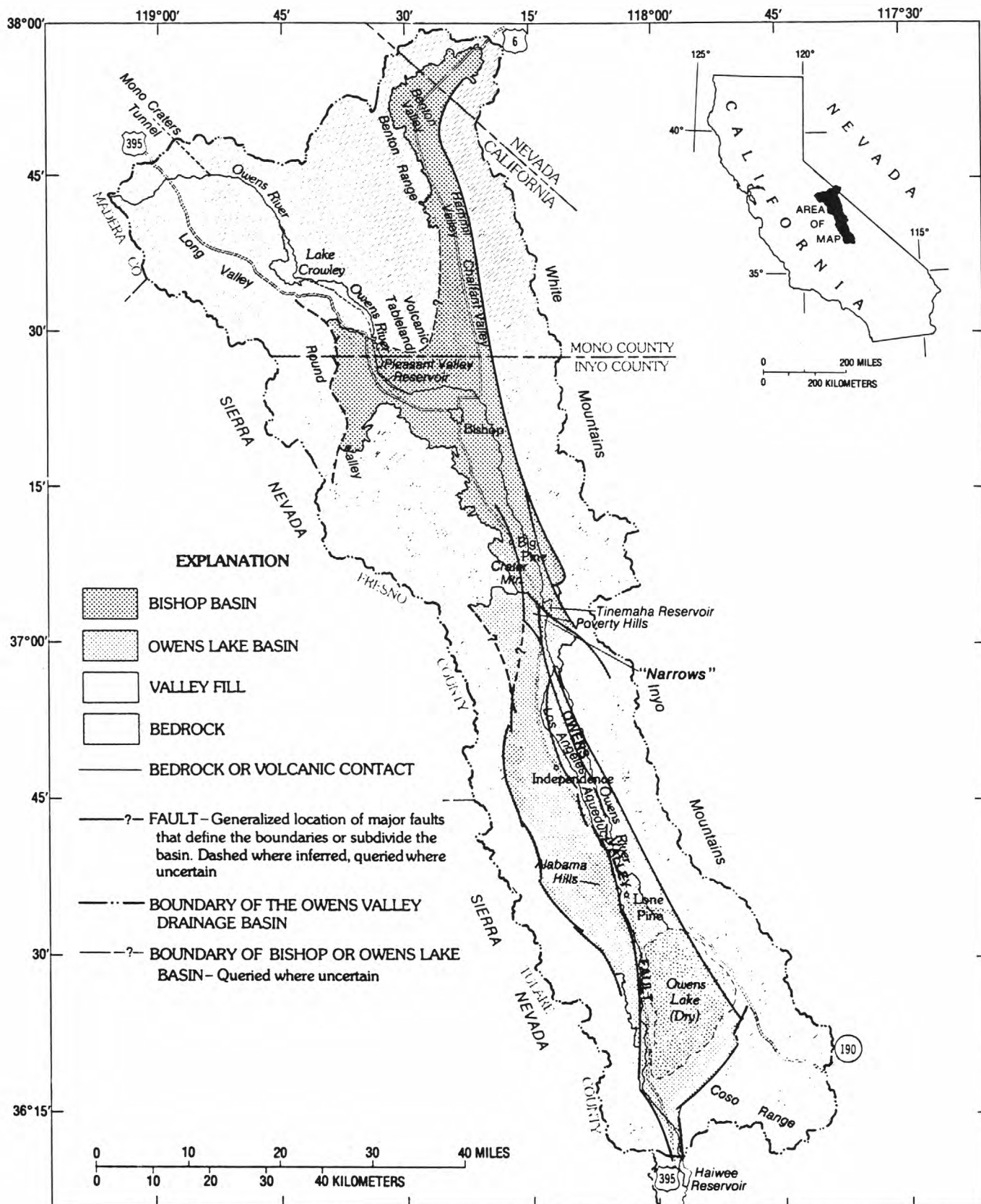


Figure 12. Location and structural division of Owens Valley into Bishop and Owens Lake basins, hydrologically connected through the geomorphic "narrows" east of and adjacent to Poverty Hills. (Modified from Hollett and others, 1991, fig 11.)

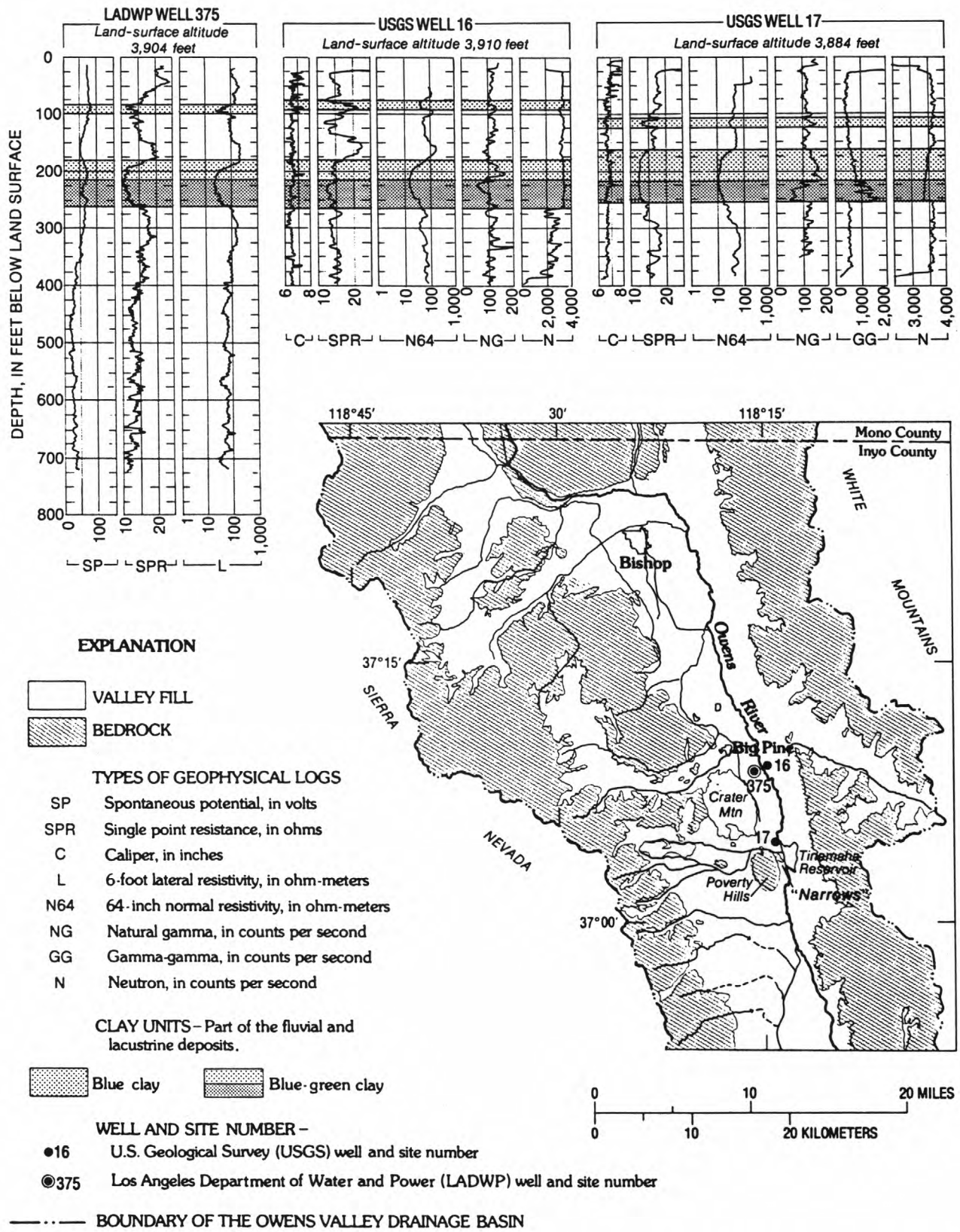


Figure 13. Borehole-geophysical logs of three wells, location of the three wells in Bishop basin, and geophysical correlation of major clay layers in the southern part of the Bishop basin. (Modified from Hollett and others, 1991, fig 12.)

USE OF BOREHOLE-GEOPHYSICAL LOGS TO DELINEATE THE
POSITION OF THE FRESHWATER/SALINE-WATER INTERFACE IN THE MICHIGAN BASIN
By D.B. Westjohn¹

The presence of shallow saline ground water (less than 30 m deep) in the Michigan Basin is known from chemical analyses of ground water collected in some areas of the basin. However, the position of the freshwater/saline-water interface for most of the State is unknown. Borehole-geophysical logs were used² to delineate the altitude of the base of freshwater within a 75,000-km² area, where rocks of Mississippian to Jurassic age underlie Pleistocene glacial deposits. The position, thickness, and character of a transition zone between units containing freshwater (<1,000 mg/L dissolved solids) and units containing brine (>100,000 mg/L dissolved solids) also were interpreted from geophysical logs (Westjohn, 1989).

Electrical-resistivity/spontaneous-potential logs (formerly termed electric log; Hilchie, 1979) made of hydrocarbon-exploration boreholes drilled in the 1940s provide the data set most useful for delineating the freshwater/saline water interface. These logs were run in mud-filled boreholes, open to glacial deposits or to freshwater-bearing bedrock aquifers, and they provide electrical-resistivity data for aquifers that contain the range of dissolved solids present in the aquifer system (107 to 297,000 mg/L; Dannemiller and Baltusis, 1990). Electrical-resistivities of freshwater, saline-water, and brine-saturated aquifers were established by interpreting more than 600 logs. Formation fluid resistivities were also inferred from the electrical properties of aquifers invaded by drilling mud. Old electric logs were run in boreholes filled with freshwater-base muds (electrical resistivities of 1 to 4 ohm-meters), and mud invasion inferred from the separation of lateral and long- and short-normal log traces delineates aquifers that contain pore water that is more or less resistive than drilling mud (fig. 14). In figure 14, formation water appears more resistive than borehole fluid (lateral log to the right of the short-normal log) above a depth of 180 m, and less resistive (short-normal log to the right of the lateral log) below a depth of 180 m. Mud-invasion profiles can also be related to hydraulic properties of the aquifer units studied, because mud invasion occurs only in hydraulically-conductive intervals. However, the extent of invasion commonly depends on formation porosity and permeability. Resistivity, dual-porosity, and gamma-ray logs were run in drill holes that were cored for laboratory measurements of hydraulic properties to establish relations among log data and hydraulic properties (fig. 15). Separations of the intermediate and deep resistivity-log traces are observed for aquifers that have hydraulic conductivities greater than 10^{-6} cm/s.

Electrical-resistivity/spontaneous-potential logs provide a semiquantitative means of estimating formation-water resistivity (R_w), and dissolved-solids concentrations can be extrapolated from these R_w estimates (Hearst and Nelson, 1985, p. 100). Several empirical methods for determining of R_w , made on the basis of relation of resistivity to porosity, have been established (Archie, 1942; Asquith and Gibson, 1982, p. 5). The general form of the Archie (1942) equation was derived from electrical-resistivity measurements of brine-saturated sandstone cores. The cementation exponent needed to apply the Archie relation (1942) was determined from laboratory

¹U.S. Geological Survey, 6520 Merchantile Way, Lansing, MI 48911

measurements made of cores from the Michigan Basin. For the case illustrated in fig. 16, calculated values of R_w (0.17 to 0.30 ohm-m) using the Archie relation (table 4) are consistently higher than measured values of R_w (0.14 ohm-m) for formation water produced from sandstone below a depth of 570 ft (fig. 15). Differences in calculated and measured R_w are, in part, related to porosities determined from geophysical logs. A comparison of measured porosities in 870 cores to porosities estimated from cross plots of neutron density log data shows that log-based porosities are 2 to 3 percent higher than measured porosities. A similar situation exists for the example illustrated in fig. 16, in that measured porosities (table 4) are lower than geophysical-log-based porosities. If measured porosities of core specimens are used, estimates of R_w more closely approximate measured R_w of water from the formation. The porosity-resistivity relation does provide useful approximations of R_w , but limitations that need to be considered include petrophysical properties (for example, cementation factor) are variable and commonly unknown, and state-of-the-art logging tools are generally not available to produce the types of resistivity and porosity logs needed for this type of analysis.

Borehole geophysical logs show that freshwater transects the glacial-deposits/bedrock contact. Although the freshwater section exceeds 300 m in thickness in many areas of the basin, water-quality data are available for only the upper 100 m of the aquifer system. Areas where the thickness of freshwater is greatest are dominated by glaciofluvial deposits that overlie, and are in direct hydraulic connection with, freshwater-bearing Pennsylvanian, or Mississippian age sandstones. The thickness of the transition zone is fairly uniform, freshwater overlies and grades downward into saline water over a zone 75 to 125 m thick in most of the basin. In most situations, the transition zone consists of Pennsylvanian sandstones and shaly sandstones that contain saline water. The shallowest brine-bearing sandstones generally are confined to the Upper Mississippian to Lower Pennsylvanian age rock sequence, and the Parma Sandstone Member of the Saginaw Formation (considered Lower Pennsylvanian age) is an extensive brine reservoir in the central Michigan Basin. The presence of brine in the Parma Sandstone is interpreted entirely on the basis of geophysical logs, because water-quality data for this aquifer are sparse. In many areas of the basin, Pennsylvanian sandstones (as much as 75 m above the Parma Sandstone) also contain brine, especially where shale units greater than 20 m thick form confining layers for these aquifers.

Geophysical logs also show that formation-water salinity is stratified in sandstone aquifers in which lithological breaks are not obvious. In these areas, as little as 15 m difference in altitude separates freshwater from underlying ground water containing concentrations of dissolved solids equivalent to those in seawater (35,000 mg/L). This stratification of pore-fluid salinity identified from geophysical logs is supported by chemical analyses of ground water withdrawn from selected sandstone intervals during double-packer aquifer tests.

REFERENCES

Archie, G.E., 1942, The electrical resistivity log as an aid in determining some reservoir characteristics: American Institute of Mining and Metallurgical Engineers Transactions, v. 146, p. 54-62.

Asquith, G.B., and Gibson, C.R., 1982, Basic well log analysis for geologists: American Association of Petroleum Geologists, Tulsa, Oklahoma, 216 p.

Dannemiller, G.T., and Baltusis, M.A., Jr., 1990, Physical and chemical data for ground water from the Michigan basin, 1986-1989: U.S. Geological Survey Open-File Report 90-368, 155 p.

Hearst, J.R., and Nelson, P.H., 1985, Well logging for physical properties: New York, McGraw-Hill, 571 p.

Hilchie, D.W., 1979, Old electric log interpretation: Golden, Colorado, D.W. Hilchie, Inc., 161 p.

Westjohn, D.B., 1989, Application of geophysics in the delineation of the freshwater/saline-water interface in the Michigan basin: Annual American Water Resources Association, Monograph Series No. 13, p. 111-134.

Table 4. Cementation exponents and porosities measured of sandstone core samples from selected depths; porosities from neutron-porosity formation density log (fig. 16) derived by the cross-plot method of Asquith and Gibson, (1982, p. 100); electrical-resistivities of brine-saturated sandstone from dual-induction log (fig. 16), and calculated resistivities¹ of pore fluid for selected depths

Depth below land surface (ft)	Cemen- tation exponent	Porosity of core (in percent)	Porosity from log (in percent)	Formation resistivity (in ohm-m)	Calculated water resistivity (in ohm-m)
578	1.80	20	22	4.6	0.30
594	1.84	17	20	4.5	0.23
606	1.88	18	20	4.4	0.21
616	1.87	19	19	3.7	0.17
624	1.93	18	20	5.0	0.22
632	1.92	15	18	4.5	0.17
646	2.03	19	20	4.9	0.19
656	1.97	13	19	6.0	0.23

¹Resistivities of formation water as calculated by using the formula modified from Archie (1942): $R_w = R_t(\phi^m)$, where R_w is formation-water resistivity (in ohm-m), R_t is resistivity of water-saturated formation derived from deep-reading resistivity trace (in ohm-m), ϕ is porosity from neutron porosity formation density log (in percent), and m is measured cementation exponent (from core).

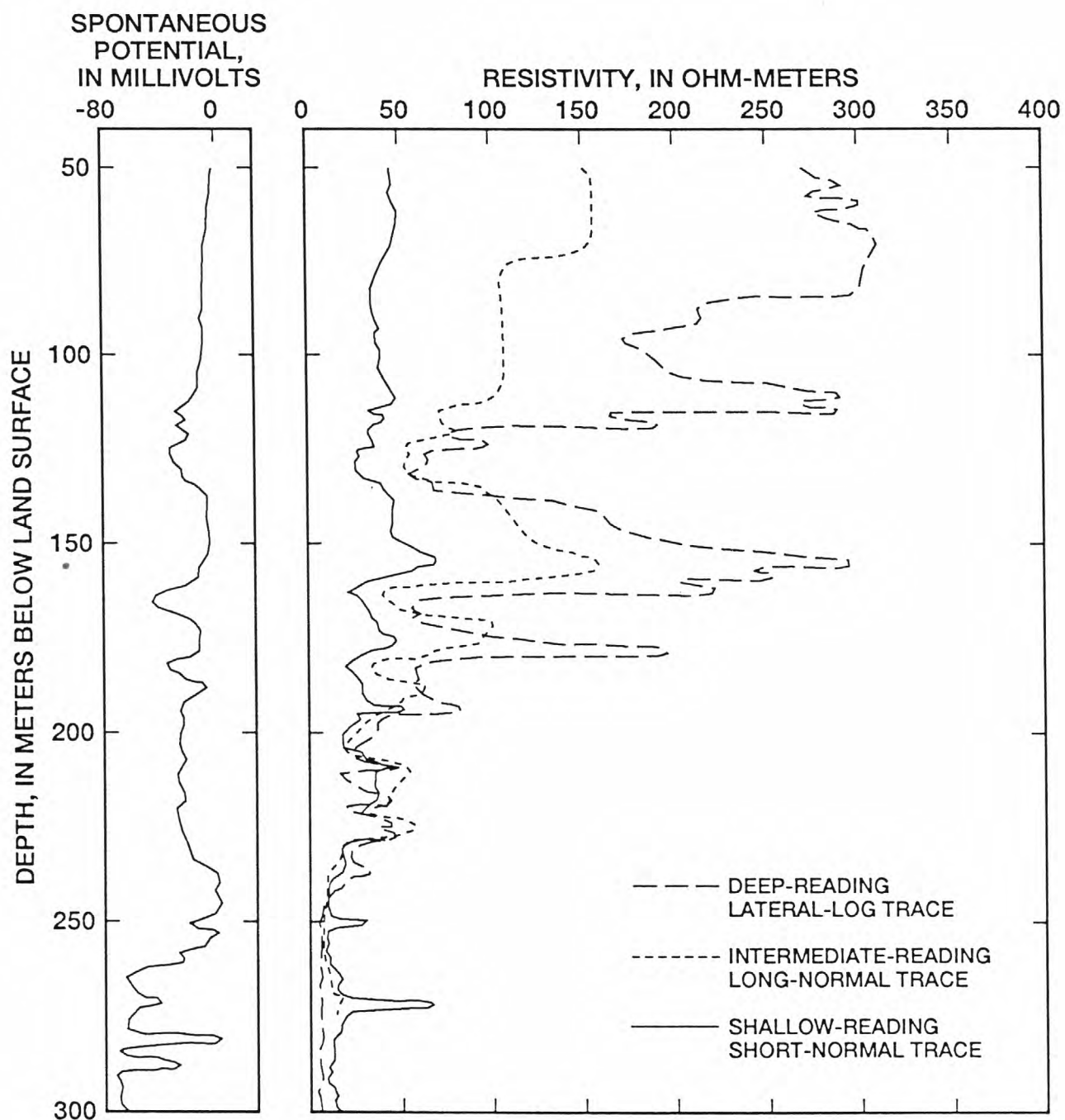


Figure 14. Electrical-resistivity/spontaneous potential log indicating the presence of freshwater to a depth of 180 meters.

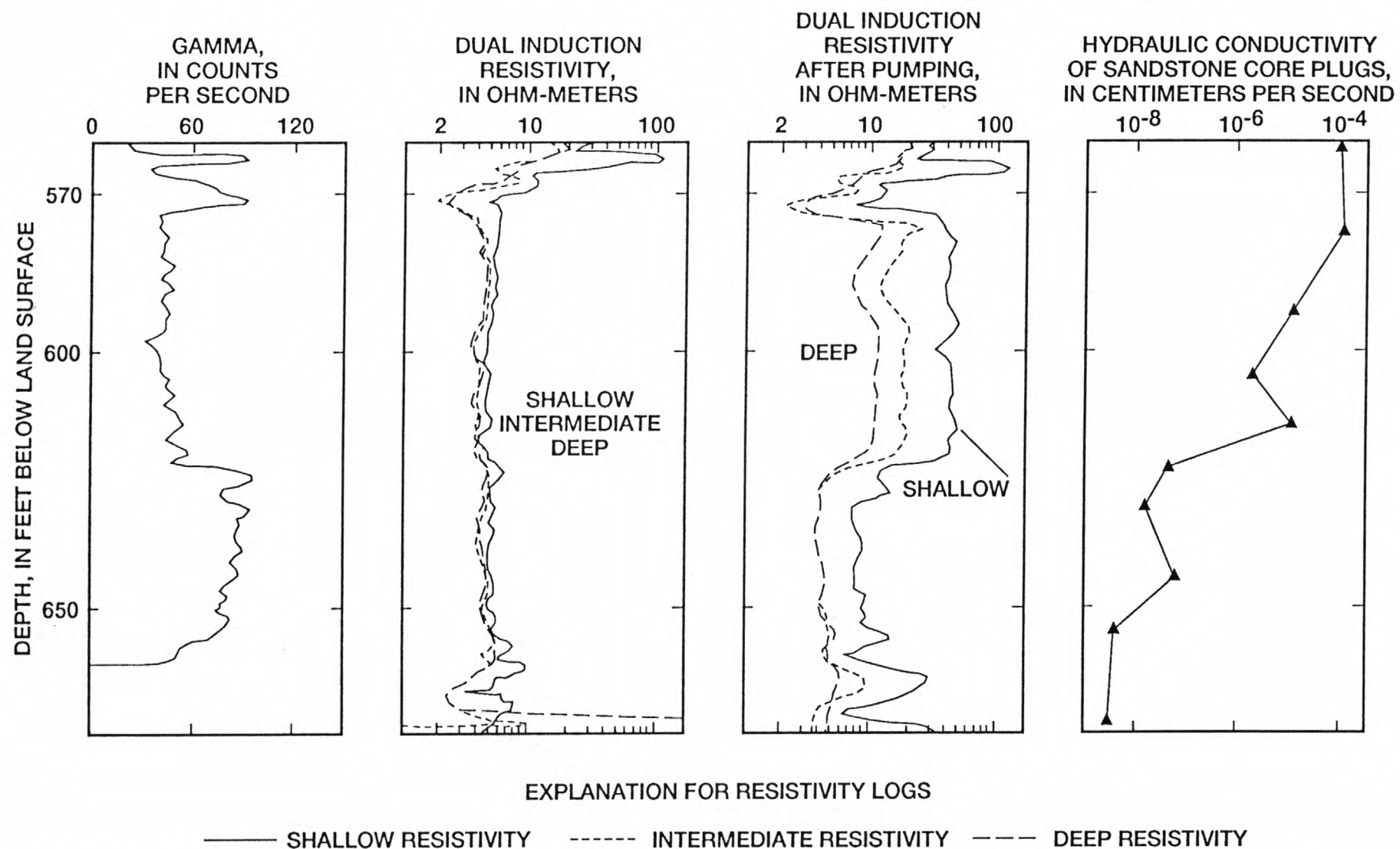


Figure 15. Dual-induction resistivity logs before and after pumping 17,000 gallons of brine from an interval packed-off at a depth of 570 feet.

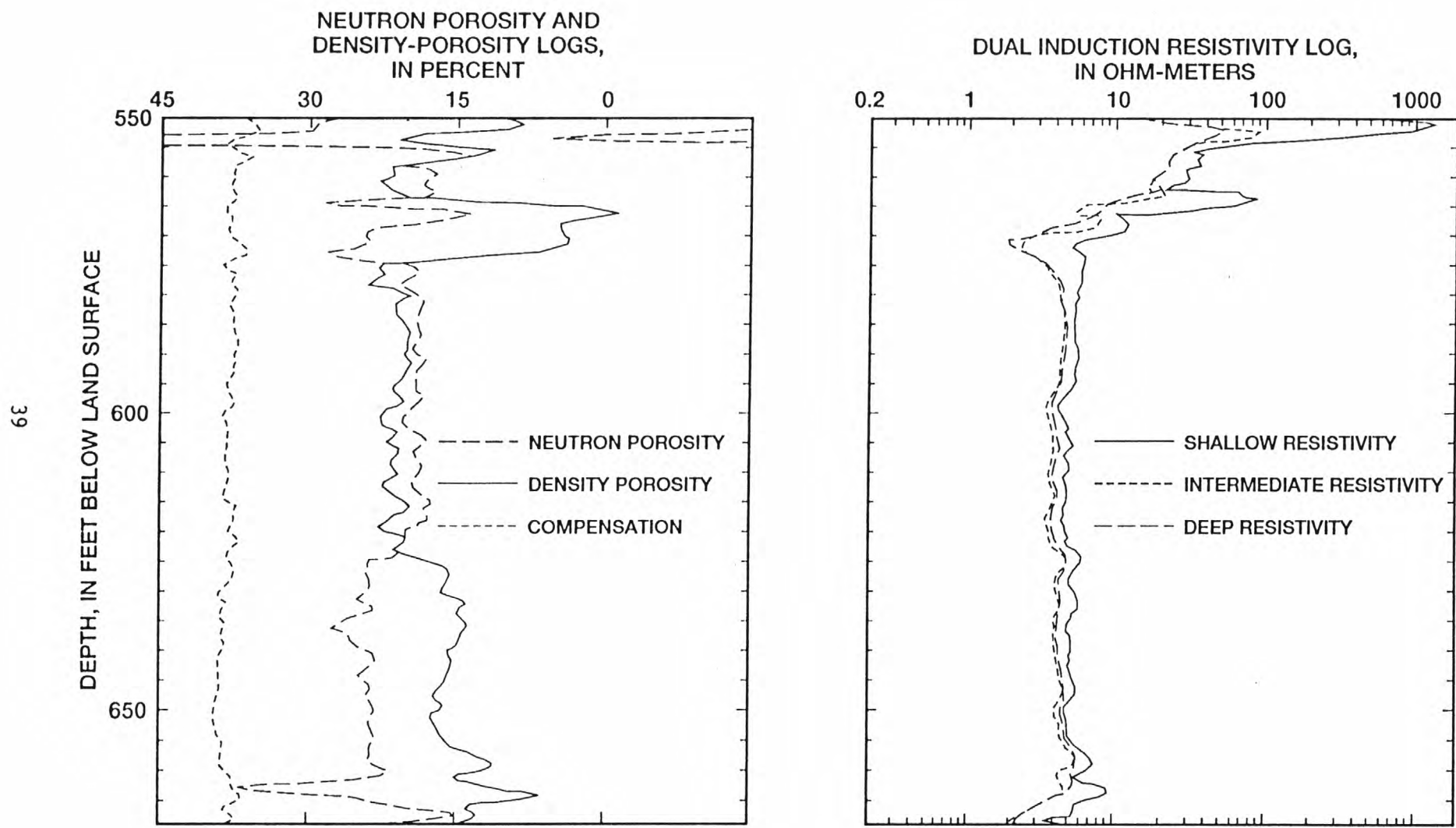


Figure 16. Suite of neutron-porosity/dual-induction logs run in borehole shown in figure 15. (See table 4 for list of measured porosities and cementation factors.)

USE OF BOREHOLE GEOPHYSICS FOR DELINEATION OF THE CONTRIBUTING AREA
TO A SUPPLY WELL IN A DIPPING, SEDIMENTARY-BEDROCK AQUIFER
By Gary J. Barton¹ and Randall W. Conger²

Data used to develop a conceptual, three-dimensional, hydrogeologic model of a well field in the Piedmont Physiographic Province of southeastern Pennsylvania, was obtained by borehole geophysical logging aquifer testing. Borehole logs were essential for identifying geologic formations, the position of the water table, and the presence of confined water-bearing beds. Borehole logs were also used to (1) determine the depth, thickness and horizontal hydraulic conductivity of minor and major water-bearing beds, (2) identify those observation wells located in the supply well's zone of diversion, and (3) collect information needed to estimate hydraulic head in the deepest confined water-bearing bed in the aquifer. The contributing area to the supply well was delineated by integrating data obtained from the geophysical logs with the results of a water-budget analysis and a conceptual hydrogeologic-model study of the aquifer (U.S. Environmental Protection Agency, 1987).

HYDROGEOLOGIC MODEL

A supply-well (NP61) and four adjacent observation wells comprise the Hospital well-field operated by the North Penn Water Authority in Lansdale, Pennsylvania (fig. 17). These open-hole wells are completed in the Brunswick and Lockatong Formations of Triassic age (mudstone, siltstone, shale, and sandstone) and are about 400 ft deep. Beds in the Brunswick Formation strike N. 38°E. and dip 10°NW. The base of the Brunswick Formation approximately coincides with a thin, black shale bed, enriched with radioactive elements, which intersects the borehole of NP61 270 ft below land surface (fig. 18). This bed emits natural-gamma radiation at a rate that is two to three orders of magnitude greater than that of the surrounding beds and, therefore, can easily be identified by natural-gamma logging. The Lockatong Formation intersects the borehole of NP61 at depths greater than 270 ft and crops out 800 ft southeast of this well. The median horizontal hydraulic conductivity of the Brunswick Formation in southeastern Pennsylvania is 1.4 ft/d, or about one order of magnitude higher than that of the Lockatong Formation. The Brunswick Formation contains thin, water-bearing beds commonly less than 1 ft thick and consisting of beds of highly fractured sandstone interbedded with thick beds of low-permeability shale and massive mudstone (fig. 19). Hydraulic connection between individual water-bearing fractures commonly is low (Wood, 1980). A conceptual model, based on the borehole logging summarized below, is shown in figure 20.

Caliper, fluid-resistivity, and fluid-temperature logs (Keys, 1990; Williams and Conger, 1990) show that under ambient hydraulic-head conditions ground water enters boreholes from extensively fractured thin beds in a confined-aquifer system, flows upward in the boreholes (figs. 18 and 21), and exits from boreholes into shallow water-bearing beds. Measurements of vertical flow made by brine-trace logging, which traces the movement of injected slugs of brine with a fluid-resistivity probe (Patten and Bennett,

¹U.S. Geological Survey, 6520 Mercantile Way, Lansing, MI 48911

²U.S. Geological Survey, 840 Market St., Lemoyne, PA 17043

1962) show upward flow in boreholes at rates up to 8 gal/min. The maximum depth in each well where water flowing up boreholes exits into water-bearing beds is 55 to 124 ft and is considered the base of a shallow aquifer. The shallow aquifer (Brunswick Formation) commonly contains several water-bearing beds, and the bedrock tends to be heavily weathered. Water-table conditions probably prevail within this aquifer. On the basis of depths where ground water enters open boreholes, confined water-bearing beds are present at depths of 140 to 313 ft. The deepest bed is in well NP61 and yields 4 gal/min to wells. Each borehole intersects one to three confined water-bearing beds. Bed thickness ranges from <1 to 3 ft. Intervening confining beds have an average thickness of 65 ft.

Simultaneous pumping and brine-trace logging were conducted in three wells to identify aquifer(s) that contribute significant quantities of water to NP61 during pumping and to calculate the horizontal hydraulic conductivity of water-bearing beds. Brine-trace logging was conducted before pumping began to measure the rate and direction of ambient flow. Water was pumped from the top and bottom of the wells at rates of 15 to 28 gal/min. Flow in these boreholes is assumed to be laminar (Moody, 1944). Brine-trace logging was conducted when the water level in each well stabilized and flow to the well approached near-steady state. The use of simultaneous pumping and brine-trace logging to calculate horizontal hydraulic conductivities is described in Molz and others (1989) and Rehfeldt and others (1989). Results show that the deepest water-bearing bed that yields several gal/min is at a depth of 217 ft in well NP61 (fig. 18) and at depths of 160 and 142 ft in wells NP58 and NP62, respectively. The water-bearing bed at a depth of 313 ft in NP61 has a very low horizontal hydraulic conductivity and, thus, a small yield (fig. 18). The horizontal hydraulic conductivity of the water-table aquifer ranges (uppermost part of the Brunswick Formation) from 1.4 to 16 ft/d. The hydraulic conductivity of the confined-aquifer system (including deeper conductive beds in the Brunswick Formation and in the underlying Lockatong Formation) to a depth of 217 ft ranges from 1.5 to 5.2 ft/d, and 0.2 ft/d below 217 ft (fig. 18). Water pumped from well NP61 is derived primarily from the water-table aquifer; some water is derived from the upper part of the confined-aquifer system.

CONTRIBUTING AREAS

Analytical methods (Blandford and Huyakorn, 1989) may not delineate contributing areas to well NP61 realistically because these methods do not include ground-water flow through thin, dipping aquifers confined by thick beds. A complex, digital ground-water-flow model may be able to incorporate virtually all information about the aquifer system obtained through logging and other testing. One approach is to use a simple water balance based on pumping (200 gal/min; permitted pumping rate for well NP61) and estimated aquifer recharge rates (10 in/yr; R.A. Sloto, 1992) to estimate a zone of contribution (ZOC) and adjust the boundaries of the contributing area to reflect the conceptual model. The well field's 1 year time-of-travel ZOC and adjacent surface areas beyond the outcrop of the aquifer contributing flow to the well are shown in figure 17. Results from borehole logging that are used to identify the contributing area to the well field are summarized below.

Wells NP59, NP62, and NP58 are within the ZOC of well NP61. Fluid-resistivity and brine-tracing logs show that vertical flow in boreholes

OB59 and OB62 is upward when well NP61 is not pumped, and upward and downward when well NP61 is pumped (fig. 21). Well NP61 withdraws water from confined water-bearing beds that extend to wells NP59 and NP62. At wells NP59 and NP62, water from a shallow, water-bearing bed moves down the borehole to recharge ground water in deeper beds in direct hydraulic connection with the pumped well (fig. 21). Upward vertical flow is induced in borehole OB58 after pumping begins.

On the basis of the hydrogeologic model, the ZOC of well NP61 extends from the well to the southeast to the recharge area of the deepest confined water-bearing bed penetrated by well NP61 (fig. 20). The altitude of the water level in this bed is approximately 380 ft above sea level at well NP61, as calculated by use of the Theim equation (Theim, 1906). The hydraulic head at this altitude is 10 ft higher than the elevation of land surface 1,800 ft southeast of well NP61, where the bed is assumed to cropout. The recharge area of this bed probably is an additional 400 ft farther upslope from well NP61 (fig. 20). Also, the ZOC extends approximately 1,000 ft from well NP61 to the northwest, where the aquifer is overlain by a thick confining unit. The shallowest water-bearing zone penetrated by well NP61 is 65 ft below land surface, and it dips to depths of between 100 and 250 ft and at a distance from 200 to 1,000 ft northwest of the well. At a depth of 100 ft, this bed is assumed to be confined (fig. 20). On the basis of simultaneous pumping and brine-trace logging, few water-bearing beds are present below a depth of 250 ft.

REFERENCES

Blandford, T.N., and Huyakorn, P.S., 1989, An integrated semianalytical model for the delineation of wellhead protection areas: U.S. Environmental Protection Agency contract 68-08-003, variously paginated.

Keys, W.S., 1990, Borehole geophysics applied to ground-water investigations: U.S. Geological Survey Techniques of Water-Resources Investigations, book 2, chap. E-2, 149 p.

Molz, F.J., Morin, R.H., Hess, A.E., Melville, J.G., and Guven, Oktay, 1989, The impeller meter for measuring aquifer permeability variations--evaluation and comparison with other tests: Water Resources Research, v. 25, no. 7, p. 1677-1683.

Moody, L.F., 1944, Friction factors for pipe flows: Transactions of the American Society of Mechanical Engineers, v. 66, p. 671-684.

Patten, E.P., Jr. and Bennett, G.D., 1962, Methods of flow measurement in wellbores: U.S. Geological Survey Water-Supply Paper 1544-C, 28 p.

Rehfeldt, K.R., Hufschmied, P., Gelhar, L.W., and Schaefer, M.E., 1989, Measuring hydraulic conductivity with the borehole flowmeter: Massachusetts Institute of Technology, 250 p.

Sloto, R.A., and Davis, P.K., 1983, Effect of Urbanization on the Water Resources of Warmwater Township, Bucks County, Pennsylvania: U.S. Geological Survey Water-Resources Investigations Report 82-4020, 72 p.

Thiem, G., 1906, Hydrologic methods: J.M. Gebhardt, Leipzig, 56 p.

U.S. Environmental Protection Agency, 1987, Guidelines for delineation of wellhead protection areas: EPA 440 per 6-87-010, 50 p.

Williams, J.H. and Conger, R.W., 1990, Preliminary delineation of contaminated water-bearing fractures intersected by open-hole bedrock wells: Ground Water Monitoring Review-Fall 1990, p. 118-126.

Wood, C.R., 1980, Groundwater resources of the Gettysburg and Hammer Creek Formations, southeastern Pennsylvania: Pennsylvania Geological Survey 4th series, Water Resources Report 49, 87 p.

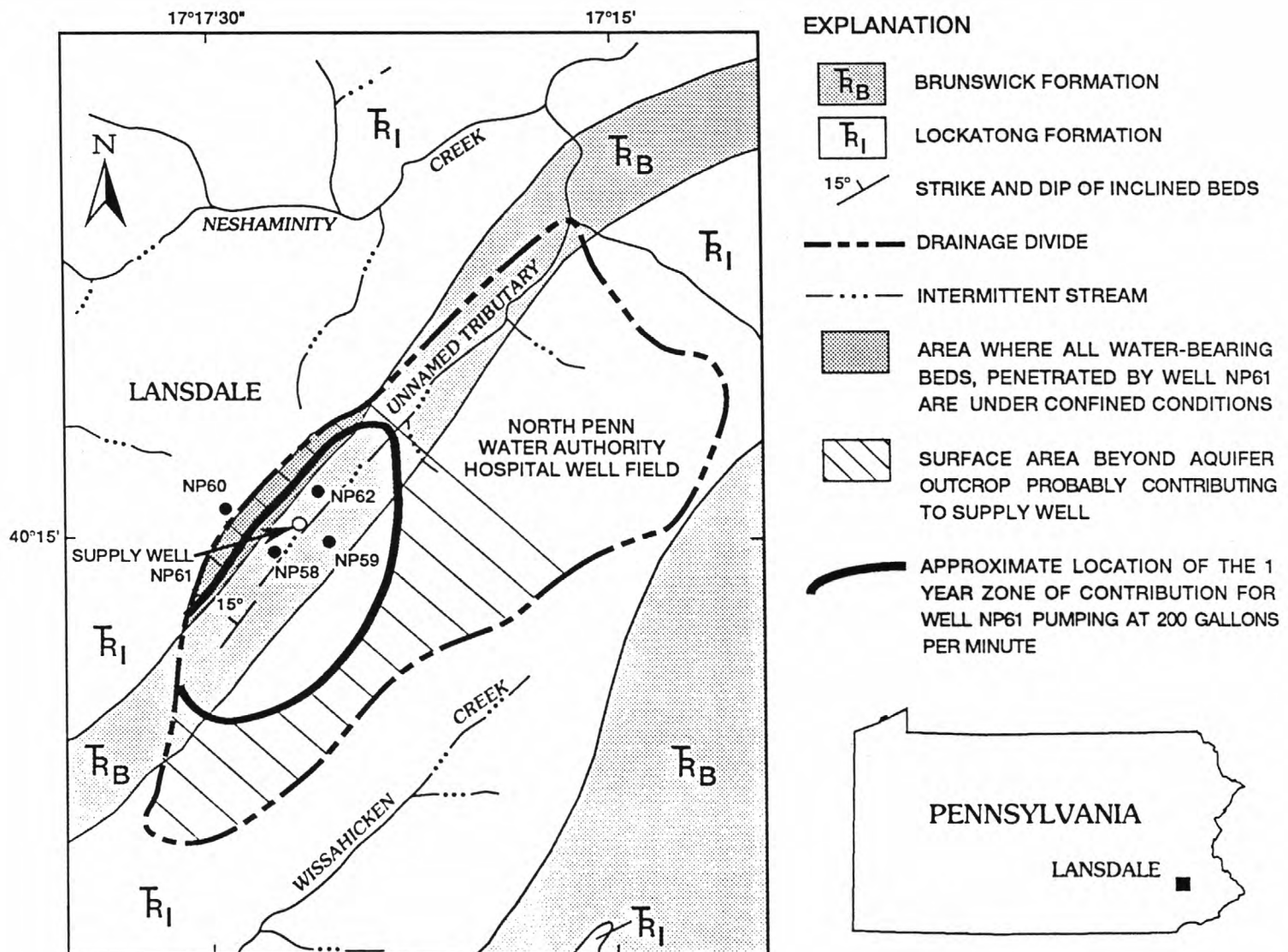


Figure 17. Geology and zone of contribution for supply-well NP61 at the North Penn Water Authority Hospital well field, Lansdale, Pennsylvania.

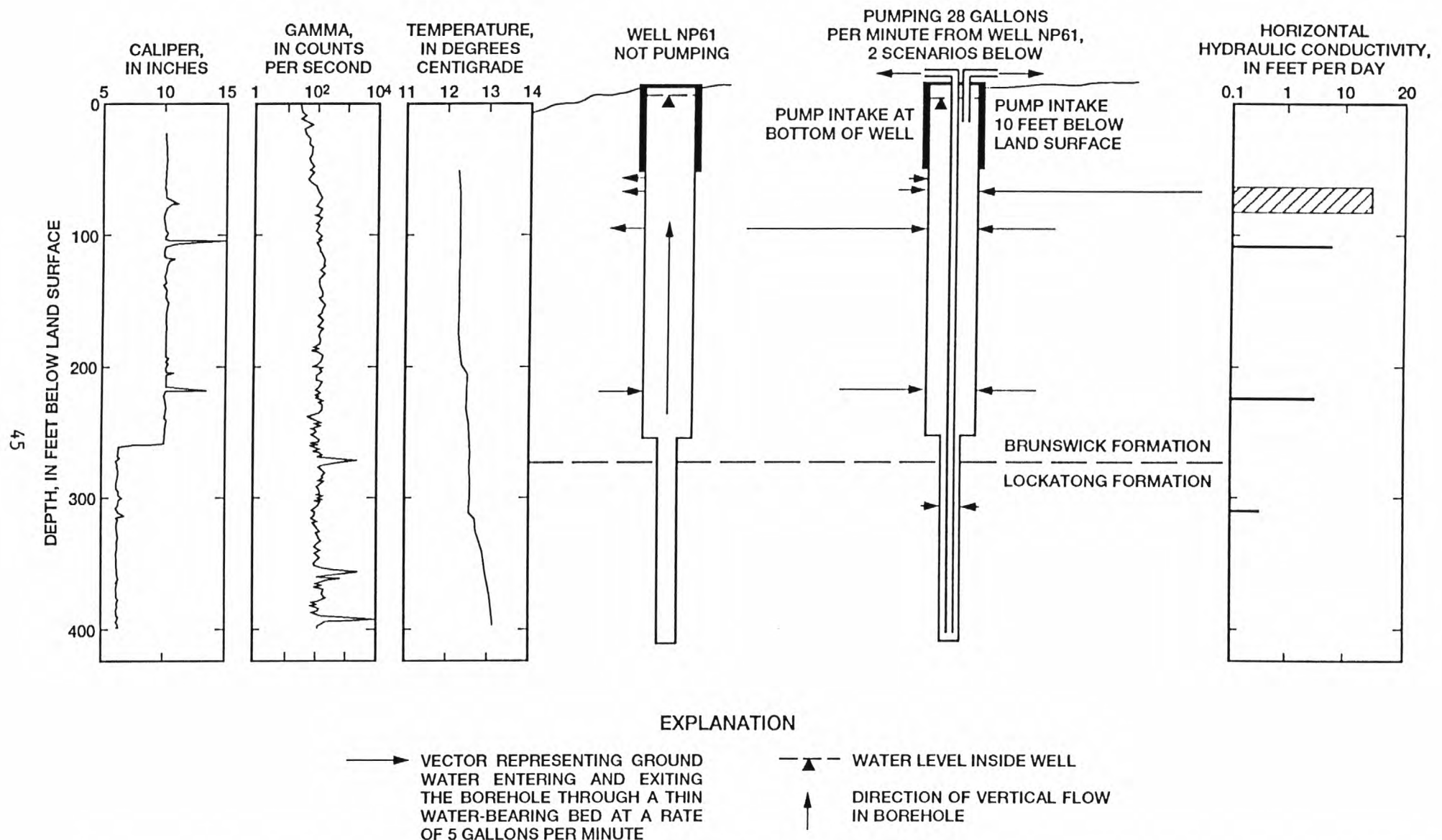


Figure 18. Geophysical logs of supply-well NP61, at Hospital well field, Lansdale, Pennsylvania, flow directions for ground water entering and exiting NP61's borehole through water-bearing beds under nonpumping conditions and while pumping NP61 at a rate of 28 gallons per minute under laminar-flow conditions, and distribution of horizontal hydraulic conductivity.

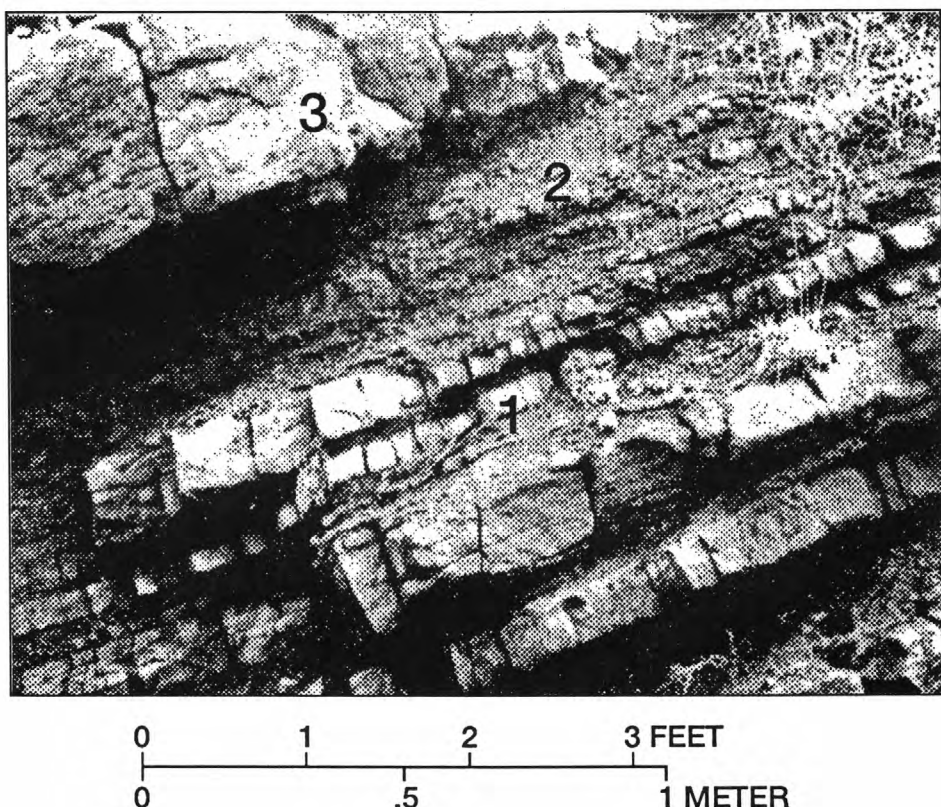
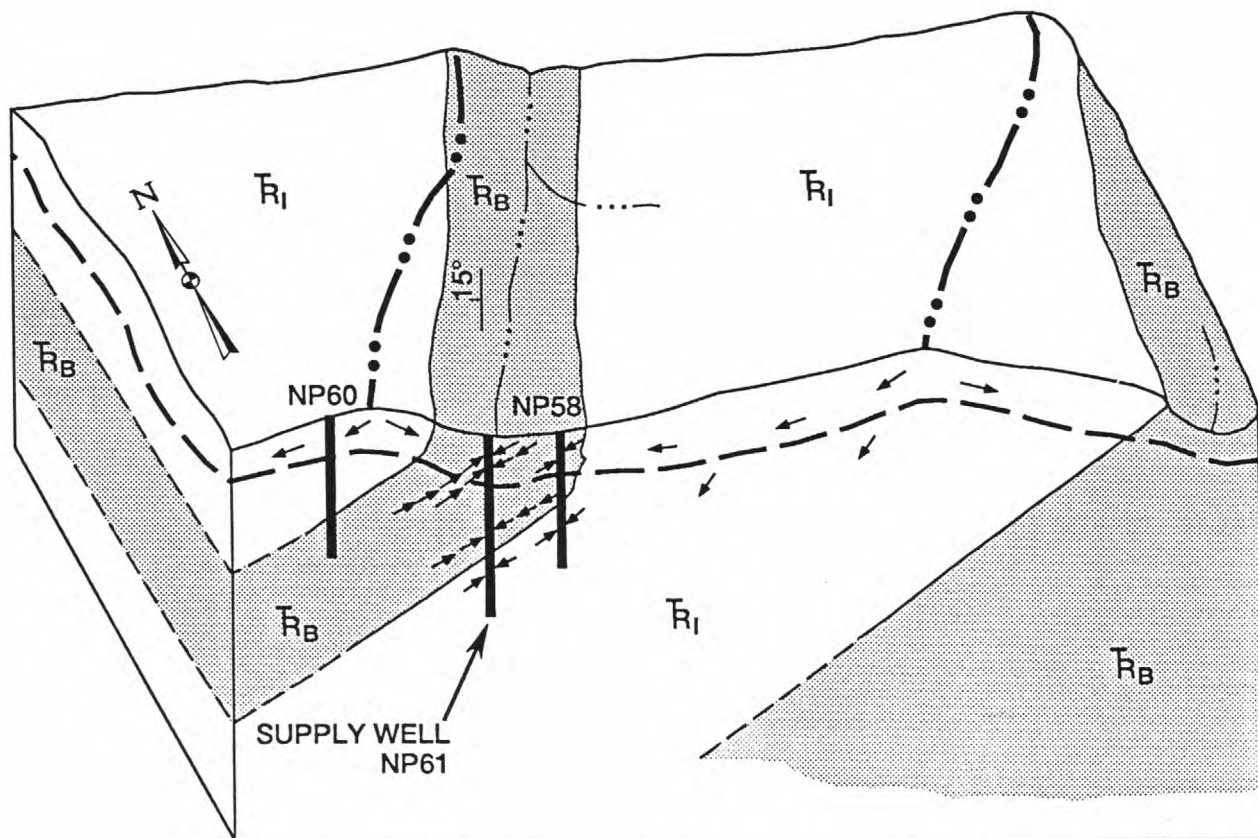


Figure 19. Hydrogeologic characteristics of sedimentary bedrock of Triassic age in the vicinity of the Hospital well field, Lansdale, Pennsylvania. Hydrogeologic characteristics include (1) very thin water-bearing beds that consist of highly fractured sandstone between beds of (2) soft, low-permeability shale and (3) massive mudstone. (Modified from Wood, 1980)



HORIZONTAL SCALE
 0 2000 4000 FEET
 0 500 1000 METERS
 VERTICAL EXAGGERATION: 7:1

EXPLANATION

- NP58 LOCAL WELL IDENTIFIER AND GROUND-WATER FLOW PATHS INTERSECTING A BOREHOLE INDICATE THAT WATER ENTERS AND EXITS THE BOREHOLE THROUGH WATER-BEARING BEDS AND FLOW IS VERTICAL IN THE WELL
- BRUNSWICK FORMATION
- T_L LOCKATONG FORMATION
- GROUND-WATER FLOW
- 15° STRIKE AND DIP OF INCLINED BEDS
- — — BASE OF WATER-TABLE AQUIFER
- · · — INTERMITTENT STREAM
- · — BASIN DIVIDE

Figure 20. Conceptual hydrogeologic model of the North Penn Water Authority Hospital well field, Lansdale, Pennsylvania. Flow lines for the water-table and confined aquifers when the supply well is not being pumped are presented.

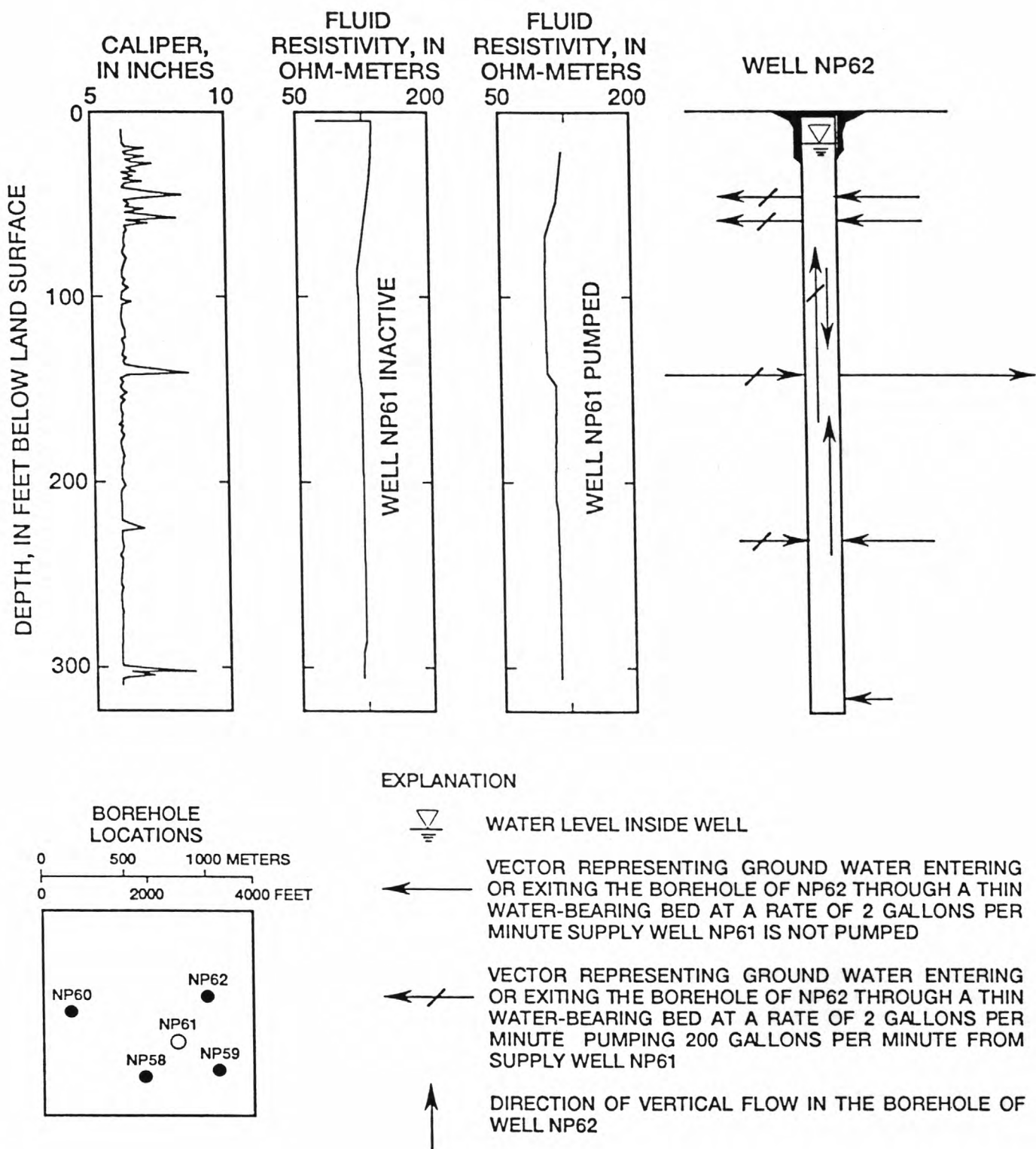


Figure 21. Geophysical logs of observation-well NP62 at the North Penn Water Authority Hospital well field, Lansdale, Pennsylvania, and flow vectors for water entering and exiting the well bore through water-bearing beds while supply well NP61 is inactive and while it is pumped.

USE OF GEOPHYSICAL LOGS IN HYDROGEOLOGIC INVESTIGATIONS AT
SELECTED SUPERFUND SITES IN NORTH-CENTRAL ILLINOIS²
by P.C. Mills¹, James Ursic¹, R.T. Kay¹, and D.J. Yeskis²

Detailed hydrogeologic and water-quality investigations were conducted at three Superfund sites (Byron Salvage Yard, Acme Solvents, and Parson's Casket Hardware; fig. 22) in north-central Illinois during 1985-92 (Paillet and others, 1993; Kay and others, 1989, R.T. Kay, U.S. Geological Survey, written commun., 1991, and Mills, 1993a, 1993b). Geophysical logs were an important source of hydrogeologic information in the investigations.

The bedrock units of Ordovician age evaluated at the sites include, from oldest to youngest, the St. Peter Sandstone, the Glenwood Formation, and the Platteville and Galena Groups (referred to collectively as the Galena-Platteville dolomite because of the lithologic similarity of the two units) (Willman and others, 1975). Quaternary deposits of glacial origin overlie the Galena Group at all the study sites (fig. 23). The water table is within the Quaternary deposits at the Parson's Casket Hardware site and within the Quaternary deposits or the Galena-Platteville dolomite at the other study sites.

Lithologic (rock-core) data and gamma logs (fig. 24) indicate that the Galena-Platteville dolomite at the three study sites thickens to the northeast. Acoustic-televIEWER logs and borehole-radar data (Niva, 1991a, 1991b) indicate the presence of substantial secondary porosity in the dolomite unit resulting from matrix dissolution (vesicles and vugs), solution along bedding-plane partings (bedding-plane fissures), and fracturing (which is generally inclined).

The borehole-geophysical data, rock-core data, and discrete-interval (packer) aquifer-test data indicate that the Galena-Platteville dolomite is substantially more permeable at the Byron Salvage Yard site than it is at the other study sites, probably because of an increase in the number of fractures and solution openings in the dolomite at the Byron Salvage Yard site.

Lithologic (rock-core) data and gamma logs (fig. 24) indicate that the clay content in the Glenwood Formation decreases to the northeast, probably because of the diminishing thickness of the Harmony Hill Shale Member of the Glenwood Formation in that direction and a general decrease in matrix clay in the underlying dolomite and sandstone members (figs. 23 and 24). The Harmony Hill Shale Member has been shown to semiconfine the underlying St. Peter sandstone aquifer (Kay and others, 1989).

Hydraulic data, including water levels, borehole heat-pulse-flowmeter measurements of flow under ambient hydraulic-head conditions, and aquifer properties estimated from discrete-interval aquifer tests, indicate that natural vertical hydraulic gradients within and between the three Ordovician bedrock units are typically downward. Discrete-interval, water-quality sampling indicates that volatile organic compounds are distributed throughout the thickness of the Galena-Platteville dolomite and apparently are transported both vertically and horizontally through fractures and bedding-plane fissures. Concentrations of the compounds often are highest in the fractured or fissured intervals. The extent of ground-water flow and

¹U.S. Geological Survey, 102 E. Main St., 4th Floor, Urbana, IL 61801

²U.S. Environmental Protection Agency, Region 5, 77 W. Jackson Blvd., Chicago, IL 60604

contaminant movement into the St. Peter Sandstone differs among the three sites and is apparently related to the variable thickness of the semiconfining Harmony Hill Shale Member of the Glenwood Formation (Paillet and others, 1993; Kay and others, 1989; Mills, 1993).

Use of the standard suite of geophysical logs (three-arm caliper, gamma, spontaneous potential, and single-point resistance) at the sites provided only a preliminary understanding of the hydrogeology of the fractured Galena-Platteville dolomite and its relation to ground-water flow and contaminant movement. Reliable characterization of contaminant hydrogeology in the fractured-bedrock system required the use of a greater variety of geophysical-logging techniques than that provided by the standard suite of logs, as well as discrete-interval aquifer testing and water-quality sampling.

REFERENCES

Kay, R.T., Olson, D.N., and Ryan, B.J., 1989, Hydrogeology and results of aquifer tests in the vicinity of a hazardous-waste disposal site near Byron, Illinois: U.S. Geological Survey Water-Resources Investigations Report 89-4081, 56 p.

Mills, P.C., 1993a, Hydrogeology and water quality of the Galena-Platteville aquifer at the Parson's Casket Hardware site Belvidere, Illinois, 1991: U.S. Geological Survey Open-File Report 93-403, 86 p.

Mills, P.C., 1993b, Hydrogeology and water quality of the Galena-Platteville aquifer at the Parson's Casket Hardware site Belvidere, Illinois, 1991-92: U.S. Geological Survey Open-File Report 93-404, 29 p.

Paillet, F.L., Kay, R.T., Yeskis, D., and Pedler, W., 1993, Integrating well logs into a multiple-scale investigation of a fractured sedimentary aquifer: *The Log Analyst*, v. 34, no. 1, p. 24-40.

Niva, Borje, 1991a, Results from borehole radar test at Parson's Casket Superfund site: Abem AB, Mala, Sweden, 16 p.

_____, 1991b, Results from borehole radar tests at Dirks Farm: Abem AB, Mala, Sweden, 31 p.

Willman, H.B., Atherton, Elwood, Buschbach, T.C., Collinson, Charles, Frye, J.C., Hopkins, M.E., Lineback, J.A., and Simon, J.A., 1975, Handbook of Illinois stratigraphy: Illinois State Geological Survey Bulletin 95, 261 p.

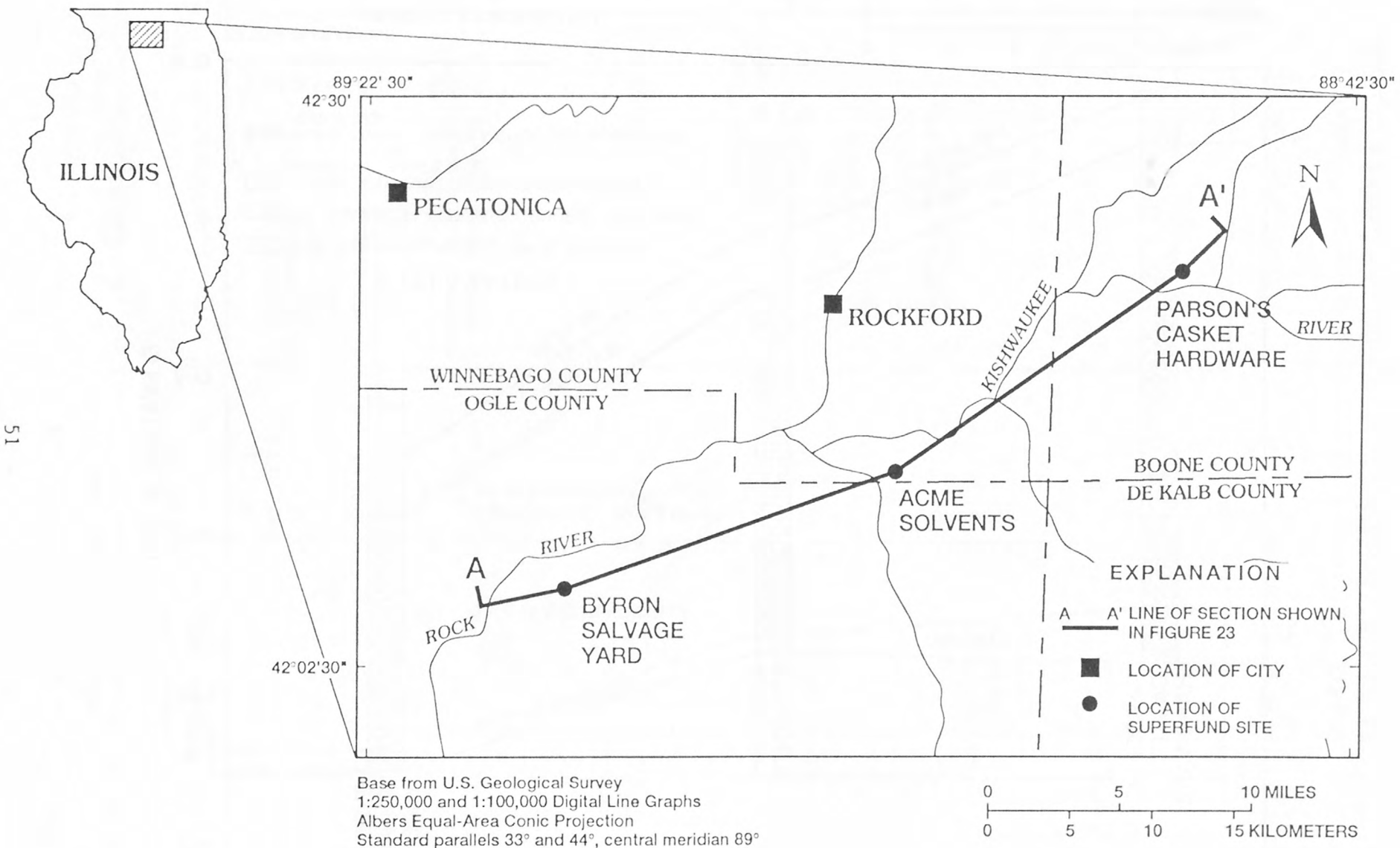


Figure 22. Location of U.S. Environmental Protection Agency Superfund sites in north-central Illinois.

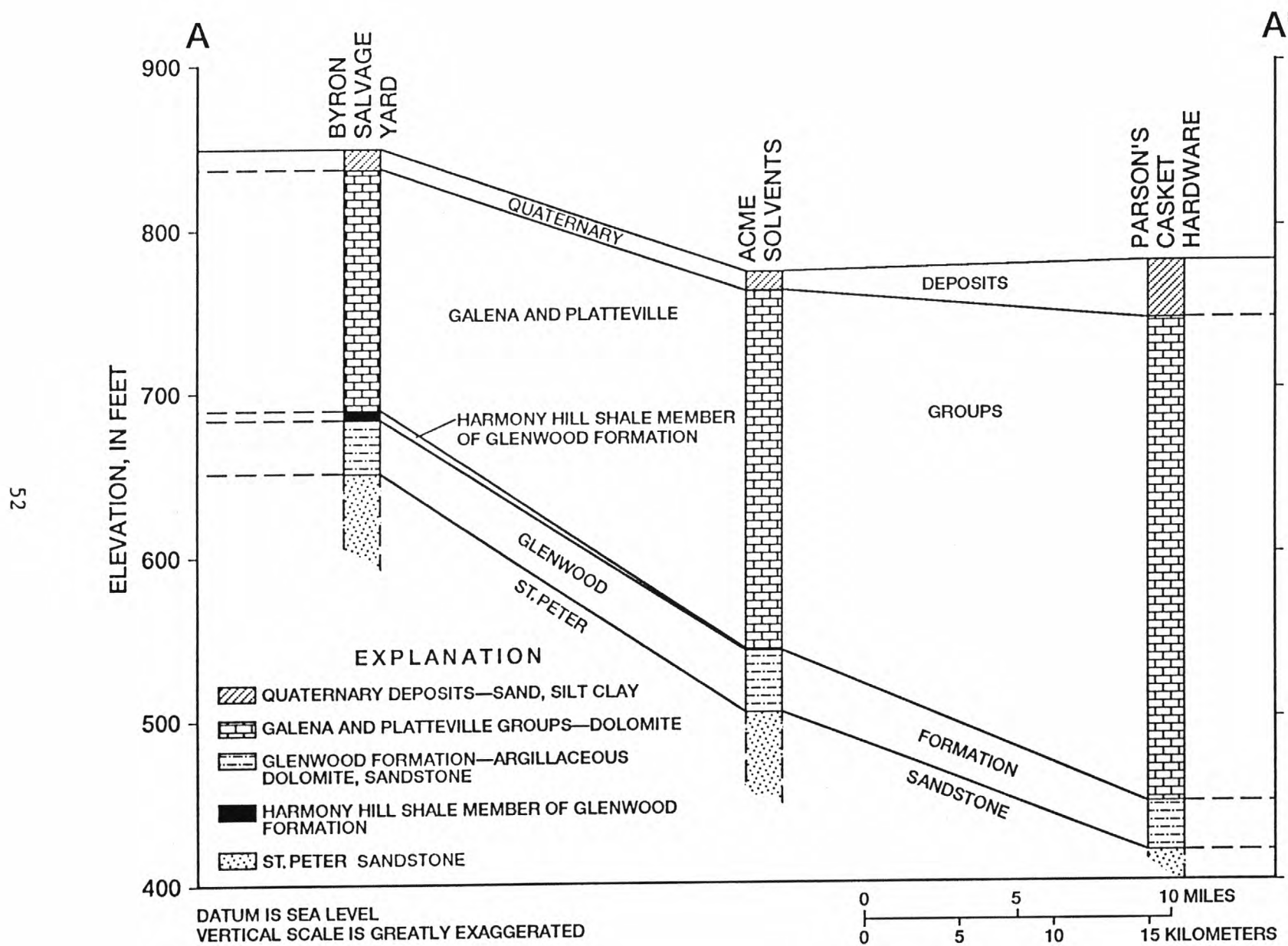


Figure 23. Correlation of geologic units at three U.S. Environmental Protection Agency Superfund sites in north-central Illinois.

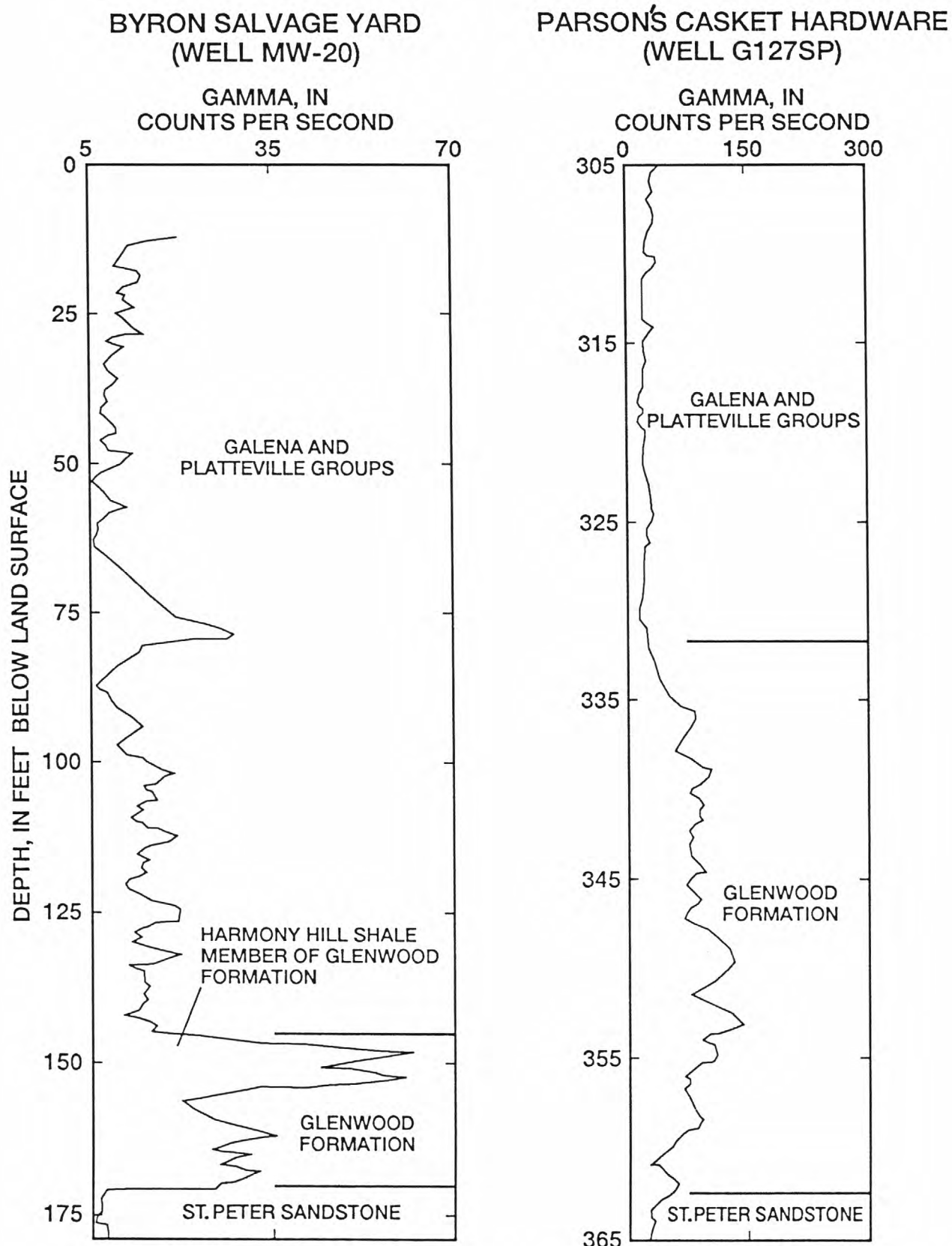


Figure 24. Natural-gamma logs for the bedrock units of Ordovician age at the Byron Salvage Yard and Parson's Casket Hardware Superfund sites in north-central Illinois.

USE OF BOREHOLE GEOPHYSICAL METHODS TO INVESTIGATE AQUIFER
CROSS CONTAMINATION BY VOLATILE ORGANIC COMPOUNDS IN THE
STOCKTON FORMATION, HATBORO, PENNSYLVANIA

By Ronald A. Sloto¹, Paola Macchiaroli², and Michael T. Towle³

Abandoned industrial and public supply wells and improperly constructed observation wells open to multiple water-bearing zones in the Stockton Formation of Triassic age in Pennsylvania affect directions of ground-water flow and act as conduits for the downward transport of volatile organic compounds (VOCs). Sediments of the Stockton are of predominantly fluvial-deltaic origin, but may include some sediments of near-shore lacustrine origin (Turner-Peterson and Smoot, 1985). In the Hatboro area, the Stockton Formation strikes approximately N.65°E. and dips approximately 9°NW. The rocks are chiefly arkosic sandstone, siltstone, and mudstone. Natural gamma, single-point resistance, caliper, borehole-fluid temperature, and borehole-fluid resistivity logs were run in 16 boreholes, which are 150 to 470 ft deep (fig. 25) and completed as open holes with shallow casings.

The Stockton Formation is a multiaquifer system (Sloto and Davis, 1983). Siltstone-mudstone beds of low permeability are confining units for the more permeable sandstone beds; however, water-bearing fractures are present in the siltstone-mudstone and sandstone units. Hydraulic head in each water-bearing fracture or zone typically is different, and water in a borehole open to more than one water-bearing zone will flow in the direction of lower head. Water moves downward through the aquifer system in response to a downward head-gradient, which is caused, in part, by the pumping of deep public-supply wells.

A three-dimensional, lithostratigraphic model of the dipping sedimentary rocks of the Stockton Formation was constructed primarily on the basis of natural gamma, single-point resistance, and caliper logs. Geophysical logs were compared to a 200-ft-long rock core from one borehole to determine the relative responses shown in the geophysical logs to lithology. Four general lithologic units were identified in the core: (1) red siltstone-mudstone; (2) reddish-grey, silty, fine-grained sandstone; (3) grey to buff, fine-grained sandstone; and (4) grey to buff, medium- to coarse-grained sandstone. This comparison was used as the basis for lithologic interpretation of the geophysical logs of the other boreholes. Because lithologic units grade, interfinger, and coalesce, none of the units can be used as location indicators (marker beds) within the lithostratigraphic sequence. Therefore, the lithology was first interpreted and subsequently fit together to construct the lithostratigraphic model. The interpreted lithostratigraphy correlates well from borehole to borehole (fig. 26). The correlations show the thinning and thickening of units across the area consistent with lens like deposition in an alluvial-fan environment. Correlation of geophysical logs was less certain when the distance between boreholes exceeded 400 ft along strike and 300 ft up-dip or down-dip.

Fluid-producing and receiving zones in the wells were identified on the basis of caliper, single-point resistance, borehole-fluid resistivity, and

¹U.S. Geological Survey, 111 Great Valley Parkway, Malvern, PA 19355

²Geology Department, University of Pennsylvania, Philadelphia, PA 19104

³U.S. Environmental Protection Agency, Region III, 841 Chestnut Bldg., Philadelphia, PA 19107

borehole-fluid temperature logs. Caliper logs were used to identify fractures and possible water-bearing openings. Producing and receiving zones were identified by sharp changes in fluid resistivity. Intervals of borehole flow were identified by a low fluid-resistivity gradient between producing and receiving zones. Intervals of vertical borehole flow also were identified by a small or absent temperature gradient. Temperature logs from wells where borehole flow does not occur generally showed a decrease in fluid temperature with depth in the upper part of the borehole and an increase in fluid temperature with depth, as a function of the geothermal gradient in the lower part of the borehole.

The direction and rate of fluid flow in the borehole were determined by injecting a slug of high-conductance fluid at a specific depth in a borehole and monitoring movement of the slug with the fluid-resistivity tool (the brine-tracing method of Patten and Bennett, 1962). The lower limit of flow measurement is about 0.5 gal/min in a 6 in.-diameter borehole. A slug of high-conductance fluid was injected at selected depths in 15 boreholes. Downward movement flow of fluid at rates up to 5.9 gal/min was measured in 13 boreholes. Generally, fluid flow is downward from fractures in siltstone-mudstone and sandstone units in the upper part of the aquifer system to fractures in sandstone units in the lower part.

After intervals of borehole flow were determined, samples of moving fluid from nine boreholes were collected with a nitrogen-driven bladder pump at a rate less than that of the measured borehole flow and analyzed for VOCs. These samples represent water flowing from the shallow to the deeper part of the aquifer system. Concentrations of trichloroethylene were as great as 5,800 $\mu\text{g}/\text{L}$, concentrations of 1,1,1-trichloroethane were as great as 1,400 $\mu\text{g}/\text{L}$, and concentrations of 1,1-dichloroethylene were as great as 260 $\mu\text{g}/\text{L}$.

The annual quantity of VOCs moving downward through the aquifer system was estimated on the basis of measured borehole flow rates and results of chemical analyses of the moving borehole fluid. Because the wells were sampled once and concentrations of VOCs in borehole fluid may vary temporally, the sampling should be considered a reconnaissance. An estimated 14.65 gal/yr of VOCs (table 5) are moving downward through the nine open boreholes sampled, from the contaminated, upper part of the aquifer system to the lower part, which is tapped by public-supply wells. Trichloroethylene accounts for 93 percent and 1,1,1-trichloroethane accounts for 3 percent of the VOCs by volume.

Table 5. Estimated quantity of volatile organic compounds moving downward in borehole fluid in nine sampled boreholes

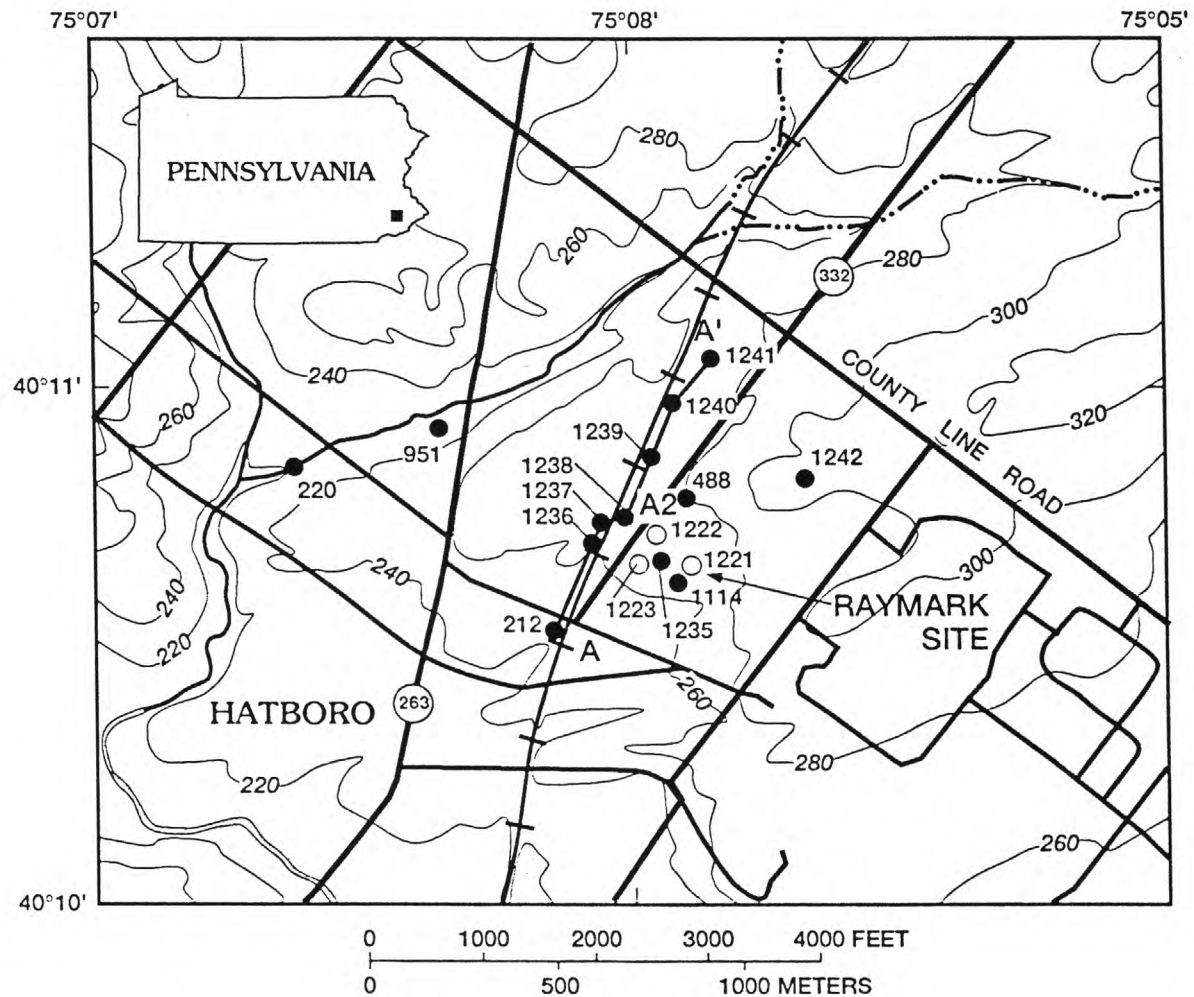
Compound	Grams per year	Gallons per year
Carbon tetrachloride	570	0.09
1,1-Dichloroethane	200	.05
1,2-Dichloroethane	8.2	<.01
Chloroform	36	.01
1,1-Dichloroethylene	730	.16
1,2,-trans-Dichloroethylene	250	.05
1,2-Dichloropropane	450	.16
Tetrachloroethylene	450	.08
1,1,1-Trichloroethane	2,050	.41
1,1,2-Trichloroethane	1	<.01
Trichloroethylene	75,900	13.65
Total	80,645	14.68

REFERENCES

Patten, E.P., Jr., and Bennett, G.D., 1962, Methods of flow measurement in well bores: U.S. Geological Survey Water-Supply Paper 1544-C, 28 p.

Sloto, R.A., and Davis, D.K., 1983, Effect of urbanization on the water resources of Warminster Township, Bucks County, Pennsylvania: U.S. Geological Survey Water-Resources Investigations Report 82-4020, 78 p.

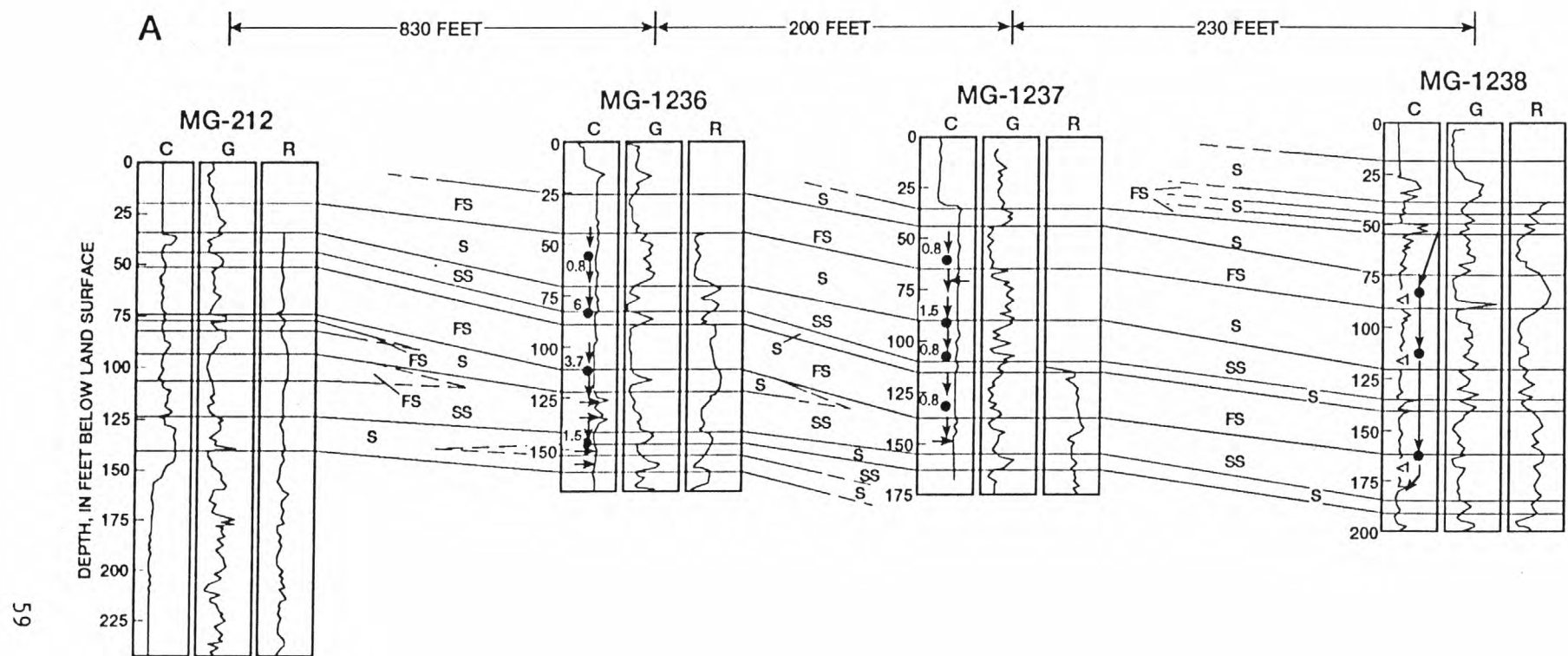
Turner-Peterson, C.E., and Smoot, J.P., 1985, New thoughts on facies relationships in the Triassic Stockton and Lockatong Formations, Pennsylvania and New Jersey: U.S. Geological Survey Circular 946, p. 10-17.



EXPLANATION

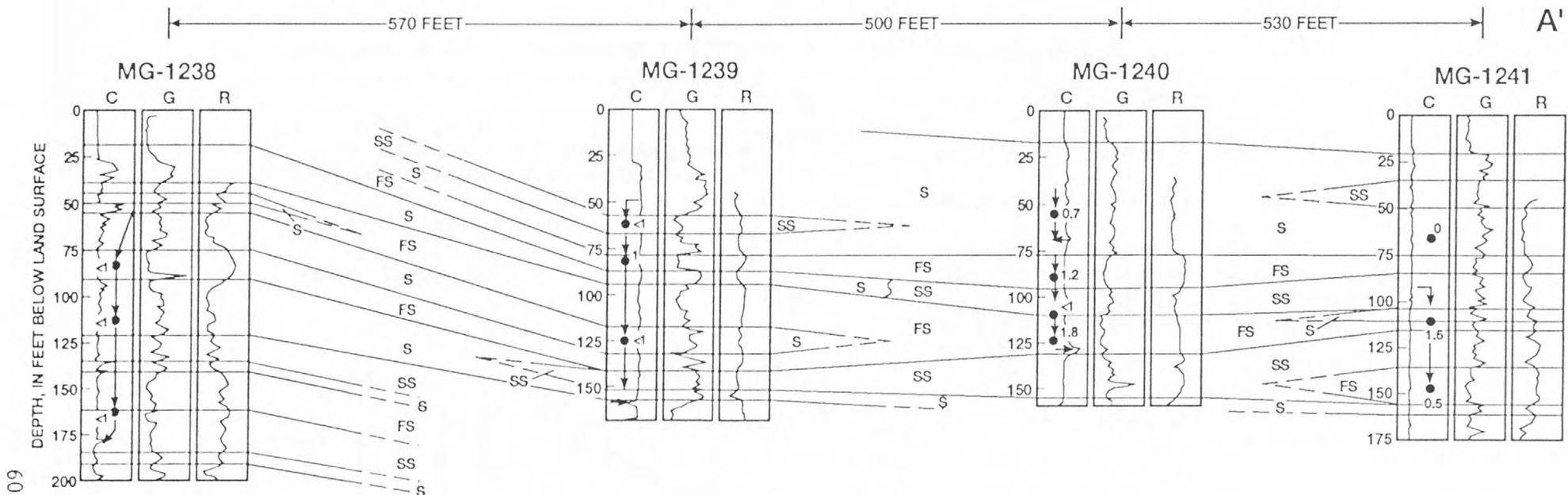
- 1236 BOREHOLE AND IDENTIFIER. (PREFIX MG OMITTED FROM IDENTIFIER)
- 1221 MONITOR WELL CLUSTER AND IDENTIFIER. (PREFIX MG OMITTED FROM IDENTIFIER)
- A — A' LINE APPROXIMATELY ALONG STRIKE. (SECTION SHOWN IN FIGURE 26)

Figure 25. Location of study area, boreholes, and monitoring-well clusters.



- C CALIPER LOG
- G NATURAL-GAMMA LOG
- R SINGLE-POINT RESISTANCE LOG
- 6 BOREHOLE FLOW MEASUREMENT—CIRCLE AT DEPTH OF SLUG INJECTION. NUMBER IS MEASURED FLOW IN GALLONS PER MINUTE
- ↓ DIRECTION OF VERTICAL BOREHOLE FLOW—ARROW POINTING DOWN INDICATES DOWNWARD FLOW
- FLOW INTO OR OUT OF BOREHOLE—ARROW POINTING AWAY FROM CALIPER LOG INDICATES FLOW INTO BOREHOLE. ARROW POINTING TOWARD CALIPER LOG INDICATES FLOW OUT OF BOREHOLE
- MS MEDIUM- TO COARSE-GRAINED SANDSTONE
- FS FINE-GRAINED SANDSTONE
- SS SILTY, FINE-GRAINED SANDSTONE
- S SILTSTONE AND MUDSTONE

Figure 26. Diagram showing lithostratigraphic correlation approximately along strike (of the line A-A' shown in figure 25).



EXPLANATION

- C CALIPER LOG
- G NATURAL-GAMMA LOG
- R SINGLE-POINT RESISTANCE LOG
- 6 BOREHOLE FLOW MEASUREMENT—CIRCLE AT DEPTH OF SLUG INJECTION. NUMBER IS MEASURED FLOW IN GALLONS PER MINUTE
- ↓ DIRECTION OF VERTICAL BOREHOLE FLOW—ARROW POINTING DOWN INDICATES DOWNWARD FLOW
- FLOW INTO OR OUT OF BOREHOLE—ARROW POINTING AWAY FROM CALIPER LOG INDICATES FLOW INTO BOREHOLE. ARROW POINTING TOWARD CALIPER LOG INDICATES FLOW OUT OF BOREHOLE
- MS MEDIUM- TO COARSE-GRAINED SANDSTONE
- FS FINE-GRAINED SANDSTONE
- SS SILTY, FINE-GRAINED SANDSTONE
- S SILTSTONE AND MUDSTONE

Figure 26. Continued.

DELINERATION OF THE SALTWATER-FRESHWATER INTERFACE IN
GREAT NECK, LONG ISLAND, NEW YORK
By Frederick Stumm¹

Great Neck is a peninsula about 1.5 mi wide and 3.0 mi long in northwestern Nassau County, Long Island, New York (fig. 27). The peninsula is underlain by unconsolidated deposits of the Lloyd Sand and Raritan clay of Cretaceous age and upper Pleistocene age (Kilburn, 1979). These deposits form three major freshwater aquifers and two confining units that rest unconformably upon bedrock. A number of public supply wells screened within the Lloyd aquifer have become adversely affected by saltwater intrusion.

The entire Great Neck area is underlain by the Pleistocene upper glacial aquifer, which is composed of tills and clays (Suter and others, 1949; Kilburn, 1979) (fig. 28). The upper glacial aquifer is unconfined and underlain by a gray clay throughout the study area. The clay appears to be equivalent to the Port Washington confining unit identified by Kilburn (1979).

An unnamed aquifer confined by this clay was encountered during drilling. The aquifer consists of gray and brown sand and gray silt and appears to be of Pleistocene (?) age; it is in hydraulic connection with the Magothy aquifer to the south (fig. 28).

Underlying this confined aquifer is the Raritan clay, which consists of gray, red, and multicolored solid clays of Cretaceous age (Smolensky and others, 1989; Suter and others, 1949). Parts of the Raritan clay appear to have been scoured by glacial erosion that removed the unit entirely in the peninsula's northern part and created a unit of variable thickness throughout the southern part (fig. 28).

The Raritan clay confines the underlying Lloyd aquifer, which consists of discontinuous layers of gravels, sands, and clay lenses of Cretaceous age (Smolensky and others, 1989; Suter and others, 1949). The Lloyd aquifer is present throughout most of the peninsula, except in the northernmost part (at wells GN-4 and 8, figs. 27 and 28).

On the basis of geologic samples collected during drilling, glacial erosion completely removed the Lloyd aquifer and Raritan clay in the peninsula's northernmost part in the vicinity of well GN-6. In the northernmost part of the peninsula, an aquifer consisting of fine, gray sand unconformably overlies the bedrock surface. The aquifer appears to be equivalent to the Port Washington aquifer that was identified by Kilburn (1979) (fig. 28). The aquifer is in hydraulic connection with the Lloyd aquifer to the south. The Port Washington aquifer is overlain by the Port Washington confining unit.

Geologic data obtained during drilling that indicates the entire peninsula is underlain by medium- to high- grade metamorphic bedrock, the upper zone which consists of saprolite about 50 to 100 ft thick. The bedrock surface is considered to be an impermeable boundary (Franke and McClymonds, 1972).

Ten wells were drilled to bedrock within the study area as part of a geologic, geophysical, and geochemical survey (fig. 27). During drilling of each well, split-spoon cores were collected to provide filter-press and geologic samples. Filter-press sampling uses a nitrogen gas pressurized

¹U.S. Geological Survey, 5 Aerial Way, Syosset, NY 11791

chamber to force interstitial water from pore space of a core sample; it is assumed that this interstitial water represents water typical of that in the formation and was not introduced during drilling (Luszynski, 1961). The resulting filtered water sample is then analyzed to determine the chloride concentration of the formation at a specific depth. The combination of induction and gamma logs from these wells indicated the distribution of saltwater intrusion (fig. 29) (Keys and MacCary, 1971; Keys, 1990).

Induction and gamma logs and geochemical data indicate three major areas of saltwater intrusion within the Lloyd and parts of the Port Washington aquifers immediately above the bedrock surface. Induction logs of these wells substantiate the low permeability of the bedrock below these aquifers, because permeable bedrock saturated with electrically conductive sea water would show much higher conductivities than those indicated on the logs (fig. 29). Data from exploration wells GN-4 and GN-8 (figs. 27 and 29) indicate the presence of a zone of saltwater in the northernmost part of Great Neck, in which chloride concentrations are higher (15,300 mg/L) and the vertical extent of the saltwater larger (100 ft) than they are in any other part of the study area.

A second zone of saltwater was penetrated in wells GN-2 and GN-6 but not in well GN-9 (figs. 27 and 29). At well GN-2 the chloride concentration was 1,900 mg/L and the saltwater zone indicated by aquifer concentrations greater than about 50 millisiemens per meter was about 20 ft thick. This zone of saltwater was the cause for the abandonment of two public-supply wells near well GN-2.

The third zone of saltwater was detected on the northwestern shore of Great Neck at well GN-5 (fig. 27). The saltwater wedge had a thickness of about 30 feet and an estimated chloride concentration of 8,000 mg/L on the basis of the induction-log response (fig. 29).

Data derived from filter-press samples, induction logs, and well-screen water samples suggest that the extent of saltwater intrusion was much greater than had been previously thought. The average slope of the saltwater wedge is very shallow and contains a narrow transition zone between saltwater and freshwater in the Lloyd aquifer and in parts of the Port Washington aquifer. Induction logging provided a high-resolution cross-sectional view of the peninsula's saltwater zones, delineating peak chloride concentrations and thicknesses of saltwater zones.

REFERENCES

Franke, O.L., and McClymonds, N.E., 1972, Summary of the hydrologic situation on Long Island, New York, as a guide to water management alternatives: U.S. Geological Survey Professional Paper 627-F, 59 p.

Keys, W.S., 1990, Borehole geophysics applied to ground-water investigations: U.S. Geological Survey Techniques of Water-Resources Investigations, book 2, chap. E2, 150 p.

Keys, W.S., and MacCary, L.M., 1971, Application of borehole geophysics to water-resources investigations: U.S. Geological Survey Techniques of Water-Resources Investigations, book 2, chap. E1, 126 p.

Kilburn, Chabot, 1979, Hydrogeology of the town of North Hempstead, Nassau County, Long Island, New York: Long Island Water Resources Bulletin LIWR-12, 87 p., 4 pl.

Luszynski, N.J., 1961, Filter-press method of extracting water samples for

chloride analysis: U.S. Geological Survey Water-Supply Paper 1544-A,
8 p.

Smolensky, D.A., Buxton, H.T., and Sernoff, P.K., 1989, Hydrologic framework
of Long Island, New York: U.S. Geological Survey Hydrologic
Investigations Atlas HA-709, 3 sheets, scale 1:250,000.

Suter, Russel, de Laguna, Wallace, and Perlmutter, N.M., 1949, Mapping of
geologic formations and aquifers of Long Island, New York: New York
State Power and Control Commission Bulletin GW-18, 212 p.

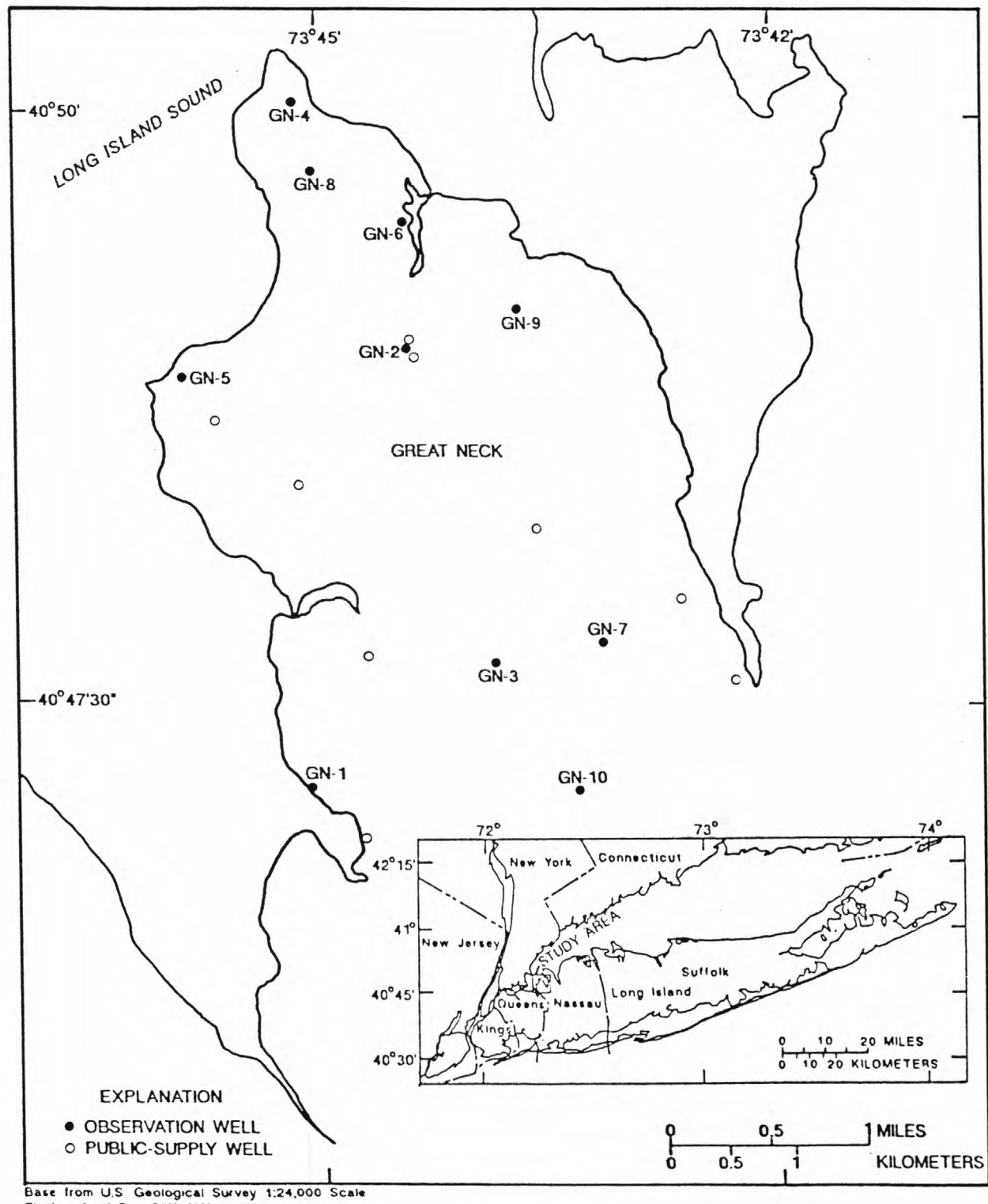


Figure 27. Location of the Great Neck study area and observation wells GN-1 to GN-10.

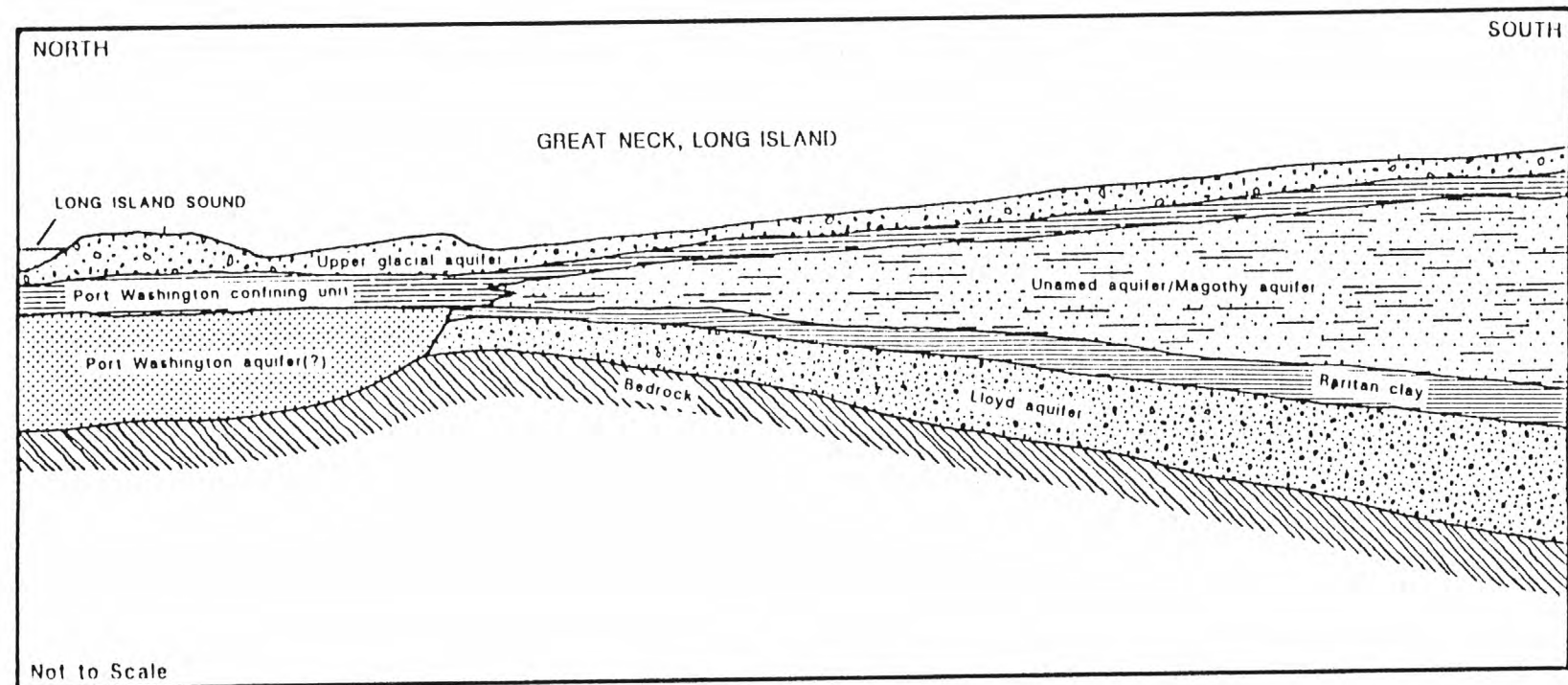


Figure 28. Generalized geologic section of the Great Neck peninsula.

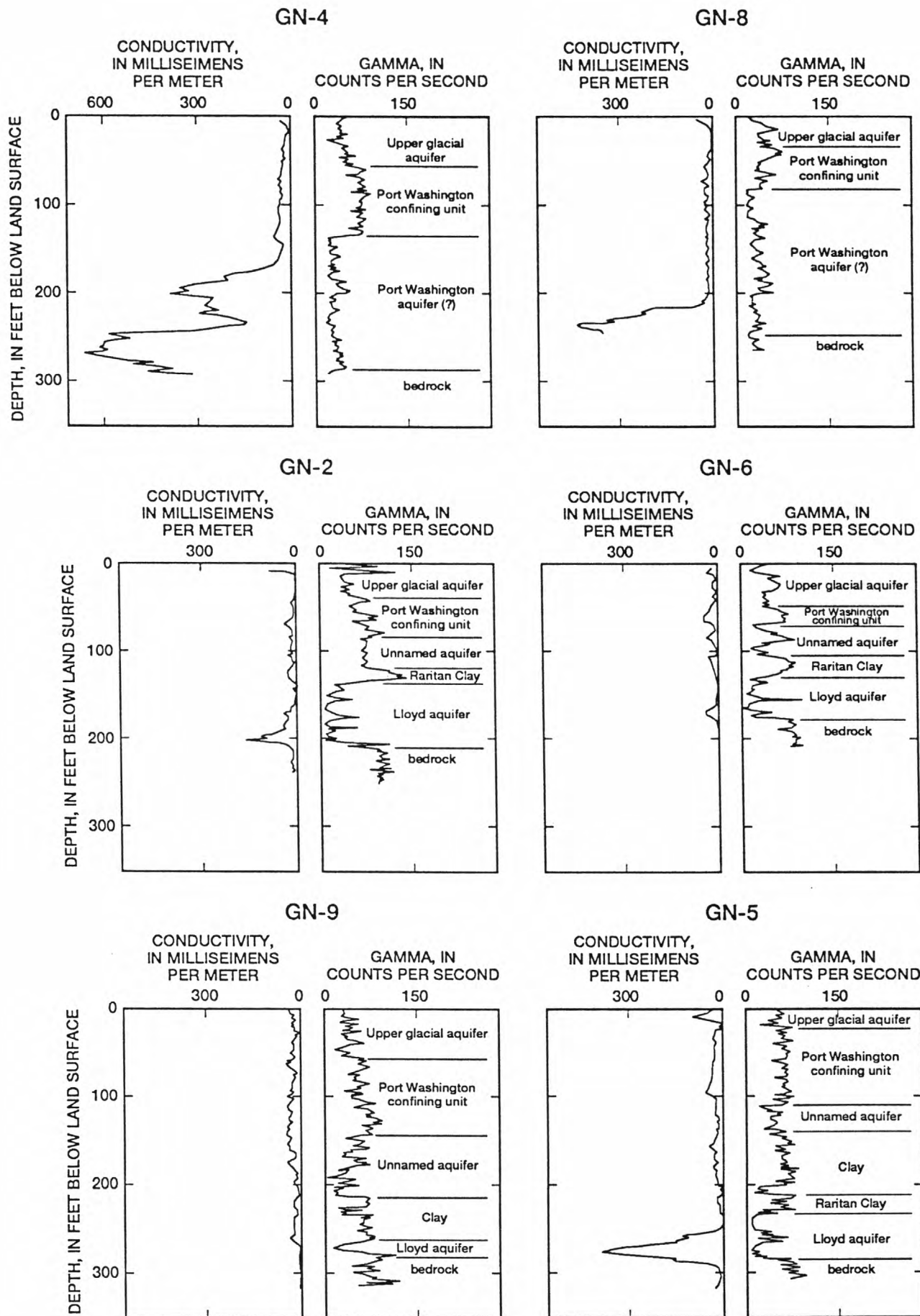


Figure 29. Geophysical logs (gamma and electromagnetic induction) of observation wells.

DELINeATION AND ESTIMATED TIME OF TRAVEL OF A ROAD-SALT PLUME
BY USE OF BOREHOLE INDUCTION LOGS
By Peter E. Church¹ and Paul J. Friesz¹

Vertical distribution and temporal fluctuation of ground water contaminated with road salt in a glacial sand and gravel aquifer downgradient from a recently completed six-lane highway in southeastern Massachusetts (fig. 30) is being monitored by borehole induction logging. The induction logger measures the combined electrical conductivity of the aquifer material and pore fluid surrounding an observation well (Hearst and Nelson, 1985; Keys, 1990). Induction logs made in wells upgradient and downgradient from the highway have shown the presence of a plume of ground water having relatively high electrical conductivity downgradient from the highway. The high-electrical-conductivity water is present in a thin zone near the water table. Induction logs also have shown that the electrical conductivity of this zone varies on an approximate annual cycle. Analysis of water-quality samples collected from clusters of wells with 1.5-m-long screens concurrently with induction logging indicate that the vertical distribution of solutes and the ionic content of the water samples are consistent with a plume that originated as the result of application of deicing salt to the highway during the winter (fig. 31).

A method to determine the hydraulic conductivity of the road-salt-contaminated zone has been developed on the basis of this annual fluctuation in electrical conductivity. The road-salt plume consists primarily of sodium cations and the conservative, nonreactive chloride anion, and is assumed to travel at about the same rate as the ground water. On the basis of Darcy's law, hydraulic conductivity can be calculated, whereby average linear velocity is replaced by the distance between two observation wells along the same path of ground-water flow divided by the time of travel of the road-salt plume.

The time of travel of the annual road-salt plume was calculated on the basis of the time interval between the temporal centroids (first moment) (Fischer and others, 1979) of the areas defined by the temporal distributions of the maximum electrical conductivities through their annual cycles. Temporal variations of the maximum road-salt plume electrical conductivities are shown for two observation wells, B2303 and B2403 (fig. 32), both of which are screened in the same ground-water flow path. The temporal centroid is an estimate of when one-half the plume, as detected by electrical-conductivities, has passed by the observation well.

Induction-log data previously collected on a nearly monthly basis in 1989 and 1990, indicate that times of travel range from 68 to 103 days--equivalent to horizontal hydraulic conductivities of 46 to 66 m/d. This range of hydraulic conductivities compares reasonably with horizontal hydraulic conductivities of 35 to 48 m/d obtained from slug tests completed within this road-salt contaminated zone. Because of this similarity of hydraulic conductivities, this method was pursued by collecting logs on a weekly basis from wells installed in November 1990 to refine the delineation of the pulse of salinity associated with annual peaks in road salt use for purposes of improving time-of-travel measurements. The time of travel from the road-salt plume defined from these weekly measurements was 84 days,

¹U.S. Geological Survey, 28 Lord Road, Suite 280, Marlborough, MA 01752

resulting in a horizontal hydraulic conductivity of 61 m/d.

The induction logger has proved to be an efficient and effective instrument for monitoring road-salt contamination of ground water. Induction logs have been used in the design of wells and placement of screens by defining the vertical location and extent of a road-salt plume downgradient from the highway. Induction logs continue to be used to verify that the well screens span the full vertical extent of the plume. Induction logs can be used to detect or monitor any contaminant plume, if its electrical conductivity differs from that of the surrounding ground water.

Favorable results were achieved in developing a method to determine horizontal hydraulic conductivity from induction-log data by monitoring travel times of annual road-salt plumes between wells along the same ground-water flow path. Although this method requires frequent monitoring over a relatively long period of time, it does not require injection of a tracer and collection of water samples to detect the arrival of the tracer.

REFERENCES

Fischer, H.B., List, E.J., Koh, R.C.Y., Imberger, J., and Brooks, N.H., 1979, Mixing in inland and coastal waters: New York, Academic Press, Inc., 483 p.

Hearst, J.R., and Nelson, P.H., 1985, Well logging for physical properties: New York, McGraw-Hill, 570 p.

Keys, W.S., 1990, Borehole geophysics applied to ground-water investigations: U.S. Geological Survey Techniques of Water-Resources Investigations, book 2, chap. E2, 150 p.

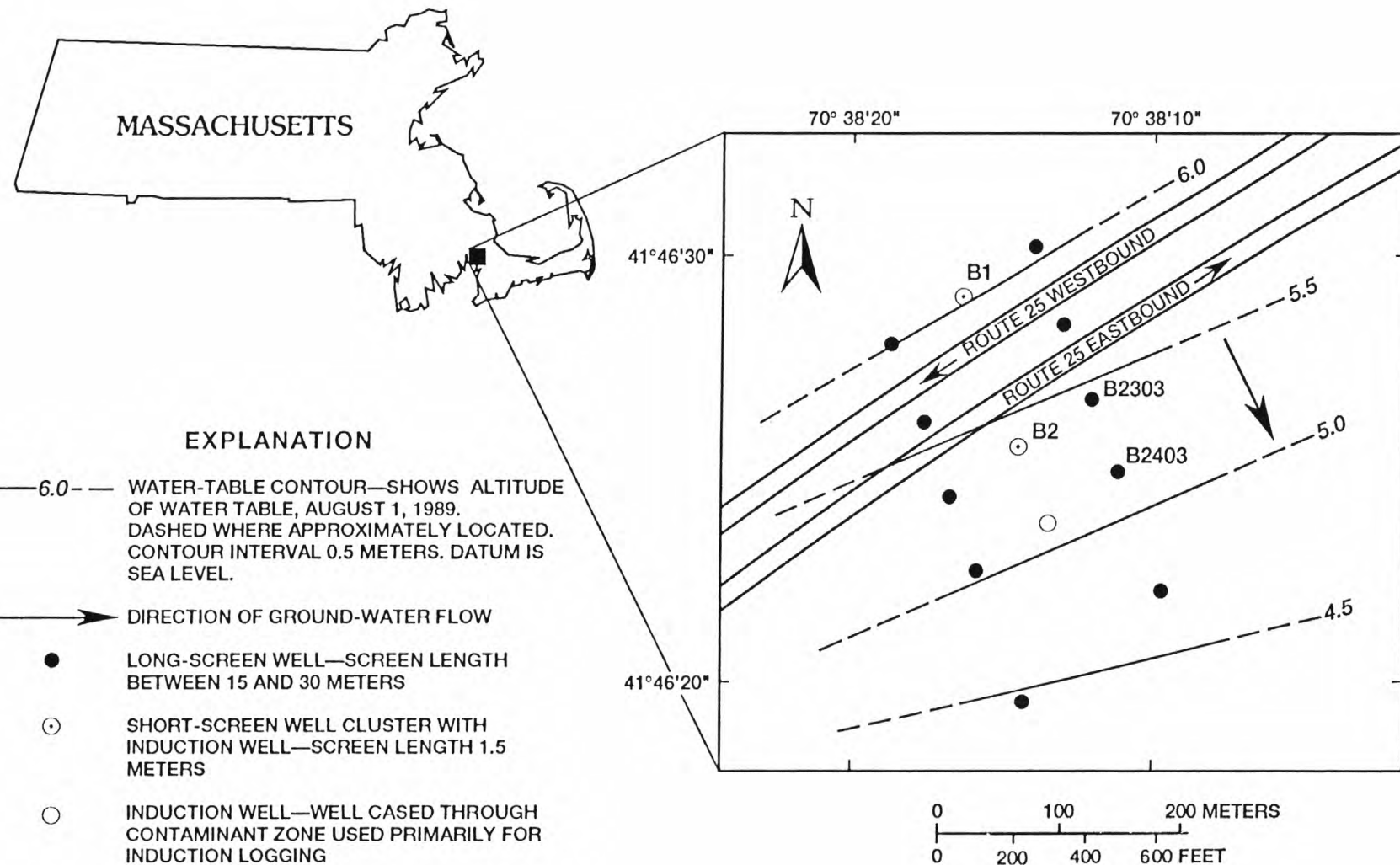
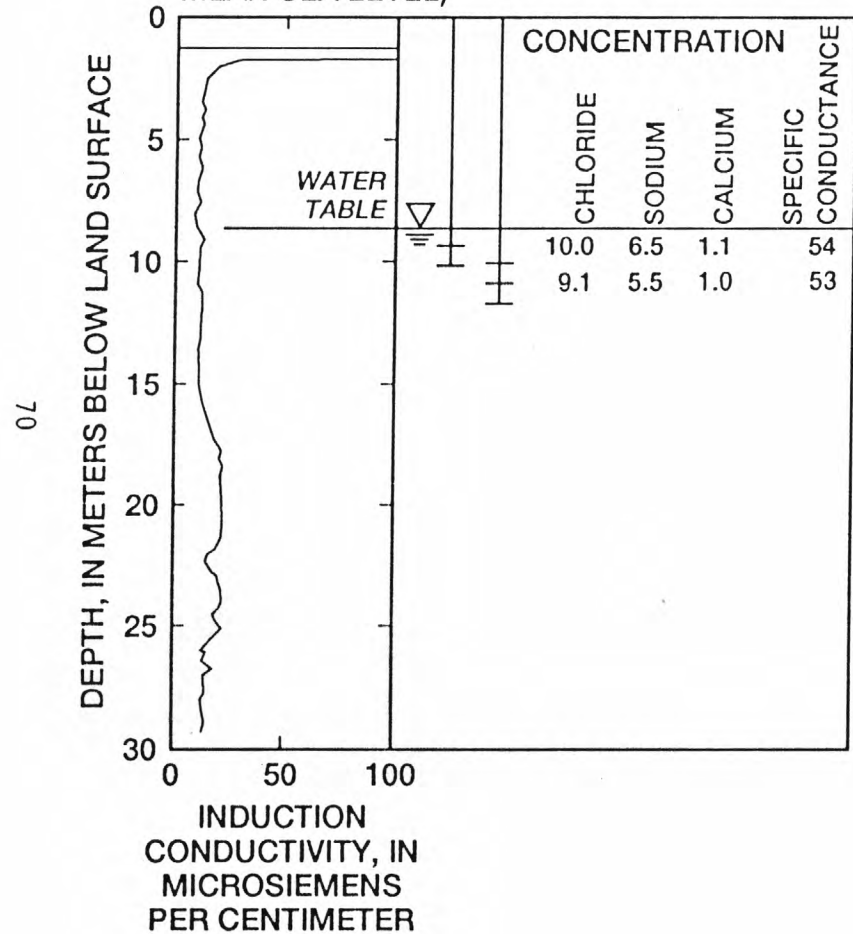


Figure 30. Location of study area in southeastern Massachusetts and location of wells relative to Route 25, altitude of water table on August 1, 1989, and the direction of ground-water flow at site B in Wareham, Massachusetts.

WELL CLUSTER B1

(30 METERS UPGRAIDENT FROM HIGHWAY;
ALTITUDE OF LAND SURFACE 14.78 METERS,
MEAN SEA LEVEL)



WELL CLUSTER B2

(30 METERS DOWNGRADIENT FROM HIGHWAY;
ALTITUDE OF LAND SURFACE 14.23 METERS,
MEAN SEA LEVEL)

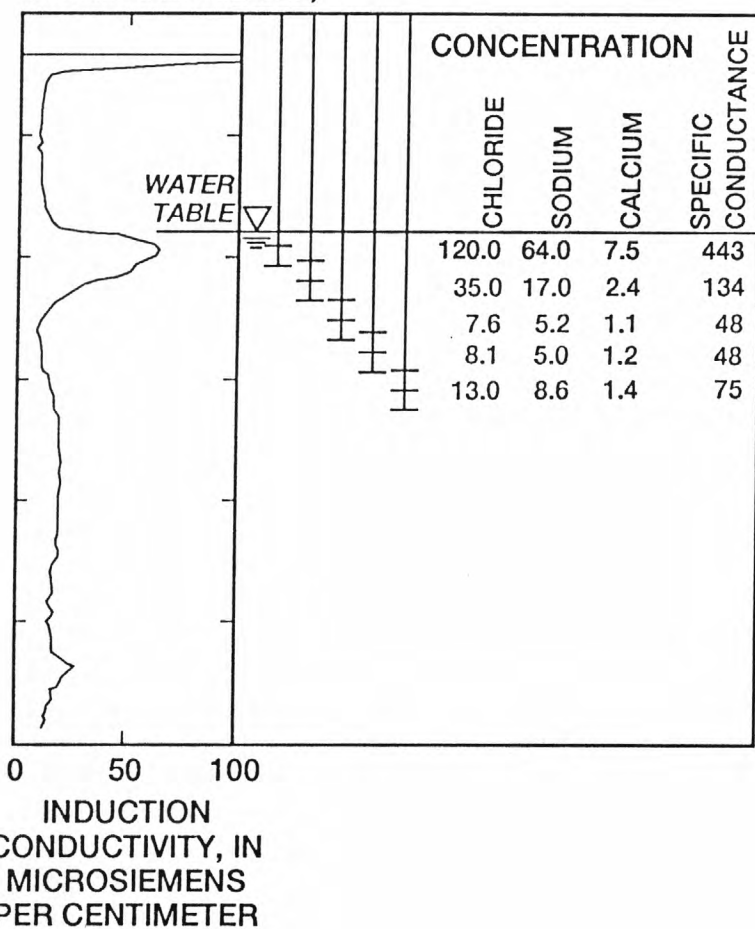


Figure 31. Induction logs and water-quality data collected on July 25, 1991, from well clusters B1 (upgradient from the highway) and B2 (downgradient from the highway) along the same path of ground-water flow; (concentrations in milligrams per liter; specific conductance in microsiemens per centimeter at 25 degrees Celsius).

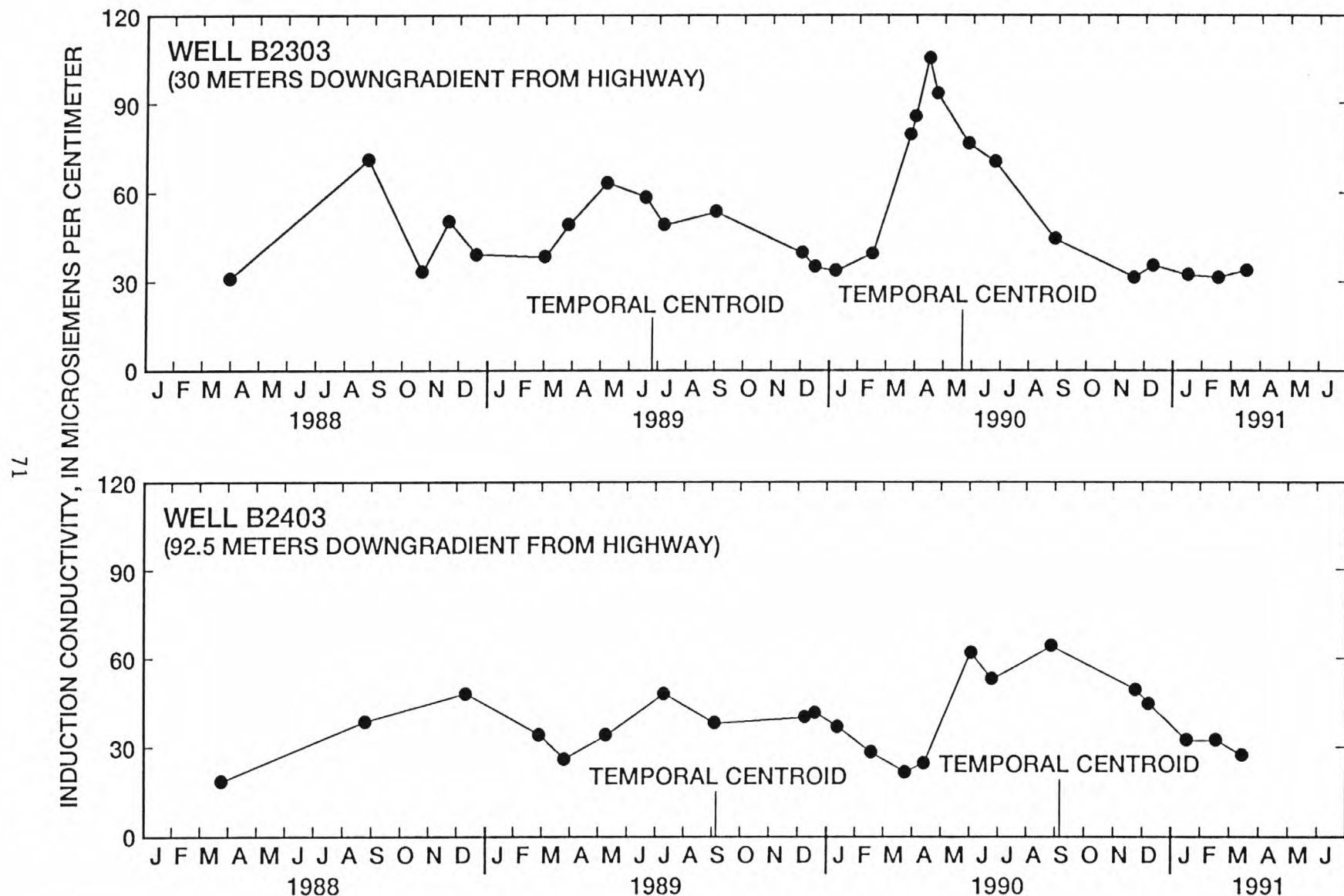


Figure 32. Maximum induction conductivities of the road-salt plumes from March 1988 through March 1991, at monitoring wells B2303 and B2403, 30 meters and 92.5 meters downgradient from highway, respectively, along the same path of ground-water flow.

DETECTION OF CONTAMINANT PLUMES BY BOREHOLE GEOPHYSICAL LOGGING
By Thomas J. Mack¹

Two borehole-geophysical methods, electromagnetic-induction and natural-gamma logs, were used to delineate the vertical extent of leachate plumes in ground water beneath two landfills in a glacial sand-and-gravel aquifer in west-central Vermont (fig. 33). Geophysical logging of observation wells greatly aided in the interpretation of lithologic logs, creation of detailed hydrogeologic sections, and placement of observation-well screens to sample landfill-leachate plumes (Keys, 1990; Hearst and Nelson, 1985).

Zones of high electrical conductivity were delineated in the induction logs run in wells near two landfills. Some of these zones were found to correlate with silt and clay units on the basis of natural-gamma logs (fig. 34). Observation wells were screened specifically in zones of high electrical conductivity that did not correspond to a silt or clay unit. Zones of high electrical conductivity that did not correspond to a silt or clay unit were caused by the presence of ground water with a high specific conductance (generally 1,000 to 2,370 $\mu\text{S}/\text{cm}$). Ambient ground water in the study area has a specific conductance of approximately 200 to 400 $\mu\text{S}/\text{cm}$. Landfill-leachate plumes in ground water were found to be approximately 5 to 20 ft thick and to be near the water table (fig. 34 and 35).

REFERENCES

Hearst, J.R., and Nelson, P.H., 1985, Well logging for physical properties: New York, McGraw-Hill, 570 p.
Keys, W.S., 1990, Borehole geophysics applied to ground-water investigations: U.S. Geological Survey Techniques of Water-Resources Investigations, book 2, chap. E2, 150 p.

¹U.S. Geological Survey, 525 Clinton St., Bow, NH 03304

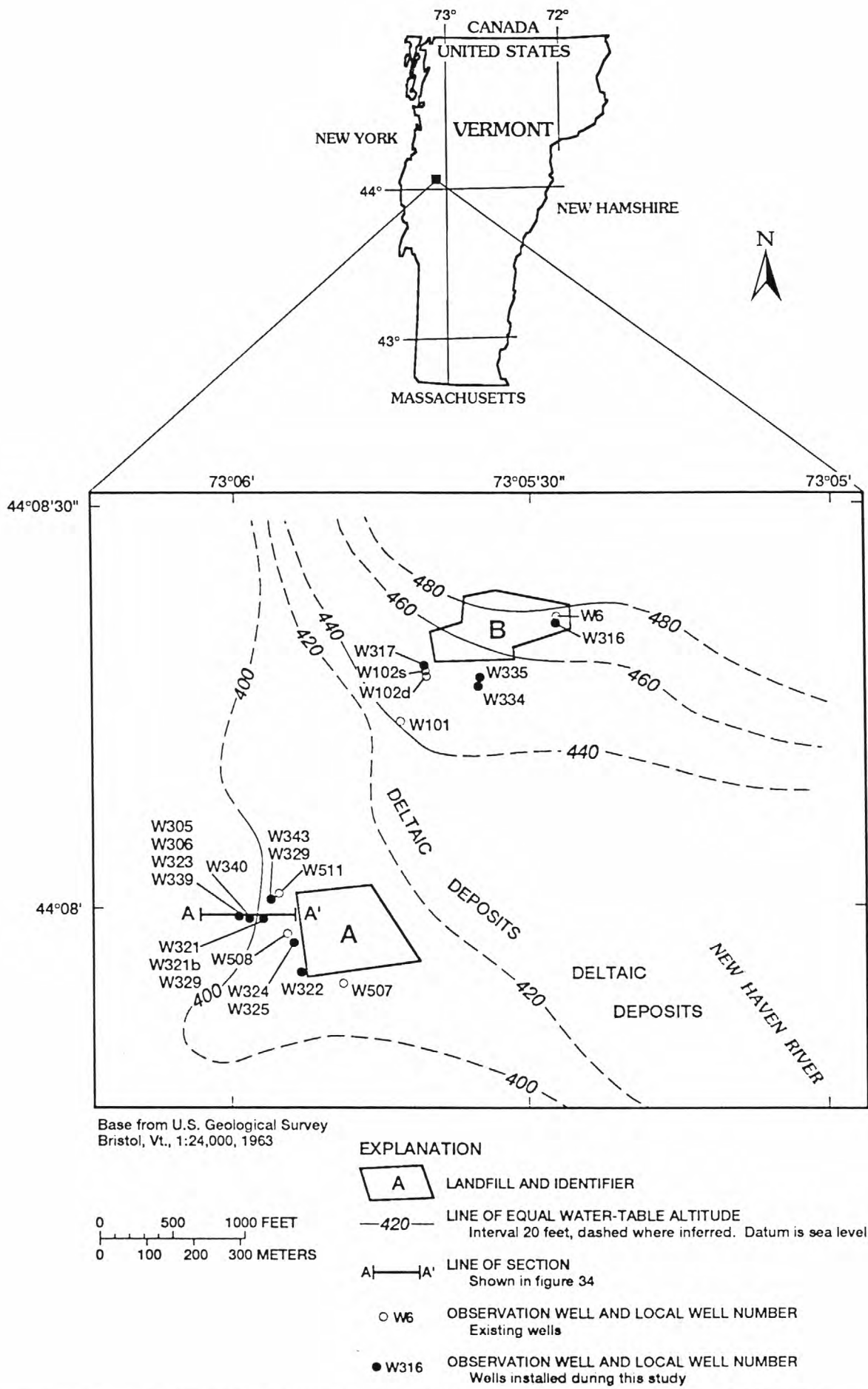
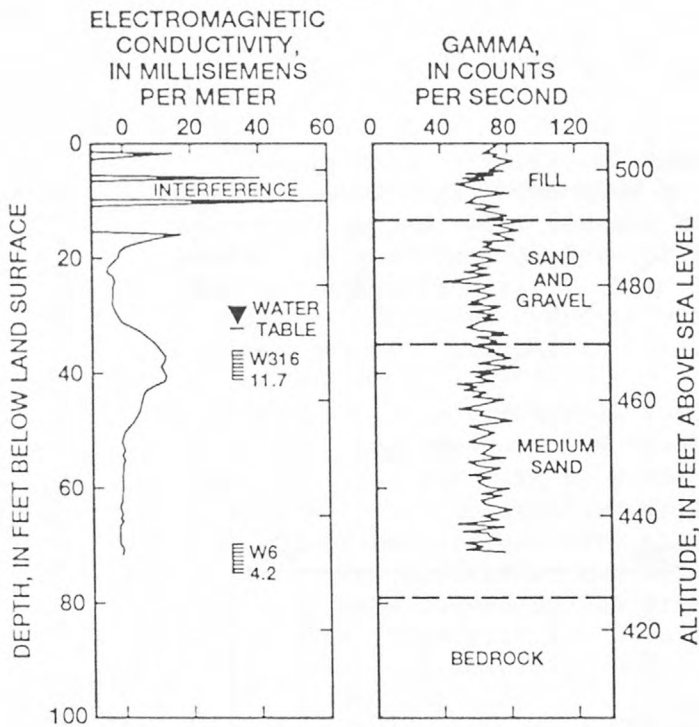
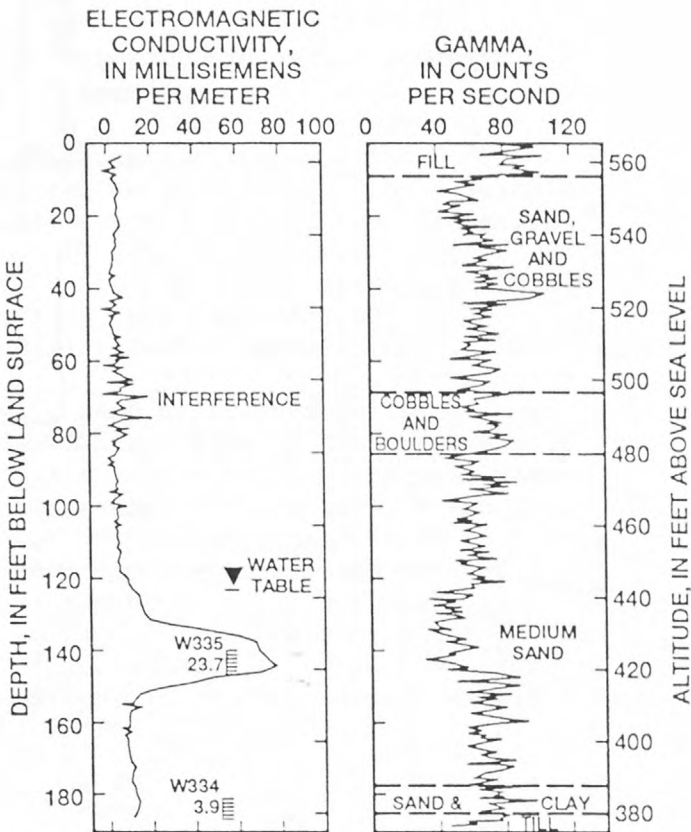


Figure 33. Location of study area, landfills, and monitoring wells and water-table altitude in September 1991.

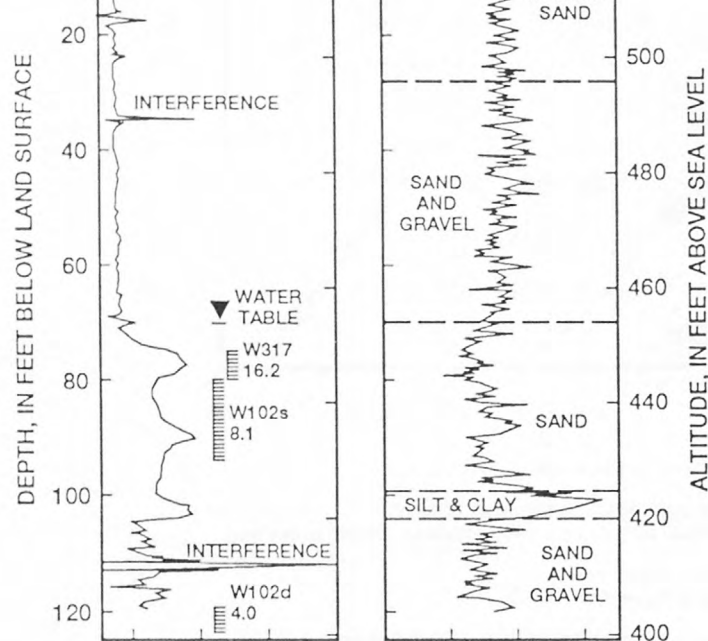
WELL W6



WELL W334



WELL W102d



EXPLANATION

 SCREENED INTERVAL OF OBSERVATION
 WELL—Top number is well number.
 Bottom number is specific conductance of water samples from the screened interval, in millisiemens per meter at 25 degrees Celsius.

Figure 34. Diagram showing borehole geophysical logs, geologic section, screened intervals, and associated specific conductance of ground water at Landfill B.

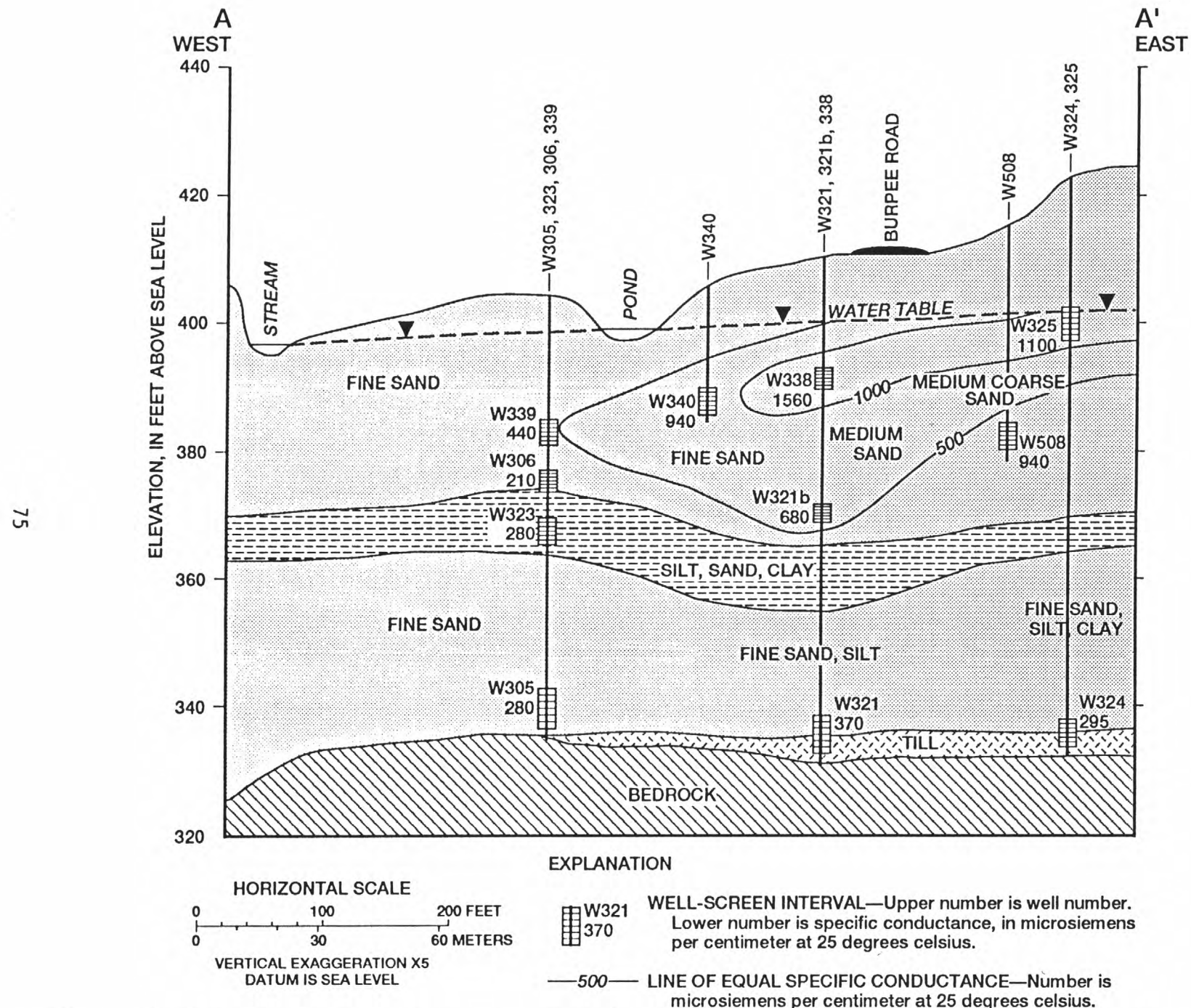


Figure 35. Geologic section, electromagnetic-induction log screened intervals and associated specific conductance of ground water at Landfill A along section A-A'. (Location of section is shown in fig. 33.)

USE OF BOREHOLE ELECTROMAGNETIC LOGGING TO DELINEATE A SEPTAGE-EFFLUENT PLUME IN GLACIAL OUTWASH,¹ ORLEANS, MASSACHUSETTS
By Leslie A. DeSimone¹ and Paul M. Barlow¹

The location and monitoring of an advancing plume of contaminated ground water can be a difficult, costly, and time-consuming endeavor. Borehole electromagnetic(EM)-induction logging has proved to be an efficient, cost-effective means for delineating and monitoring a plume of treated-septage effluent in glacial outwash on Cape Cod, Massachusetts. The heterogeneity of the outwash has caused the plume to have a complex, three-dimensional structure that would have been difficult to define accurately, while remaining within the budget of the investigation, had the induction logger not been used.

The plume originated from the infiltration of treated-septage effluent that had been discharged to infiltration beds since February 1990 (fig. 36). The effluent contained high concentrations of dissolved ions, including chloride, calcium, and sodium, that caused the plume to be electrically conductive (mean specific conductance was 3,500 $\mu\text{S}/\text{cm}$). This specific conductance is an order of magnitude higher than the specific conductance of uncontaminated ground water at the site. Consequently, the highly conductive plume was readily detected by the induction logger, which measured the electrical conductivity of the aquifer (McNeill, 1986). Exact concentrations of dissolved constituents could not be determined from the electrical conductivity of the aquifer, because the measured conductivity depends on both the electrical conductivity of the water saturating the formation and that of the minerals in the formation. However, the occurrence and relative concentrations of dissolved ions could be inferred from the anomalously high conductivity measurements, which were detected by the induction logger at contaminated sites. Induction logs were made at about 1-month intervals at 10 to 15 observation wells. These wells span the vertical extent of the plume at contaminated locations and the anticipated vertical extent of the plume at uncontaminated locations.

The goal of the field investigation was to observe the development of the effluent plume, and the induction logger has been used in several facets of the investigation. Induction logs have provided a detailed history of the plume's development at several observation-well sites. Repeated induction logging at these sites prior to and during the plume's arrival made it possible to identify contaminated zones, because the logs indicated changes in induction conductivity relative to precontamination measurements, regardless of the level of background (precontamination) conductivity. This method is particularly useful at sites where low-conductivity sand and naturally, more electrically conductive silt- and clay-rich layers are present. The response of the induction logger to such layers results in a peak in conductivity that would be difficult to distinguish from a peak resulting from elevated concentrations of dissolved ions, if repeated induction logs were not available to show that the peak did not change with time. As indicated by the induction logs at the two sites (fig. 37; sites located on fig. 36), the location and time of arrival of the plume at the individual well sites varied greatly. The induction logs were used to define the vertical extent of the plume and determine, by inference, the variability

¹U.S. Geological Survey, 28 Lord Road, Marlborough, MA 01752

of contaminant concentrations within the plume. This information was used to select sites for additional wells that would intersect the plume's center and boundaries. Precise siting of wells is necessary for obtaining the data needed to understand the biogeochemical processes that affect transport of the contaminants and for making accurate mass-balance estimates of constituents dissolved within the plume. The timing of water-quality sampling also is based on the induction logs. Water-quality samples were collected at a particular site only when the logger detected arrival of the plume or an apparent increase in contaminant concentrations; this increased the efficiency of the sampling effort.

The induction logger was used in conjunction with lithologic and natural-gamma logs to determine the complex shape and path of the plume. Delineation of the vertical extent and location of peak concentrations of the plume by means of water-quality sampling alone would have required a greater number of observation wells than were needed for delineation using the induction logger. Horizontal and vertical movement of the plume is controlled, to a large extent, by the heterogeneous lithology of the glacial outwash underlying the study area. The plume split into two horizontal lobes (fig. 36). This split is hypothesized to have been caused by a laterally discontinuous and sloping fine-grained unit, composed of very fine to fine sand and silt (the unit 18 to 62 feet below sea shown level in fig. 36A). A local high in the altitude of this unit could have caused the bifurcation of the plume and the consequent uncontaminated area between the lobes. Vertically, the fine-grained unit constricted the plume to the upper 30 ft of the saturated zone at well site 93, which is 25 ft downgradient from the infiltration beds (fig. 37B). However, the unit pinches-out within 125 ft of the infiltration beds, allowing the plume to plunge downward more than 40 ft under the effects of infiltration and fluid density gradients between sites 93 and 96 and to spread to a total thickness of 70 ft at site 96 (fig. 37B). The plume's downward movement was consistent with steep, downward vertical hydraulic-head gradients that have been measured between the two sites. As shown in figure 37, there was good correlation between the location of the plume at these two well sites, as defined by the induction logs, and the lithologic and natural-gamma logs at these sites. Correlation between the induction and gamma logs clearly indicated that the plume was located primarily within the coarse-grained middle unit at each site.

REFERENCES

McNeill, J.D., 1986, Geonics EM39 borehole conductivity meter theory of operation: Mississauga, Ontario, Geonics Limited Technical Note TN-20, 17 p.

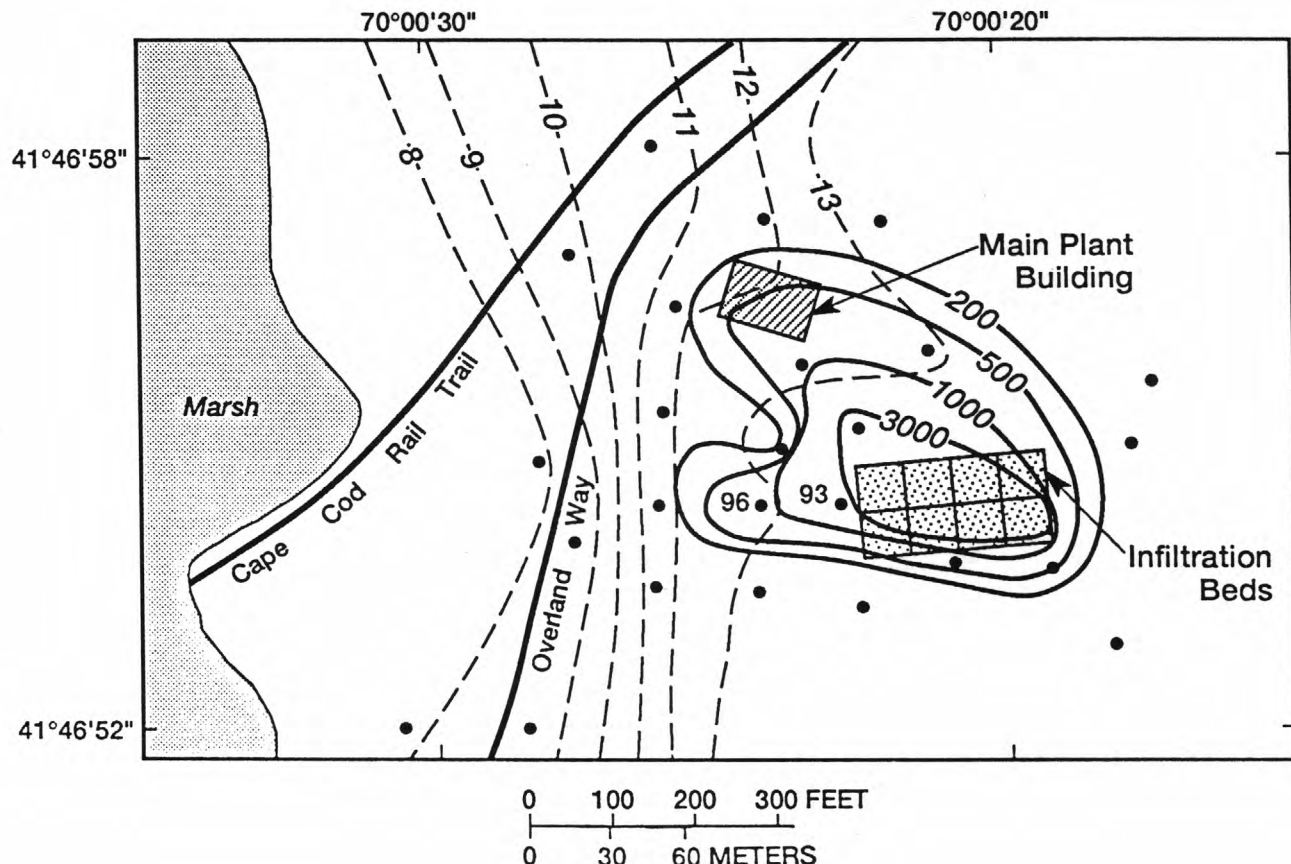


Figure 36. Map showing water-table altitude and configuration, and areal distribution of specific conductance of ground water, March 1991.

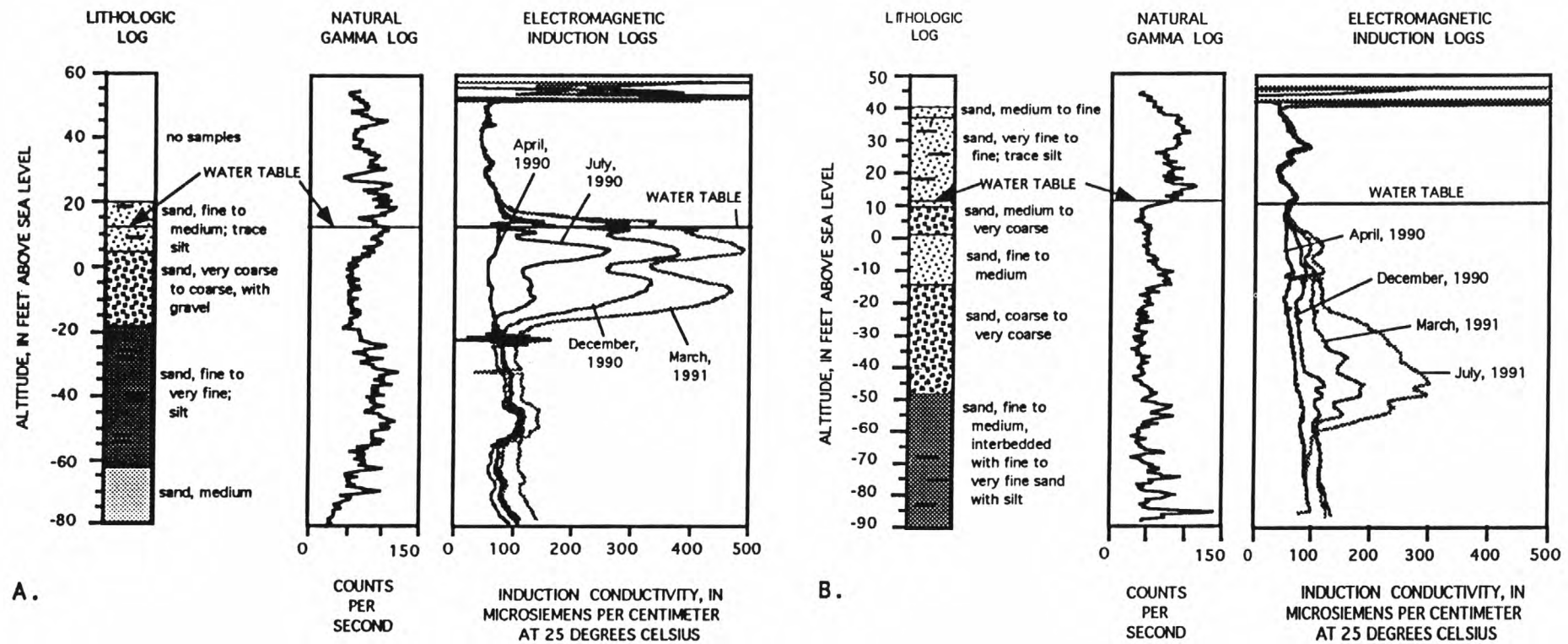


Figure 37. Lithologic log, natural-gamma log, and induction logs for (A) Well 93, (B) Well 96. (Location of wells shown in figure 36.)

USGS LIBRARY - RESTON



3 1818 00198077 8